Granular Activated Carbon for the Removal of Seasonally Present Microcystin-LR

by

Victoria Anne Inez Chennette

A thesis

presented to the University of Waterloo

in fulfilment of the

thesis requirements for the degree of

Master of Applied Science

in

Civil Engineering (Water)

Waterloo, Ontario, Canada, 2017

Author's declaration

I hereby declare that I am the sole author of this thesis. This is a true copy of the thesis, including any required final revisions, as accepted by my examiners.

I understand that my thesis may be made electronically available to the public

Abstract

Microcystin-LR (MC-LR) is a potent hepatotoxin, produced by cyanobacteria. MC-LR is the most commonly regulated cyanotoxin. MC-LR typically occurs seasonally in late summer in temperate regions, such as the North American Great Lakes region. Nutrient and temperature conditions lead to the annual formation of cyanobacterial blooms, most notably in shallower Lake Erie.

Adsorption using granular activated carbon (GAC) is a promising treatment technology for the removal of cyanotoxin MC-LR. The operation of a GAC contactor on a seasonal basis, and the storage of GAC between annual events were the focus of this work. A typical GAC in the study geographic area, Calgon Filtrasorb ® 300 (F300), was selected for this work.

In order to simulate one season of use, the F300 was preloaded with 20,000 bed volumes of post-filtration Lake Ontario water from a full-scale drinking water treatment plant. The preloading period was determined from the volume of water passed through the full-scale plant when cyanobacterial metabolites geosmin and 2-methylisoborenol had historically been detected. During preloading the water quality was consistent in terms of Total (TOC) and dissolved (DOC) organic carbon. The largest contributor to natural organic matter (NOM) was humics as determined by liquid chromatography organic carbon detection (LC-OCD).

The virgin and preloaded F300 were evaluated in terms of ultimate capacity and kinetics for MC-LR adsorption. The bottle point method was used, with samples taken daily for

the first ten days, and every two days following until less than 1% change in percentage removal was observed. MC-LR was quantified using LC-MS/MS (liquid chromatography tandem mass spectrometry). The virgin F300 reached equilibrium after 18 days, and the preloaded reached equilibrium after 49 days. The preloaded and virgin F300 did not show significantly different Freundlich isotherm parameters, indicating that the preloaded F300 was not significantly exhausted following one season of preloading. This finding should be interpreted with caution, as there may be differences which are not detectable at the selected confidence level.

The preloaded F300 was then stored under four conditions for eight months (the typical portion of the year in which cyanobacterial blooms are uncommon in temperate regions). Storage conditions included high moisture content (HMC) and low moisture content (LMC), to represent the bottom and top, respectively, of a drained GAC contactor. Two fully saturated conditions were explored; the F300 was stored completely submerged in post-filtration water from the full scale facility, and the F300 was stored fully submerged in a 20 g/L salt (sodium chloride) solution. In addition, a continuous operational control located at the full-scale pant was maintained at the same hydraulic loading rate as the full-scale filters in order to simulate a GAC contactor which remained in service year round.

The time to equilibrium for each carbon was evaluated; the salt storage samples reached equilibrium (less than 1% change in percent removal) after 41 days, and displayed the fastest kinetics for MC-LR removal. The submerged storage method displayed the slowest

kinetics, and reached equilibrium after 57 days. At the 95% confidence level, all of the stored F300 Freundlich isotherm parameters were significantly different from the continuous operational control, indicating that there may be a benefit from storage under any of the considered conditions. When the broader prediction intervals are considered, there was no significant difference in any of the predicted MC-LR solid phase concentrations when considering various MC-LR liquid phase concentrations. This finding indicates that non-detectable differences may be present, due to the data quality.

When compared with the virgin and preloaded F300, the continuous operational control is distinct from the virgin and preloaded isotherm parameters at the 95% confidence level. At the 95% confidence level, the virgin, preloaded and LMC stored carbon parameters for MC-LR removal are not distinct. Although capacity for MC-LR cannot be directly determined simply by examining the Freundlich parameters, the results suggest that the storage of the F300 under LMC conditions provides a benefit in terms of equilibrium capacity.

Overall, this research indicates that there is a benefit in terms of capacity and kinetics from the storage of the preloaded F300, under any of the considered conditions. There is an indication that the LMC storage may provide the most benefit, however additional confirmation is required to establish this finding with statistical significance.

Acknowledgments

Firstly, I would like to acknowledge the aid of my supervisors Drs. William B. Anderson, Peter M. Huck and Sigrid Peldszus. Throughout the course of this work, and the challenges faced, they have never failed to provide insight and guidance. I am truly grateful for their advice and expertise. I would also like to thank Dr. William A. Anderson and Dr. Susan L. Tighe for their review of this thesis.

I would also like to acknowledge the Region of Durham and Staff, including Barry Ward, Richard Jones, Andy Sapkowski and Thom Sloley, for their help in this project, including water sampling and chlorine analysis.

My sincerest thanks go to former NSERC Chair in Water Treatment students Dr. Feisal Rahman and Silvia Vlad for their aid in getting this work off the ground through providing valuable background knowledge. I would also like to thank current NSERC Chair in Water Treatment students Sabrina Bedjera, Andy (Zhanyang) Gong, Chuan Liu, Yanting Liu, Paul Markin, and Jangchuck Tashi for their guidance in analytical methods and procedures, and their companionship in the lab. I gratefully acknowledge the work of undergraduate research assistants Sara Abu-Obaid, Rachel Blowes and Juan Park in providing additional lab work, including some water sample preparation and analysis.

I would like to thank Justin Harbin from the Department of Earth and Environmental Sciences for freeze drying my carbon samples over the course of this work. I would also like to thank Tom Dean from Chemical Engineering for providing the shakers used for this work.

Dr. Monica Tudorancea completed the LC-OCD analysis for this work, and provided valuable lab advice and support, and I wish to express my thanks for her compassion and hard work.

Mark Merlau and Mark Sobon provided incredibly valuable advice and aid throughout the course of this works, and the exceptional number of equipment challenges faced through this work. They provided a never ending source of ideas and troubleshooting tips without which this project would not have been completed.

I would also like to thank the Department of Civil and Environmental Engineering for providing me with so many incredible opportunities to become involved over the course of my degree, including the opportunity to learn and grow as a teaching assistant and lecturer.

Ultimately, I would like to thank my family and friends for all they have done for me over the course of this degree; the level of their support and understanding is impossible to put into words. Special thanks to Drew Dutton and Lindsay Bowman for their support. Put quite simply, I would not have made it here without you. Thank you.

Table of Contents

List of Figures

List of Tables

List of Abbreviations

ATP	Adenosine Triphosphate
DOC	Dissolved Organic Carbon
F300	Calgon Carbon's Filtrasorb 300 Granular Activated Carbon
GAC	Granular Activated Carbon
HMC	High Moisture Content
JCR	Joint Confidence Region
LC MS/MS	Liquid Chromatography Mass Spectrometry
LC-OCD	Liquid Chromatography-Organic Carbon Detection
LMC	Low Moisture Content
MAC	Maximum Acceptable Concentration
MC-LR	Microcystin-LR
NOM	Natural Organic Matter
PAC	Powdered Activated Carbon
pH_{PZC}	Point of Zero Charge
SSE	Sum of Squared Errors
TOC	Total Organic Carbon
UV_{254}	Ultra Violet 254 nm

1 Introduction

1.1 Problem Statement

With the progression of climate change and the growing human population, water quality concerns are changing; temperatures are getting warmer, nutrient loading (notably nitrogen and phosphorous) is increasing, and human waste volume requiring treatment is growing. With this comes changing drinking water treatment requirements to comply with ever more stringent guidelines and regulations, designed to be protective of public health. In temperate climate zones, such as the North American Great Lakes region, cyanobacterial blooms are one example of an evolving water quality concern with emerging contaminants requiring consideration for drinking water treatment.

Cyanobacteria are an ancient and diverse group of phototrophic microorganisms. They occur in bloom type developments when temperatures and nutrient availability conditions are conducive, and are typically blue-green in colour. Cyanobacteria blooms occur globally, in both fresh and salt waters. Cyanobacteria produce a range of secondary metabolites including taste and odour compounds, such as geosmin, and a wide range of toxins collectively termed cyanotoxins. Blooms are formed when conditions are conducive, typically in the late summer and fall in temperate zones. This seasonality brings additional challenges in terms of treatment, as the toxins are not always present and the concentration of toxins can change by orders of magnitude in relatively short spans of time.

One of the most prevalent and toxic cyanotoxins is microcystin-LR (MC-LR), one of at least 80 variants of microcystin (Westrick at al., 2010). MC-LR is produced by a range of cyanobacteria including *Anabaena, Anabaenopsis, Microcystis, Nostoc* and *Planktothrix* (Westrick et al., 2010). Other prominent cyanotoxins include cylindrospermopsin and anatoxin-a. MC-LR is a cyclic hepatotoxin, primarily affecting the liver and kidneys. In 1996, a hemodialysis center in Brazil experienced a MC-LR outbreak, where 101 of 124 patients receiving dialysis became ill, with 50 fatalities attributed to microcystin related illness (Jochimsen et al., 1998). The water used for dialysis was treated with alum and trucked to the facility where it was sand filtered, passed through a carbon absorber, deionized and micro-filtered; the filters had not been changed in the three months prior to the incident and no chemicals (such as chlorine) were added (Jochimsen et al., 1998). This outbreak remains the largest incidence of human death and illness associated with microcystin.

Cyanotoxin drinking water treatment regulations are developing in many parts of the world. MC-LR is currently the most widely regulated of the cyanotoxins. The World Health Organization guidelines for drinking water quality recommend a maximum acceptable concentration (MAC) of 1 μg/L for total microcystins (World Health Organization, 2011). Health Canada's proposed MAC is 1.5 μg/L for total microcystins in drinking water (Health Canada, 2016). In Ontario, MC-LR is regulated at 1.5 μg/L (Ontario, 2006).

Adsorption has shown promise as a treatment technology for the removal of MC-LR. A granular activated carbon (GAC) contactor can be used to effectively reduce MC-LR

concentrations to below guideline values (for example Huang et al., 2007; Lambert et al, 1996; Newcombe et al., 2003).

GAC is a non-specific adsorber and will become exhausted over time by adsorbing background water constituents and natural organic matter (NOM), which are typically present at concentrations orders of magnitude greater then MC-LR (Crittenden et. al., 2012; Worch, 2012). GAC contactors are typically located post-filtration, with the purpose of adsorbing more resistant contaminants, such as MC-LR. Although GAC caps on filters may be used, full depth GAC contactors are typically run year round. The targeted removal of MC-LR on a seasonal basis utilizing a GAC contactor approach remains uninvestigated. The operation of a GAC contactor on a seasonal basis may extend the useful life of the activated carbon to remove MC-LR and reduce the replacement or regeneration frequency of the GAC. This would ultimately be protective of human health, in addition to reducing the replacement and regeneration frequency of GAC contactor media involving an operational improvement and cost savings.

1.2 Research Objectives

The primary goal of this research was to evaluate the seasonal usage of a commonly used coal-based GAC for the removal of the cyanotoxin MC-LR. This included determining if the adsorption capacity of GAC can be preserved when the GAC is stored (taken off line) between the seasonal occurrences of cyanobacteria blooms. In order to accomplish this goal, the following objectives were established:

- Determine how one season of use will impact the selected coal based GAC in terms of kinetics and capacity of MC-LR removal through a comparison of virgin and preloaded GAC.
- Identify practical GAC contactor storage scenarios. Expose the preloaded GAC to these conditions for the length of time annually that cyanobacterial blooms are typically not of concern in temperate regions.
- Evaluate how the various storage conditions affect the GAC in terms of capacity and kinetics of MC-LR removal.
- Determine the preferred GAC storage technique for use between cyanobacterial seasons.

1.3 Thesis Approach and Structure

This thesis is structured as a paper based thesis around two papers, chapters 3 and 4. Chapter 2 is a literature review, providing a summary of the MC-LR knowledge base including occurrence, toxicity and removal by common drinking water treatment processes. Chapter 3 discusses the effect of NOM preloading on GAC in terms of kinetics and ultimate capacity for MC-LR removal. Chapter 4 explores the storage of GAC under four conditions in terms of kinetics and ultimate capacity for MC-LR, and seeks to determine the preferential method of GAC storage between cyanobacterial seasonal occurrences. The detailed materials and methods involved in the experimental work are included within chapters 3 and 4. Chapter 5 concludes this thesis by summarizing results and making recommendations for drinking water treatment practice as well as for future

studies concerning the seasonal removal of MC-LR. Additional information and supporting material can be found in a series of appendices.

2 Background and Literature Review

2.1 Introduction

Cyanobacteria are a diverse group of prokaryotes, first discussed in the scientific literature in 1878, when livestock deaths were attributed to a bloom in Australia (Francis, 1878). Cyanobacteria are commonly and mistakenly confused with eukaryotic algae, and have historically been called “blue green algae” (O’Neil et al., 2012). There are approximately 40 varieties of cyanobacteria, and they can exist in a very wide variety of water conditions (varying saline, nutrient levels, temperatures, etc.) (Westrick et al., 2010).

Cyanobacteria can produce a wide range of metabolites. Municipal drinking water providers have long dealt with the biogenic taste and odour compounds, such as geosmin and 2-methylisoborneol, which can be produced as secondary metabolites of some strains of cyanobacteria (Izaguirre & Taylor, 2004). A diverse group of toxins, cyanotoxins, can also be produced by cyanobacteria, and are the subject of much current research (for example Westrick et al., 2010). Cyanotoxins have a wide range of impacts on humans, with the most common being hepatotoxins, affecting the kidneys and liver. Cyanotoxins having hepatotoxic effects include microcystins, nodularins, and cylindrospermopsin (O’Neil et al., 2012; World Health Organization, 1999).

The occurrence of cyanobacteria is a seasonal concern in the Great Lakes Region of North America. Cyanobacteria can reproduce quickly, resulting in dense blooms which typically

occur in the late summer and fall. The prevalence of such blooms are becoming more common with climate change (Paerl & Huisman, 2009).

Cyanobacteria can produce a wide variety of cyanotoxins. Microcystins are by far the most common and most heavily researched. Microcystins are produced primarily by *Microcystis spp.*, but can also be produced by *Anabaena, Anabaenopsis, Hapalosiphin, Nostoc,* and *Planktothrix (Oscillatoria)* (Falconer, 2005; Ho et al., 2012; Westrick et al., 2010; World Health Organization, 1999). The most prevalent is microcystin-LR (MC-LR), one of over 80 variants of microcystin (Carmichael, 1992; MacKintosh et al., 1990; Svrcek & Smith, 2004; Westrick et al., 2010). Cyanotoxins can exist both intracellularly contained inside the cells, or extracellularly. Damage to the cells, either in natural or in drinking water treatment processes, can cause the cells to lyse and to release their toxins (U.S. EPA, 2015; World Health Organization, 2011).

Intracellular MC-LR is removed in conventional drinking water treatment similarly to particle removal. Extracellular toxin is more difficult to remove as the toxin is dissociated from the cell and present as a dissolved compound (U.S. EPA, 2015; World Health Organization, 2011). Activated carbon is a promising removal technique for MC-LR. GAC, more operationally preferable and reusable than PAC, can be used.

GAC becomes exhausted over time, as target compounds and background NOM contribute to fouling. The seasonal use of activated carbon for the removal of intermittently present compounds such as MC-LR may preserve the capacity of the GAC; however, the storage of the GAC remains uninvestigated.

2.2 Microcystin-LR Properties and Toxicity

MC-LR is a potent hepatotoxin, affecting the liver and kidneys (Falconer et al., 1983). More specifically, MC-LR has been shown to be lethal to mice at the 1-2 µg range (injected intraperitoneally) (MacKintosh et al., 1990). The LD_{50} of MC-LR is reported to be 50 µg/kg (World Health Organization, 1999).

The empirical chemical formula for MC-LR is $C_{49}H_{74}N_{10}O_{12}$ (U.S. EPA, 2015). In terms of structure, microcystins are monocyclic heptapeptides; they contain two variable L-amino acids and two novel D-amino acids (U.S. EPA, 2015). MC-LR contains leucine (L) and arginine (A), as shown in Figure 2.1 (World Health Organization, 1999, U.S. EPA, 2015). MC-LR has a molecular weight of 995.17 g/mol (U.S. EPA, 2015). The MC-LR structure contains three ionisable groups: two carboxyl and one amino acid (De Maagd et al., 1999). The pKa of these groups is presented in Table 2.1. At the pH range commonly occurring in drinking water, MC-LR contains one negatively charged group.

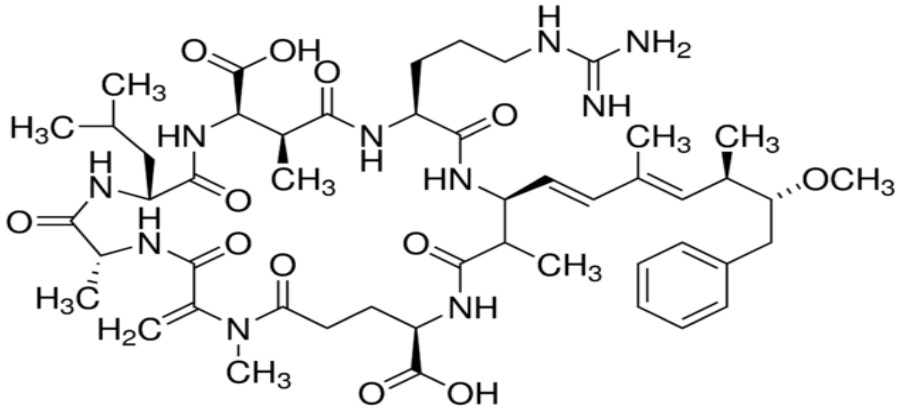

Figure 2.1 MC-LR Structure (Sigma Aldrich, 2016)

Table 2.1 MC-LR charge at various pH ranges (De Maagd et al., 1999)

pH	Dominant Species	MC-LR Net Charge
<2.09	$(COOH)_2(NH_2^+)$	+
2.09<pH<2.19	$(COO^-)(COOH)(NH_2^+)$	0
2.19<pH<12.48	$(COO^-)_2(NH_2^+)$	-
pH>12.48	$(COO\text{-})_2(NH)$	- -

MC-LR is quite stable in the environment once released from the host cell but will naturally biodegrade in days to weeks, depending on the concentrations and water chemistry (Cousins et al., 1996; Ho et al., 2006). Photolysis by natural sunlight can be effective for the destruction of MC-LR but depends on a number of conditions (Tsuji et al., 1994), for example NOM can promote photolysis (Welker & Steinberg, 1999).

2.2.1 Microcystin –LR Occurrence

Cyanobacteria, the Earth's oldest oxygen producing organisms, have existed for approximately 3.5 billion years (Schopf, 2006). Currently, cyanobacteria have a broad geographic range, existing almost globally in both fresh and salt water environments (Paerl & Paul, 2012).

Cyanobacteria drivers for formation include nutrient loading (notably nitrogen and phosphorous), temperature, atmospheric carbon dioxide levels, and water pH (O'Neil et al., 2012). Global temperatures are predicted to increase, up to 4.8°C by 2100 (IPCC, 2013). Human populations, leading to nutrient loading and carbon dioxide production

from manufacturing and farming, are predicted to increase to over 11 billion by 2100 (United Nations, 2015). These global conditions are conducive to increasing occurrence of cyanobacteria, and their accompanying cyanotoxins (Carey et al., 2012; Zhang et al., 2012).

In temperate regions, such as the North American Great Lakes, cyanobacteria blooms are becoming more common in the summer and fall, as temperature and nutrient conditions become ideal (Rinta-Kanto et al., 2005; Watson et al., 2008; Wiedner et al., 2007). For example, cyanotoxin producing species *Cylindrospermopsis raciborskii*, typical of tropical regions, has been found in temperate regions possibly due to earlier warming periods caused by climate change (Wiedner et al., 2007). The shallowest of the Great Lake, Lake Erie (also the most heavily impacted by a large basin population), has historically experienced large cyanobacterial blooms; for example *Microcystis* ssp. was detected in Lake Erie in 2003 and 2004, confirming earlier indications of potentially toxic cyanobacteria blooms forming in western Lake Erie (Rinta-Kanto et al., 2005). Lake Ontario, although less impacted than Lake Erie, has been impacted by MC-LR forming blooms (Watson et al., 2008).

The most notable incident of MC-LR related drinking water contamination occurred at a hemodialysis clinic in Brazil; 101 patients became sick and 50 died of liver failure following exposure to microcystin (Jochimsen et al., 1998). The water used for the hemodialysis was concluded to have been inadequately treated.

Lake Erie is seasonally heavily impacted by cyanobacterial blooms. In August 2014, Toledo, OH, MC-LR was detected in treated water resulting in a 3 day 'do not drink order' issued to the 500,000 water users (City of Toledo Department of Public Utilities, 2014). Bloom severity is monitored closely in Lake Erie, as the shallow conditions and heavy nutrient loading from the densely populated basin make bloom formation likely; however, the 2016 bloom severity rating was found to be 3.2 out of a possible 10 making it one of the least severe occurrences in the past 15 years, so toxin presence can be quite variable (National Oceanic and Atmospheric Administration, 2016).

2.3 Microcystin-LR Fate in Drinking Water Treatment

MC-LR can be bound within the cell (intracellular) or released from the cell (extracellular). MC-LR can be released from the cell naturally, as part of the cell life cycle, or when the cell becomes damaged. Treatment considerations vary greatly between intra- and extra-cellular MC-LR.

2.3.1 Intracellular MC-LR Removal

The removal of intracellular MC-LR focuses on the removal of the intact cells, similar to particle removal. The removal of intact cells may be achieved during conventional water treatment, including coagulation and filtration (Cheng et al., 2015; Gonzalez-Torres et al., 2014; Zamyadi et al., 2013). Dissolved air floatation (DAF) can also be effective for the removal of cyanobacterial cells, with removal rates up to 98% with no cell lysis, depending on the coagulant type and dose, and cyanobacterial species (Teixeira & Rosa, 2006). Following conventional treatment, cyanobacterial cells containing MC-LR will be trapped

in the sludge, and it is possible for the toxin to be released at this point in the process. Care should be taken to avoid rupturing the cells walls, and releasing the toxin, as extracellular toxin is much more resistant to removal. Ozonation and other strong oxidants, at high enough doses, can rupture the cell walls and release the toxins (Coral et al., 2013). Intracellular MC-LR requires higher ozone and oxidant doses than extracellular, as it is consumed when the cell becomes damaged (Onstad et al., 2007). Low pressure membrane filtration can remove cyanobacterial cells (Gijsbertsen-Abrahamse et al., 2006). Ultrafiltration has been shown to release 2% of the cell-bound toxin (Gijsbertsen-Abrahamse et al., 2006).

2.3.2 Extracellular MC-LR Removal

Conventional water treatment, involving coagulation, filtration and sedimentation is not effective for the removal of extracellular (i.e. dissolved) toxin (Himberg, et al., 1989; Hoffmann, 1976).

Chlorine is effective for the removal of dissolved MC-LR through oxidation at pH values below 8 in order to achieve removal within typical contact times, as shown in Table 2.2. (Acero et. al., 2005). For example, Ho et al. (2006) found that 90% oxidation of MC-LR occurred in two natural waters with a 1.5 mg/L chlorine dose and a 30-minute contact time at DOC levels less than 5 mg/L. Chlorination of MC-LR is more effective at lower pH levels as seen in Table 2.2 (Acero et. al., 2005, Xagoraraki et al., 2006). Elevated levels of background NOM/DOC can consume free chlorine, potentially leaving the MC-LR un-oxidized if background levels are high enough or a sudden spike in DOC occurs (Acero et

al., 2005; Ho, et al., 2006; Nicholson et al., 1994; Xagoraraki et al., 2006). If ammonia is present in sufficient quantities it too can react with free chlorine to form monochloramine, which is a much less powerful oxidant that cannot oxidize MC-LR under typical drinking water treatment conditions (Acero et al., 2005).

Table 2.2 MC-LR half-life over pH range 6-9 (Acero et al., 2005)

pH	MC-LR Half Life (min)	
	Initial Chlorine Concentration 1 mg/L	Initial Chlorine Concentration 0.5 mg/L
6	6.2	12.4
6.5	7.3	14.6
7	8.9	17.8
7.5	13.2	26.4
8	24.7	49.4
8.5	49.1	98.2
9	81.1	162.2

Chlorine dioxide is effective for the oxidation of MC-LR only when the background NOM, and specifically fluvic and humic acids, levels are low (Kull et al, 2006). Only a 17% reduction was observed by Kull et al. (2006) when DOC was present at 5 mg/L with a contact time for 40 hours.

Potassium permanganate can be an effective oxidant for MC-LR but it is not commonly used to treat drinking water (Chen & Yeh, 2005; Rodríguez et al., 2007).

MC-LR is susceptible to ozonation as it is a strong oxidant, although as with other oxidants, there is competition from DOC/NOM (Fawell et al., 1993; Rositano et al., 2001).

Chloramines are not effective for the removal of MC-LR, due to their weaker oxidizing capacity (Nicholson et al., 1994).

Biological removal through sand filtration shows promise as a removal technique (DeVries et al., 2012). Biodegradation through a rapid sand filter has been shown to be effective for MC-LR, through the bacteria with the *mlrA* gene; in one study, a 3-day lag period was required for the biomass to adjust and remove MC-LR albeit the biomass might have been exposed to MC-LR in a previous study (Ho et al., 2006). GAC has also been investigated for biological removal, in addition to the removal by adsorption. Wood-based GAC picazine was studied by Ho and Newcombe, and it was determined that biological activity was occurring in the filter column by isolating the bacteria from the media, and conducting batch experiments to evaluate biological MC-LR removal; following an 8-day lag period removal was observed (Ho & Newcombe, 2007).

Physical removal by nanofiltration is effective for the removal of microcystin, with a 96% rejection rate (Gijsbertsen-Abrahamse et al., 2006). MC-LR removal was observed to be governed by steric hindrances, with limited impacts by changes in influent water make up (Ribau and Rosa, 2006).

Alternative removal methods have been considered for MC-LR. For example, MC-LR has been shown to undergo photocatalytic decomposition in the presence of titanium dioxide (Liu et al., 2009) while glow discharge plasma oxidation degraded MC-LR at the gas-liquid interphase (Zhang et al., 2012). However, these technologies are not currently in use for water treatment.

Activated carbon can either be in powdered (PAC) or granular (GAC) form. PAC is applied on an as-needed basis, and presents some operational challenges. GAC is typically located in contactors or used to top conventional filter beds. GAC is an engineered adsorbent, typically made from various base materials including wood, coal and coconut. Activation is completed in various proprietary methods to create a final product with a high volume of pore space intended to remove contaminants (such as MC-LR). The mass transfer mechanisms of removal are as follows (Worch, 2012):

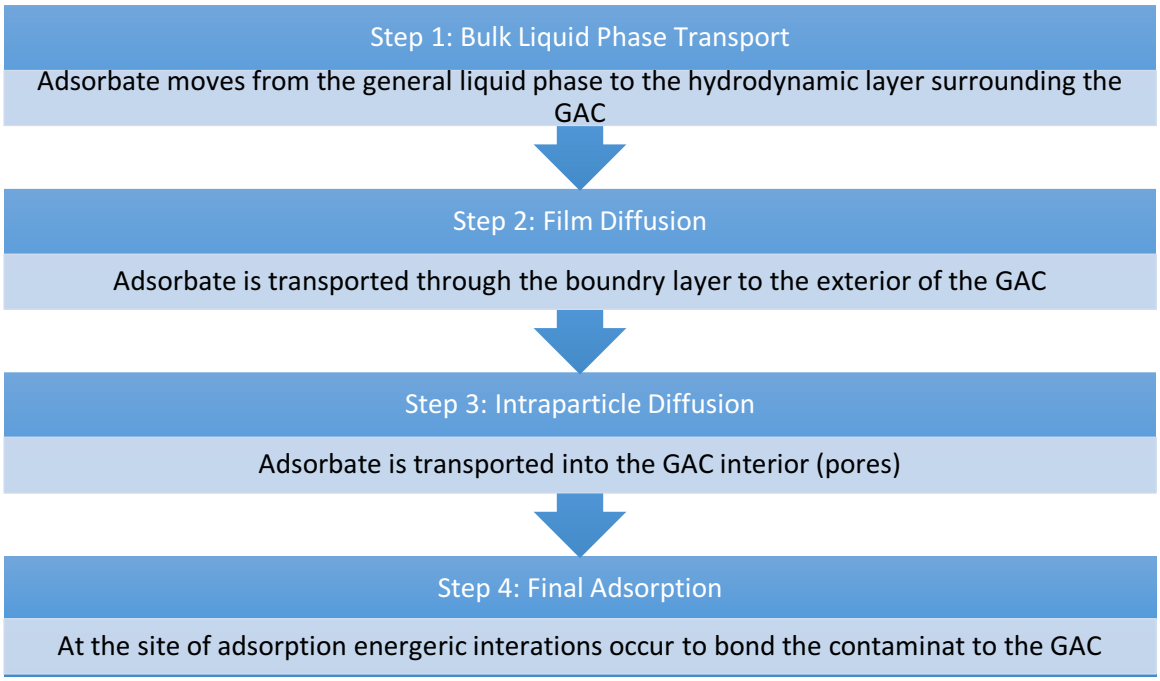

The kinetics of the reaction are typically limited by steps 2 and 3 (Worch, 2012).

Both PAC and GAC are effective for the removal of MC-LR in drinking water through adsorption (Falconer et al., 1989; Himberg et al., 1989; Hoffmann, 1976; Keijola et al., 1988). Falconer et al. (1989) examined blooms containing cyanobacteria, and determined that under lab and pilot plant conditions PAC and GAC were both able to remove the

toxins from drinking water. Himberg et al. (1989) examined common water treatment practices and found that GAC filtration and ozonation was effective for the removal of toxins. Hoffman (1976) also examined conventional water treatment practices, and found that processes with activated carbon were able to remove toxins below “active levels”. Keijola et al. (1988) further examined common water treatment practices, and found that processes including activated carbon filtration with ozonation were able to remove cyanotoxins, and that slow sand biological filtration showed promise as a treatment technology. Following these initial studies, various works have investigated MC-LR removal using activated carbon, and these are discussed in detail in Chapter 3. The operation of GAC contactors/filters on a seasonal basis remains uninvestigated, and may lead to the preservation of GAC for the targeted seasonal removal of MC-LR.

Although extracellular MC-LR can be removed by oxidation, it is a singular treatment and in combination with conventional treatment (coagulation, flocculation, sedimentation, and filtration), does not provide a multi-barrier approach. Should water quality vary significantly, and change the oxidant demand quickly, MC-LR removal may not be achieved. Implementation of an additional treatment process should be considered. Biological filtration, although effective, involves an acclimatization period, which could leave a water treatment plant vulnerable in the presence of sudden MC-LR occurrences. This makes biological filtration an effective solution in warm climates with year round blooms, such as experienced in Australia. Membrane processes, specifically nanofiltration, show promise for the removal of extracellular MC-LR on a seasonal basis as no acclimatization period is required; however, nanofiltration is expensive from an

energy standpoint, and involves frequent chemical cleaning and waste management. GAC contactors following conventional filtration, also show promise for the removal of MC-LR on a seasonal basis. GAC adsorption is non-specific, and therefore the storage of the media between seasonal occurrences may have some value; however, the storage conditions and capacity impacts remain uninvestigated.

2.4 Summary and Research Gaps

Cyanobacterial blooms may contain potent cyanotoxins, including the hepatotoxin MC-LR, a contaminant of concern in the Canadian Great Lakes region, impacting a valuable drinking water resource. With the acceleration of climate change and increasing anthropogenic driven nutrient loading, the removal of MC-LR from drinking water is a subject of concern for many municipalities. The current traditional water treatment process configuration does not provide a robust or multi-barrier approach to the removal of extracellular MC-LR. Activated carbon is an effective removal technology for MC-LR removal; however, it is non-specific and will become exhausted with continued exposure to background NOM during the MC-LR free portion of the year. The targeted and seasonal usage of GAC for the removal of MC-LR remains to be investigated.

3 Microcystin-LR Removal by Virgin and Preloaded GAC

3.1 Summary

The kinetics and equilibrium capacity of a coal based carbon for the cyanotoxin, MC-LR, were evaluated for both virgin and preloaded granular activated carbon (GAC). Filtrasorb 300 (F300) was selected as it is a common coal-based GAC used in the study geographic area. Filter effluent from a full-scale Lake Ontario drinking water treatment plant in Whitby, Region of Durham, ON was used to preload the GAC. The number of bed volumes passing through the full-scale filter during the portion of the year when cyanobacteria are present were determined. The selected GAC was preloaded with the equivalent number of bed volumes of post filtration water. Total organic carbon (TOC) breakthrough up to 75% was observed over the duration of the preloading. The surface charge of the GAC changed from positive to close to neutral upon preloading as indicated by a decrease in point (pH_{PZC}) of zero charge from 10.2 in the virgin carbon to 7.2 following preloading. The bottle point method was used to further examine the effects of preloading on the kinetics and equilibrium capacity of the F300 in ultrapure water. The virgin carbon reached equilibrium following 18 days, with up to 99% removal of MC-LR being observed. The preloaded F300 reached equilibrium much more slowly, taking more than twice the time compared to the virgin material (49 days), though up to 93% removal of MC-LR was observed. The Freundlich isotherm model was used to evaluate the equilibrium capacity of the F300; however, there was no statistically significant difference between the preloaded and virgin carbon parameters at the 95% confidence level as indicated by overlapping confidence joint confidence regions and parameter prediction intervals.

Under the conditions tested, one season of preloading of the F300 was not sufficient to alter the equilibrium capacity substantially but significant changes were observed in terms of the slowing of the preloaded F300 kinetics. Further consideration should be given to competition effects from background natural organic matter (NOM) in water to be treated by performing tests in a natural water matrix. In addition, preloading with NOM in the presence of the target adsorbate MC-LR should be evaluated to examine any possible desorption effects.

3.2 Introduction

3.2.1 Background

Microcystins are the most common and widely studied of the diverse group of cyanobacterial toxins (cyanotoxins). Microcystins are cyclic peptides; variants arise from the substitution of one of the seven amino acids that comprise the compound (Westrick et al., 2010). The molecular mass is approximately 1000 Da (Westrick et al., 2010). Of the approximately 80 known variants of microcystin, MC-LR is generally the most prevalent. MC-LR is a potent hepatotoxin, affecting the liver and kidneys. MC-LR can exist intracellularly in intact cells, or extracellularly when the cell wall ruptures and the toxin is released into the aqueous environment around the cell. Lysis may occur naturally upon cell death or when a cell is damaged by predation or other unfavorable environmental conditions.

The removal of intact cells may be achieved with conventional water treatment, comprised of coagulation, flocculation, sedimentation, and filtration (Cheng et al., 2015;

Gonzalez-Torres et al., 2014; Zamyadi et al., 2013). However, several studies have reported that conventional water treatment is only partially effective for the removal of extracellular MC-LR, and lacking in robustness (Himberg et al., 1989; Hoffmann, 1976; Lambert et al., 1996; Wheeler et al., 1942). Adsorption by activated carbon, in powdered form (PAC) has been shown to be effective for the removal of MC-LR (Falconer et al., 1989; Himberg et al., 1989; Hoffmann, 1976; Keijola et al., 1988). GAC has also been proven effective for the removal of extracellular MC-LR (Falconer et al., 1989; Himberg et al., 1989; Keijola et al., 1988).

GAC adsorbers are typically operated year-round, although blooms may not be present. Since GAC is non-specific, continual operation leads to preloading with background water constituents and natural organic matter (NOM) (Worch, 2012). This results in a loss of capacity for the removal of the target compound from adsorption. Some removal may still be achieved through biological activity, depending on the mode of filter operation (e.g. backwashing and pre-chlorination).

Adsorption kinetics are dictated by the mass transfer limitations of adsorption, and diffusion processes are typically rate limiting (Worch, 2012). When determining the limits of adsorption, it is important to consider the system once it has achieved equilibrium in order to prevent underestimating the capacity for removal (Randtke & Snoeyink, 1983). Crushing the GAC increases the rate of adsorption, and allows equilibrium to be achieved in a shorter time for virgin carbons (Randtke & Snoeyink, 1983). However, crushing the

GAC opens additional pores and overestimates removal for preloaded GAC (Carter et al., 1992; Gillogly et al., 1999; Knappe et al., 1999).

Various base materials exist for GAC, with a range of pore sizes, surface properties and intended applications. Common GAC base materials include wood, coal and coconut. Activation processes vary depending on the manufacturer, and are typically proprietary. For this work Filtrasorb (F300) was selected, as it is a commonly used coal-based GAC in the study geographic area. To data, there is insufficient information available on F300 adsorption of MC-LR.

Huang at al. (2007) examined the removal of MC-LR by coconut-, coal- and wood-based pulverized GAC; the wood-based GAC was more effective in terms of kinetics and isotherms. However, the MC-LR was prepared in methanol, which may have contributed to competition effects in adsorption (Huang et al., 2007). Kinetic studies were conducted over a 72 hour period and isotherm studies over a 24 hour period; there was no indication if equilibrium was reached or the criteria used to determine equilibrium (Huang et al., 2007). Mohamed et al. (1999) studied the removal of microcystin toxins by wood-, coal- and coconut-based PAC and GAC using an exposure period of only 7 days (without any consideration of equilibrium) and it is not clear how many toxin variants were present in the prepared toxin. They found that the wood-based GAC was the most favourable for the removal of microcystins, followed by the Calgon coal-based GAC F300. Zhang et al. (2011) examined isotherms on a custom-made adsorbent comprised of bamboo charcoal and chitosan and reported that it was effectively able to remove 80% of the MC-LR (5-50

μg/L) over a 6 hour exposure period. At present, there are no well documented isotherm studies available for MC-LR adsorption with non-crushed coal-based GAC.

Julio (2011) briefly evaluated the effect of preloading crushed Norit 0.8 Supra, an extruded peat-based GAC, with tannic acid, and found that the capacity of the GAC was reduced by an unqualified amount and the kinetics remained virtually unchanged (Julio, 2011). Ho and Newcombe (2007) compared virgin and preloaded wood-based GAC Picazine for the removal of MC-LR, and found that virgin carbon was able to adsorb approximately 30% more than preloaded GAC. There are no available studies on the direct comparison of virgin and pre-loaded coal based GAC for the removal of MC-LR.

3.2.2 Objectives

This study sought to establish the performance of virgin and pre-loaded coal based GAC namely F300 for the removal of MC-LR. The goal was to produce kinetic data for the removal of MC-LR via adsorption on uncrushed virgin and preloaded F300 GAC. This study modelled the removal kinetics using pseudo-first and –second order kinetic models to allow for a comparison.

Virgin and preloaded F300 capacities were compared in terms of equilibrium isotherms using the Freundlich isotherm equation. The isotherm parameters were compared at the 95% confidence level using joint confidence intervals.

3.2.3 Approach

The adsorption of MC-LR by virgin F300 was examined in term of isotherms and kinetics using the bottle point method.

The virgin F300 was preloaded at the Whitby Drinking Water Treatment Facility, Region of Durham, Ontario. The preloading setup was located following full-scale filtration. The volume passed through the filtration setup was dictated by the historical detection period of taste and odour compounds geosmin and 2-methylisoborneol (MIB); The historical record of taste and odour compounds greatly exceeded that of MC-LR. It should be noted that while cyanobacteria produce the taste and odour compounds geosmin and 2-methylisoborneol, in addition to cyanotoxins, there is no clear association between the presence of taste and odour compounds, and cyanotoxins. During preloading the influent water quality was monitored. Following preloading, the bottle point method was used to determine the kinetics and isotherms of the preloaded F300 for the removal of MC-LR.

The evaluation of isotherms and kinetics in ultrapure water allows for the comparison of virgin and preloaded GAC without consideration of competition from background water constituents and NOM. However, this approach is not representative of removal in natural water. The comparison of NOM preloaded and virgin carbon in terms of capacity and kinetics will evaluate how the NOM impacts target compound (MC-LR in this case) removal as adsorption sites are used and blocked during preloading. Since preloading was conducted in the detectable absence of the target compound, desorption was not a factor.

3.3 Materials and Methods

3.3.1 Materials

Calgon Filtrasorb® 300 (F300) was selected as it is a commonly used GAC in the geographic study region. It was provided at no cost by Calgon Carbon (PA, USA). MC-LR was obtained from Cedarlane (ON, CAN) as a solid. Cyclo [Arg-Ala-D-Phe-Val] was used as an internal standard and was obtained from Cayman Chemicals also as a solid (MI, USA). HPLC grade acetonitrile and formic acid were obtained from Sigma-Aldrich (WI, USA). A Millipore Milli-Q® PLUS (MA, USA) water system was used to produce the ultra-pure water for solution preparation and to conduct one set of bottle point tests.

Stock solutions were prepared by dissolving 1 mg of MC-LR in 10 mL of ultrapure water. Fresh stock solutions were prepared for each batch of isotherms. Working solutions were prepared monthly. All solutions were stored in the dark at – 20°C in glass vials.

3.3.2 Carbon Pre-loading

Virgin F300 was washed in ultrapure water to remove fines, until the water ran clear. It was then dried at 110°C for 24 h, cooled in a desiccator and stored in an airtight bottle to ensure the dry weight of the GAC could be measured (Sontheimer et. al., 1988; Worch, 2012). Virgin F300 was preloaded with approximately 20,000 bed volumes of post filtration Lake Ontario water. The preloading setup consisted of 6 preloading columns (2.5 cm internal diameter 60 cm in height). Each column was filled to capacity, resulting in the depth of the GAC being 60 cm. The influent flow to each column was controlled with a

flowmeter. The preloading columns were operated in up-flow mode at a hydraulic loading of 12 m/h. Figure 3.1 and Figure 3.2 show the preloading setup.

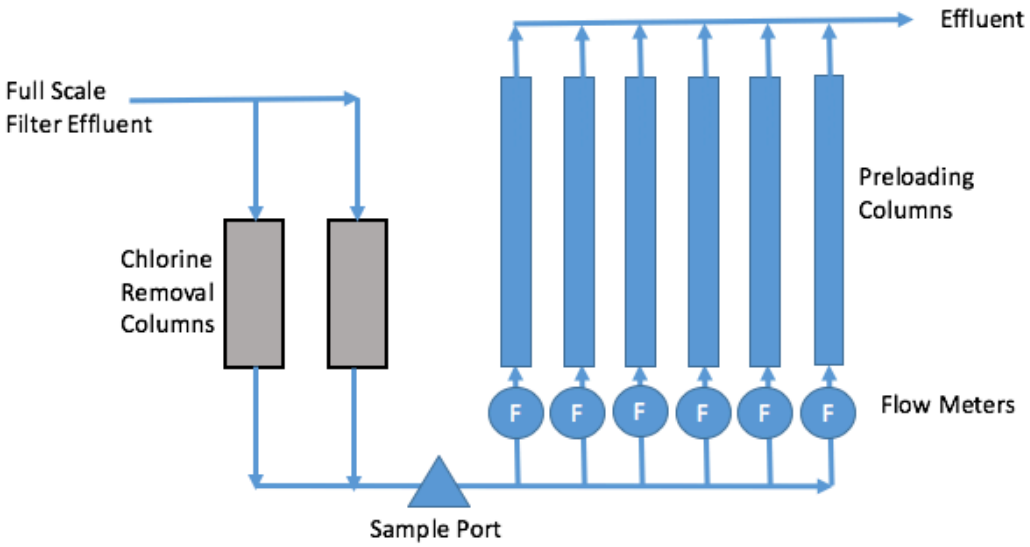

Figure 3.1 Preloading schematic showing chlorine removal columns and preloading columns.

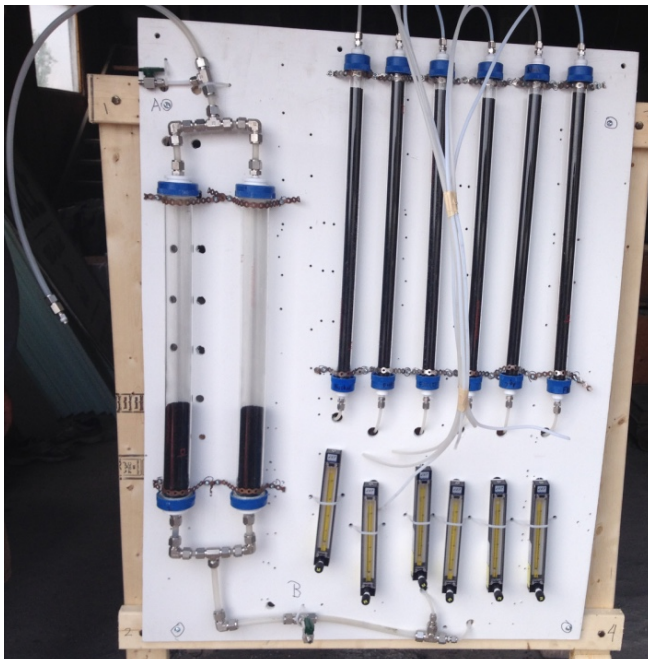

Figure 3.2 Preloading Setup photo.

The drinking water treatment facility pre-chlorinates at the entrance to the raw water intake pipe to control zebra mussels and this residual can carry through into the full-scale plant filter effluent. To avoid having chlorine reaching the preloading column, a 5 cm ID x 60 cm high chlorine removal column containing 30 cm of F300 GAC was used to dechlorinate the water. The chlorine removal column GAC depth was sized based on the iodine number relationship examined by McMlure and Megonnell (2001); the iodine number of F300 is at least 900 (Calgon Carbon, 2012), and for a bituminous coal carbon (similar product) with an iodine number of 1056 a contact time of 33.2 seconds was required to reduce the 3 mg/L free chlorine to 0.1 mg/L. The iodine number examined by McMlure and Megonnell (2001) is conservative for this application, and therefore a safety factor of 3 was applied. Some loss of GAC and compression occurred over time but free chlorine was never detected downstream of the chlorine removal columns during weekly water quality monitoring. The hydraulic loading rate in the experimental preloading setup was 12 m/h.

TOC, DOC, and NOM (as measured by LC-OCD) were monitored in the preloading setup at the influent to the setup, in the effluent of the chlorine removal columns, and in the combined effluent following the preloading columns.

3.3.3 Carbon Surface Charge Analysis

The point of zero charge (pH_{PZC}), the pH where the carbon surface charge is neutral, was determined as by Summers (1986). The initial pH (pHi) of six 40 mL vials containing 20 mL of 0.1N sodium chloride solution was adjusted to increments between 2 and 12 using 0.1

M hydrochloric and/or 0.1 M sodium hydroxide. A 100 mg mass of F300 was then added, and the vials were capped securely. The vials were placed on an orbital shaker for 24 hours at 150 RPM. The final pH (pHf) of the solutions was then measured. The pHPZC was determined by plotting the pHi against the pHf and determining the point at which the pH did not change (the intersection of the plotted data with a line of slope 1).

3.3.4 TOC and DOC Analysis

TOC and DOC analysis was performed as per Standard Methods for the Examination of Water and Wastewater, Method 5310D, for the wet oxidation method. Samples for DOC were filtered through 0.45 μm hydrophilic polyethersulfone filters.

Calibration and stock standards were prepared monthly. A blank was run with each set of samples, or on a 10% basis (whichever was more). In addition, a mid-range calibration standard was run with each set or on a 10% basis (whichever was more).

3.3.5 NOM Analysis by LC-OCD

Liquid chromatography – organic carbon detection (LC-OCD) analysis was completed as per Huber et al. (2011) to determine the NOM fractions in influent and in the combined effluent samples of the preloading columns. Samples were filtered through 0.45 μm hydrophilic polyethersulfone membranes prior to injection into the instrument.

3.3.6 Kinetic and Isotherm Sample Preparation and Handling

The bottle point method was used to evaluate the capacity and kinetics of MC-LR removal by adsorption on F300, as described in Droste (1997). The virgin F300 was washed in ultrapure water to remove fines, until the water ran clear. It was then dried at 110°C for

24 h, cooled in a desiccator and stored in an airtight bottle to ensure the dry weight of the GAC could be measured (Sontheimer et al., 1988; Worch, 2012). The preloaded carbon was removed from the preloading setup, mixed completely, and freeze dried similar to Andrews (1990), and stored in a desiccator prior to use.

Ultrapure water was collected and autoclaved prior to being allowed to sit out overnight (covered in foil) with no pH adjustment (final pH= 6.9). The TOC of the water was 0.3 mg-C/L. A solution of 9.5 L with a nominal concentration of 100 μg/L MC-LR solution was prepared by spiking 9.5 mL of a 100 mg/L MC-LR stock solution into 9.5 L ultrapure water. The actual concentration of the prepared solution was measured and determined to be 119 μg/L. A volumetric flask was used to measure 500 mL of 100 μg/L solution into individual bottles, to which the appropriate amount of F300 was added. Uncrushed F300 was used in a range of 10-65 mg/L. A positive control, initial MC-LR concentration 119 μg/L, was included to monitor for any toxin degradation (i.e. no GAC added). Following the 52 day study period, the positive control showed a 7.5% decrease. Two negative controls (no MC-LR added), one containing 50 mg/L of virgin F300, and one containing 50 mg/L preloaded F300, were included to account for any background material which may be misidentified as MC-LR.

Samples and controls were placed on orbital shakers at 150 RPM at room temperature and covered to reduce light exposure. Monitoring of the MC-LR concentration was completed by removing 1 mL per bottle for analysis. All bottles were sampled daily for the first 10 days, and every other day following, until less than a 1% change in percent

removal was observed. The lowest (10 mg/L), middle (30 mg/L) and highest (65 mg/L) carbon doses were analyzed to monitor for kinetic changes; all bottles were sampled in order to preserve the volume to carbon mass ratio. At equilibrium, the bottles were removed, and the isotherm analysis completed.

Adsorption isotherms were used to evaluate the ultimate capacity of the GAC for adsorbate MC-LR at equilibrium conditions. The bottle point method is commonly used to evaluate adsorption isotherms; various masses of GAC are added to a known concentration and volume of adsorbate and allowed to reach equilibrium. Analysis is then conducted at a constant temperature using equation 1.

$$V(C_0 - C) = M\ (q_e - q_i) \quad \text{.....(1)}$$

Where V is the volume of the aqueous solution, C_0 is the initial concentration of adsorbate, C is the equilibrium concentration of adsorbate, M is the mass of GAC added to the bottle, q_e is the equilibrium solid phase concentration and q_i is the initial solid phase concentration (typically 0) (Crittenden et al., 2012; Droste, 1997; Sontheimer et al., 1988; Worch, 2012). A commonly used model for GAC adsorption isotherms is the Freundlich isotherm (equation 2), where K_F and 1/n are constants (Freundlich, 1926).

$$q_e = K_F C^{\frac{1}{n}} \quad \text{.....(2)}$$

Where K_F is the adsorption coefficient and n is a measure of the energy diversity of the GAC surface (Worch, 2012).

3.3.7 Microcystin–LR Analysis by LC-MS/MS

MC-LR concentrations were quantified by LC-MS/MS (liquid chromatography tandem mass spectrometry) using a Shimadzu 8030 system equipped with a Shimadzu DGU-20A3R degassing unit, a Shimadzu LC-20 ADXR pump with 100 μL mixing loop and a prominence auto-sampler (SIL-20AC XR).

A Pinnacle DB C18 analytical column (50 mm x 2.1 mm internal diameter) with 1.9 μm packing was used (Restek, PA, USA). A TridentTM in-line guard cartridge holder and Pinnacle DB C18 (10x 2.1 mm with 5 μm packing) guard cartridge was used to protect the analytical column. The analytical column temperature was kept at 35 °C.

Cyclo [Arg-Ala-D-Phe-Val] was used as an internal standard at a concentration of 50 μg/L and a spiking volume of 100 μL per 1 mL sample, based on the investigation by Vlad (2015).

The LC-MS/MS analysis used a gradient, as shown in Table 3.1. Both mobile phases A and B (Milli-Q water and HPLC grade acetonitrile respectively) contained 0.1% formic acid for peak stability. The injection volume was 15 μL. Low (0.5-10 μg/L) and high (10-200 μg/L) range internal calibration curves were established. The method detection limit was established as 0.1 μg/L as per Standard Methods for the Examination of Water and Wastewater, Method 1020B.4, using seven injections of the lowest calibration point of 0.5 μg/L (Standard Methods, 2012). At a concentration of 1 μg/L, seven replicate injections yielded a concentration of 1.05 μg/L with a standard deviation of 0.02, or a

relative standard deviation of 2%. See appendix A for calibration examples and additional QA/QC data.

Table 3.1. Mobile Phase Gradient

Time	% Acetonitrile Concentration
0-1 mins	Hold at 20%
1-2 mins	Increase to 80%
2-5 mins	Hold at 80%
5-6 mins	Increase to 100%
6-10 mins	Hold at 100%
10-11 mins	Decrease to 20%
11-15 mins	Hold at 20%

3.4 Results and Discussion

3.4.1 Carbon Preloading

During the preloading phase the TOC was monitored in the influent to the chlorine removal column, the effluent of the chlorine removal column (i.e. influent to the preloading columns), and the combined effluent of the preloading columns. The chlorine removal column experienced TOC breakthrough almost immediately, and was 82% exhausted after only 2 weeks of operation. The preloading columns reached 75% TOC breakthrough at the end of the 7-week preloading period. Figure 3.3 shows the TOC results from the preloading period. Two samples were taken at each sampling location, and three TOC injections were completed for a total of 6 measurements per point.

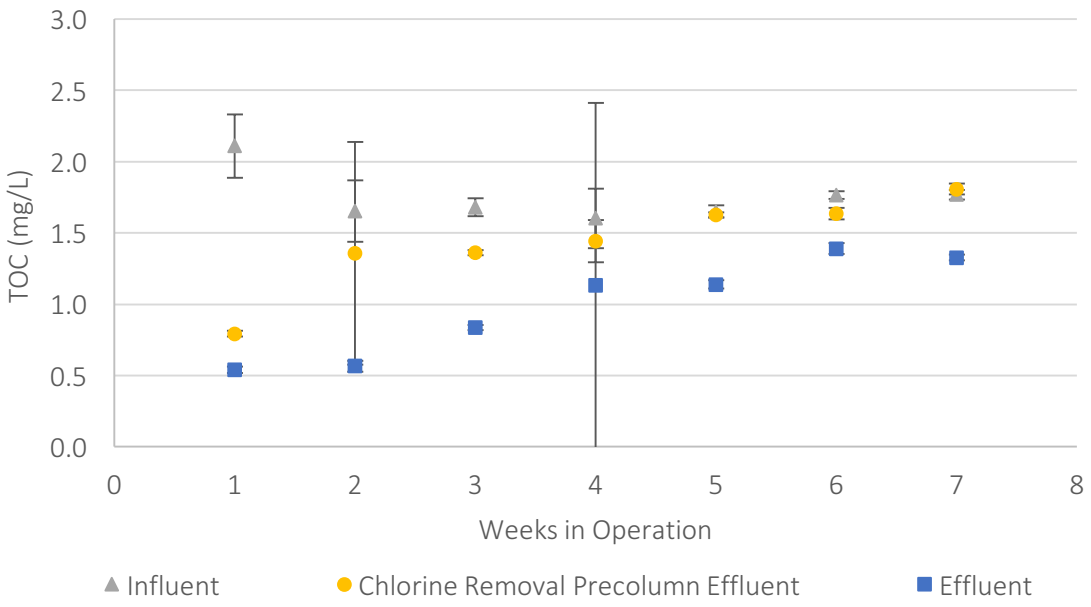

Figure 3.3. TOC profile during GAC preloading with post filtration water (n = 6). Error bars relate to duplicate samples with 3 injections each for a total of 6 measurements per point.

The chlorine removal column experienced complete DOC breakthrough following 4 weeks of operation. The preloading columns reached 73% TOC breakthrough at the end of the 7-week preloading period. Figure 3.4 shows the DOC results from the preloading period. Two samples were taken at each sampling location, and three DOC injections were completed for a total of 6 measurements per point.

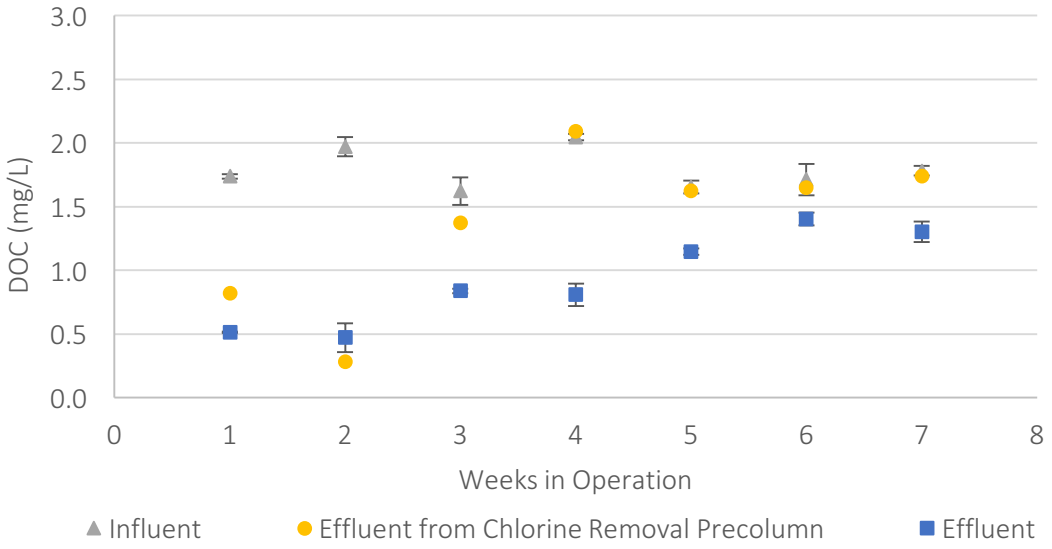

Figure 3.4 DOC profile during GAC preloading with post filtration water (n = 6). Error bars relate to duplicate samples with 3 injections each for a total of 6 measurements per point.

The largest fraction of the setup influent NOM, as determined by LC-OCD, was humics, as shown in Figure 3.5. Following the 6-week preloading period, approximately 70% humics breakthrough was observed, as shown in Figure 3.6.

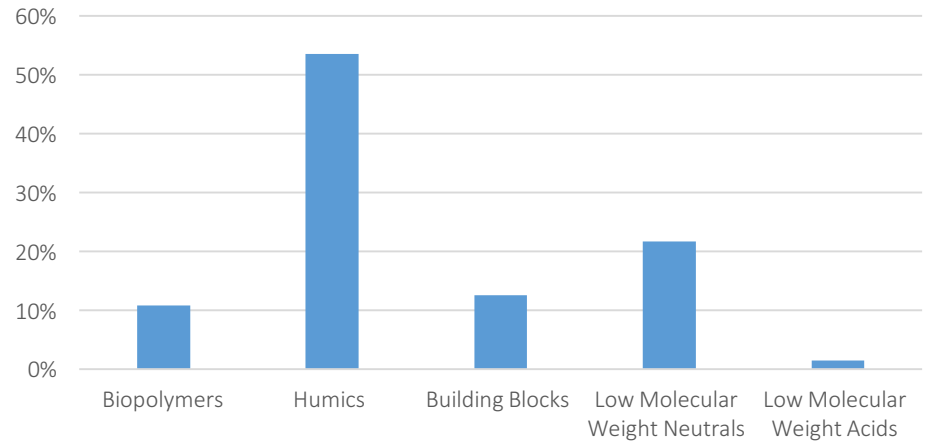

Figure 3.5 NOM Fractionation by LC-OCD of Influent to Preloading Setup (n=7)

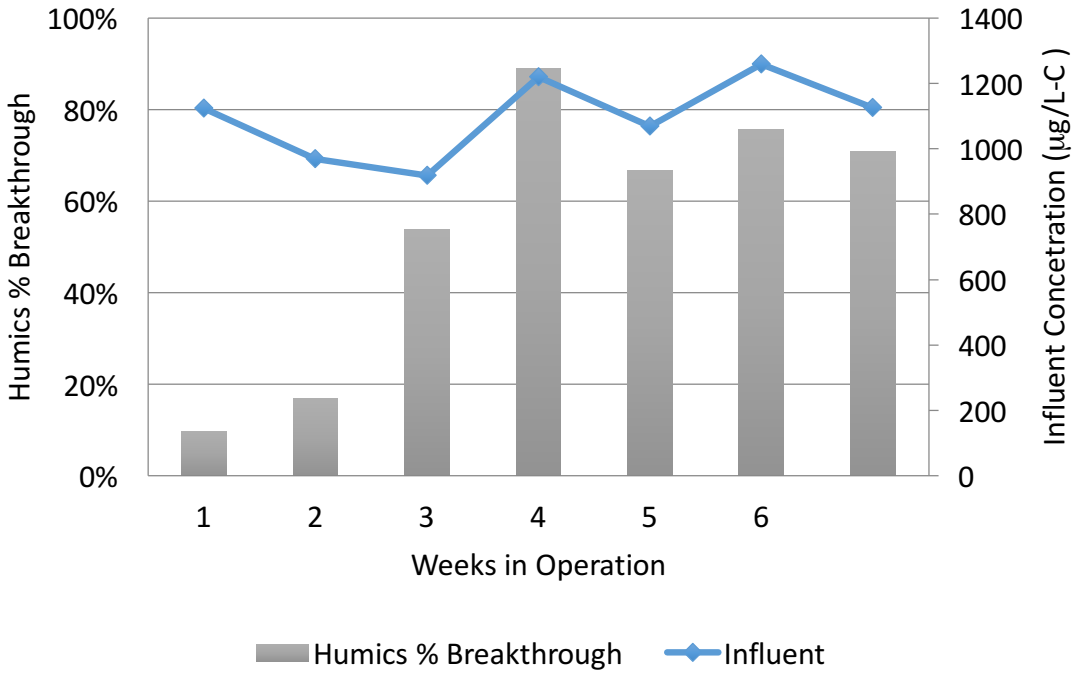

Figure 3.6 Humics Removal during Preloading Between Influent to Preloading Setup and Final Combined Effluent (n=1)

3.4.2 Carbon Characteristics

F300, a coal-based carbon, is predominantly microporous. Table 3.2 shows the virgin F300 parameters.

Table 3.2 F300 Parameters

Parameter		Value	Reference
Manufacturer		F300	(Calgon Carbon, 2012)
Base Material		Coal	
Activation Method		Steam	
Effective Size (mm)		0.80-1.00	
Apparent Density (g/cm^3)		0.56	
pH_{PZC}		10.2	This work
BET Surface Area (m^2/g)		1057	(Vlad, 2015) citing (Quantachrome, 2013)
DFT Method Pore Volume (cm^3/g)		0.551	
DFT Pore Size Distribution	Primary micropores <0.8 nm (cm^3/g)	0.23	
	Secondary micropores 0.8-2 nm (cm^3/g)	0.19	
	Mesopores (cm^3/g)	0.14	
% of pore volume in micropores		74%	

The virgin F300 pH_{PZC} 10.2. Following preloading, the pH_{PZC} was 7.2. This indicates a change from a positive to an essentially neutral carbon surface charge following preloading and was likely caused by the adsorption of predominantly negatively charged NOM during preloading. This finding is similar to that observed by Vlad (2015) who used treated Grand River water for preloading.

3.4.3 Kinetics

Kinetic studies were conducted on the virgin and preloaded F300 at three carbon doses with an initial MC-LR concentration of 100 μg/L. Based on the criteria established in section 3.3.6 the virgin F300 reached equilibrium at 18 days and the preloaded F300 reached equilibrium at 49 days. As shown by the data in Appendix D, at a 65 mg/L F300 dose the virgin carbon was able to remove 99% of the MC-LR. The preloaded F300 capacity at the 67 mg/L dose decreased by 6 percentage points to 93% removal. As is typically the case with such adsorption studies, the virgin carbon was able to remove MC-LR more quickly and had a higher equilibrium capacity. The small difference in apparent equilibrium capacity between the virgin and preloaded carbons is surprising. Biological activity may be an explanation for this small difference; however, the positive controls (containing MC-LR and no F300) did not experience any degradation over time. Biological activity could be occurring on the F300 during the isotherm analysis.

For both virgin and preloaded carbons, the observed kinetic trend was poor at the lowest carbon dose investigated. This may indicate that the experimental and analytical errors may have more impact on the removal observed at these low doses, as the changes in concentration over time are not as pronounced. Limited removal was observed initially, and therefore the results were sensitive to equipment fluctuations.

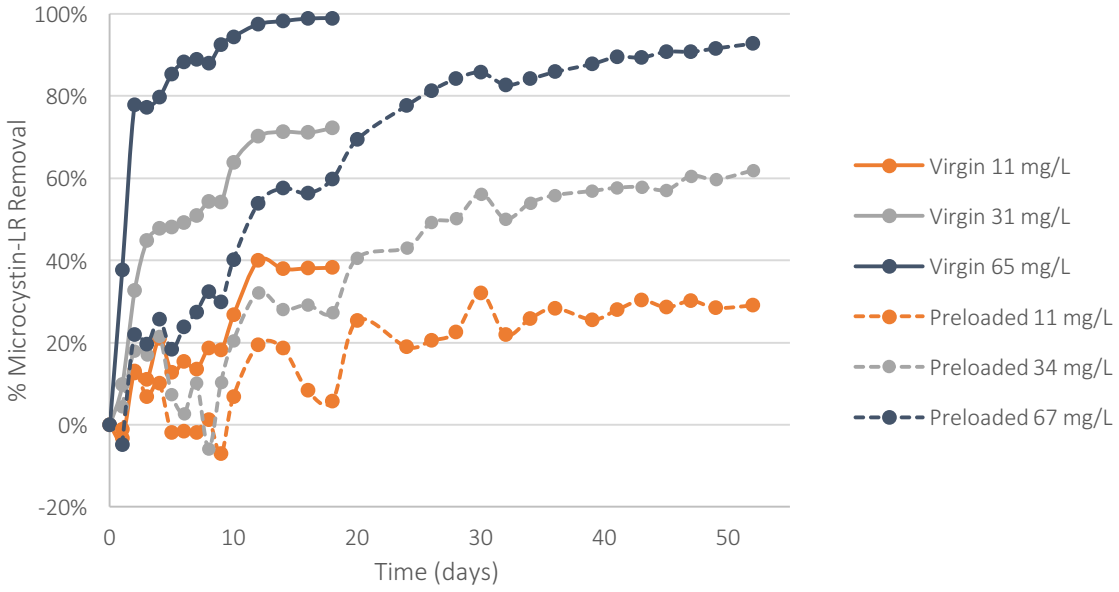

Figure 3.7. MC-LR removal over time for the highest, middle and lowest GAC dose

Adsorption kinetics can be examined using simple chemical reaction kinetics rate laws. Lagergren developed a pseudo-first order rate law, which has commonly been applied to a wide range of adsorbents (Lagergren, 1898).

$$\frac{dq}{dt} = k_1(q_{eq} - q_t) \quad \text{.....(3)}$$

Where qt is the solid phase concentration (μg/mg) at time t (days). The first order rate constant is k_1 ($days^{-1}$). The final (equilibrium) solid phase concentration is given by q_{eq}. This equation can be integrated to provide the following form of the equation (Ho & McKay, 1999; Lagergren, 1898). The equation could be transformed to the linear form, however this distorts the variance and structure of the data and prevents comparison between models.

$$q_t = q_{eq}(1 - e^{-kt}) \quad \text{.....(4)}$$

Pseudo-second order kinetics have also been shown to describe adsorption well (Ho & McKay, 1999).

$$\frac{dq}{dt} = k_2\left(q_{eq} - q_t\right)^2 \quad \text{.....(5)}$$

Where k_2 (mg/μg/days) is the second order rate constant. This equation can be integrated and becomes;

$$q_t = \frac{q_{eq}^2 kt}{1+q_{eq}kt} \quad \text{.....(6)}$$

In order to determine the pseudo-first and –second order rate constants, non-linear regression is required and was completed using least sum of squares. The equilibrium concentration was taken as predictive. The starting parameter values (required in nonlinear least sum of squares) for q_{eq}, k_1 and k_2 were obtained from a preliminary linear regression analysis and visually from Figure 3.7.

Both the pseudo-first and -second order kinetic models were investigated for MC-LR removal by virgin and preloaded F300 (Table 3.3 and Table 3.4). Both models appear to have similar data quality in terms of the Sum of Squares of Error (SSE). It is evident from the SSE that the lowest carbon doses have the poorest data quality (highest SSE), and as the carbon dose increases the data quality improves. This is likely due to the experimental variability when lower removal over time was observed initially at the lower doses.

Table 3.3. Pseudo-First Order Regression Analysis

	GAC (mg/L)	*k_1 ($days^{-1}$)*	*q_e observed (μg MC-LR /mg GAC)*	*q_e predicted (μg MC-LR /mg GAC)*	*SSE*
Virgin	11.0	5.13E-02	3.87	6.88	3.65
	31.2	2.45E-01	2.55	2.48	0.43
	65.0	6.24E-01	1.71	1.63	0.10
Preloaded	11.4	1.83E-02	2.82	5.13	9.95
	34.4	2.90E-02	2.02	2.71	1.58
	67.0	5.55E-02	1.49	1.61	0.17

Table 3.4 Pseudo-Second Order Regression Analysis

	GAC (mg/L)	*k_2 (mg/μg/days)*	*q_e observed (μg MC-LR /mg GAC)*	*q_e predicted (μg MC-LR /mg GAC)*	*SSE*
Virgin	11.0	2.80E-03	3.87	11.39	3.65
	31.2	8.44E-02	2.55	3.08	0.31
	65.0	4.82E-01	1.71	1.82	0.07
Preloaded	11.4	1.12E-03	2.82	9.15	10.01
	34.4	4.29E-03	2.02	4.34	1.62
	67.0	2.02E-02	1.49	2.23	0.20

Generally, the virgin F300 MC-LR removal kinetics were marginally better predicted by the pseudo-second order model when considering the SSE. The preloaded MC-LR removal kinetics were marginally better predicted by the pseudo-first order model. This may indicate that the presence of NOM on the carbon alters the reaction kinetics due to the interference or depletion of adsorption sites.

The pseudo-first order model best predicted the equilibrium solid phase concentration observed experimentally for both carbons; it should be noted that the observed

equilibrium solid phase concentration may not be the ultimate equilibrium solid phase concentration due to the criteria used to establish experimental equilibrium (described in section 3.3.6).

In order to examine the data fit visually and any sub-trends in the data the graphical results were plotted, and the residuals examined (Figure 3.8). The virgin F300 shows a sub-trend for the lowest F300 dose from 10 to 18 days, where a distinct plateau was observed. This may be a function of the poor data quality generally observed at the low F300 dose. Both the preloaded and the virgin F300 removal kinetics graphically showed higher variability at the lowest F300 dose, which has been attributed to experimental variability.

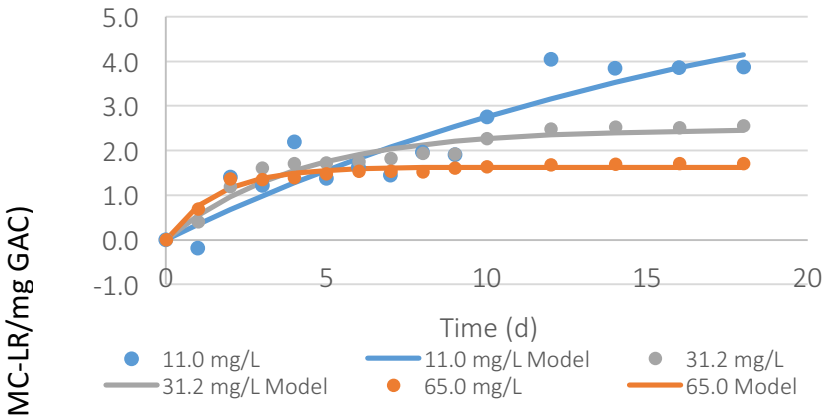

Figure 3.8 a. First Order Kinetics for MC-LR Removal by Virgin F300

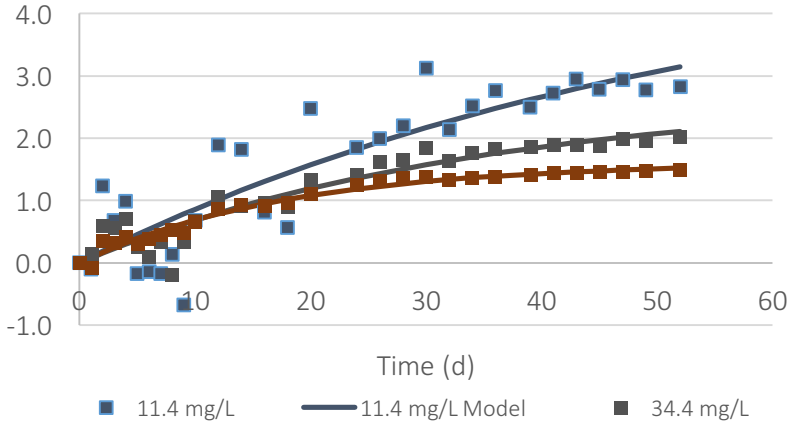

Figure 3.8b. First Order Kinetics for MC-LR Removal by Preloaded F300

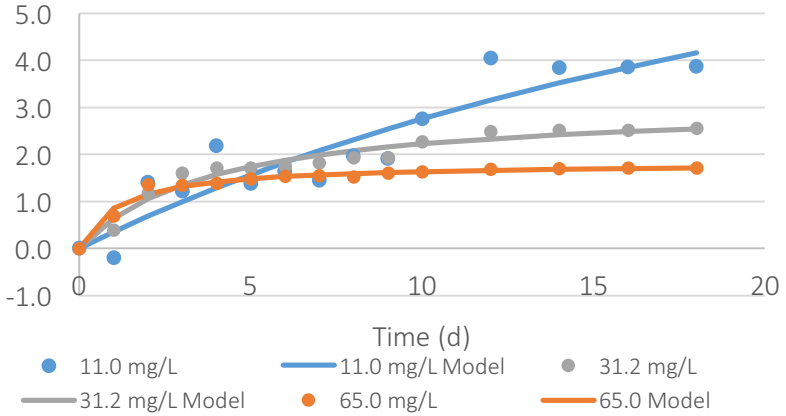

Figure 3.8c. Second Order Kinetics for MC-LR Removal by Virgin F300

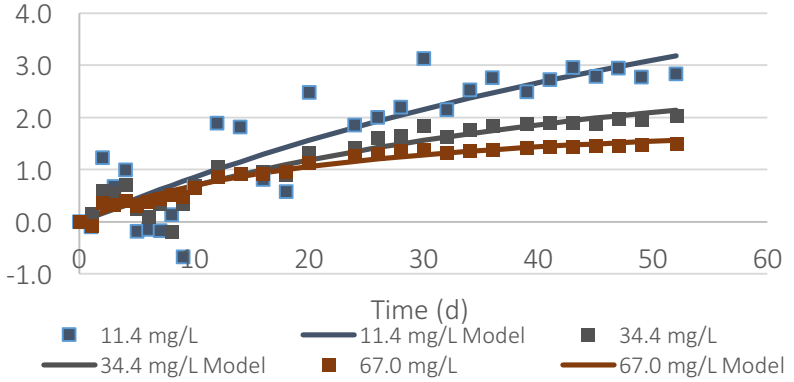

Figure 3.8d Second Order Kinetics for MC-LR Removal by Preloaded F300

Figure 3.8 Virgin and Preloaded F300 Kinetics

The fitted parameters of both models show improved kinetics for the virgin F300 which indicates that the virgin carbon will adsorb MC-LR more quickly than the preloaded carbon, with either model applied. This is supported by the observed shorter equilibrium time of the virgin carbon as compared to the preloaded carbon. The data quality (and rate constants) fit poorly at the low GAC doses; the data quality improves with increasing GAC dose.

The higher carbon doses show higher rate constants for both models. This indicates that faster MC-LR removal kinetics are achieved with higher F300 doses. This is supported by the experimentally observed results in Figure 3.8.

It should be noted that these reaction kinetic models are empirical in nature; they allow for little comparison to other systems or between models (Worch, 2012).

Although a rigorous analysis would include calculating Joint Confidence Regions (JCRs) for both models (since two parameters are being estimated), it was not considered necessary in this case, because of the generally appreciable differences between the virgin and preloaded carbon.

3.4.4 Isotherms

In order to further compare how preloading of F300 affects the adsorption of MC-LR, isotherm studies were conducted using the bottle point technique (Crittenden et al., 2012; Worch, 2012). These studies are useful in comparing between carbons, as they provide insight into the equilibrium adsorbent capacity and allow for a direct comparison

between carbons. Figure 3.9 shows the isotherm data and model fit results. One data point (circled in red) was considered to be an outlier based on visual examination and was removed from the data set following examination of the residuals data presented in Appendix C. Both the data set with and without the outlier were considered. Table 3.5 shows the modelled Freundlich isotherm parameters, as determined by non-linear regression using least-squares. Linear regression is not valid in this case, as the assumption that the residuals are normally distributed following linearization does not hold (Crittenden et al., 2012; Worch, 2012). The SEE is a better representation of the degree of model fit to the data given the non-linear regression used in this case.

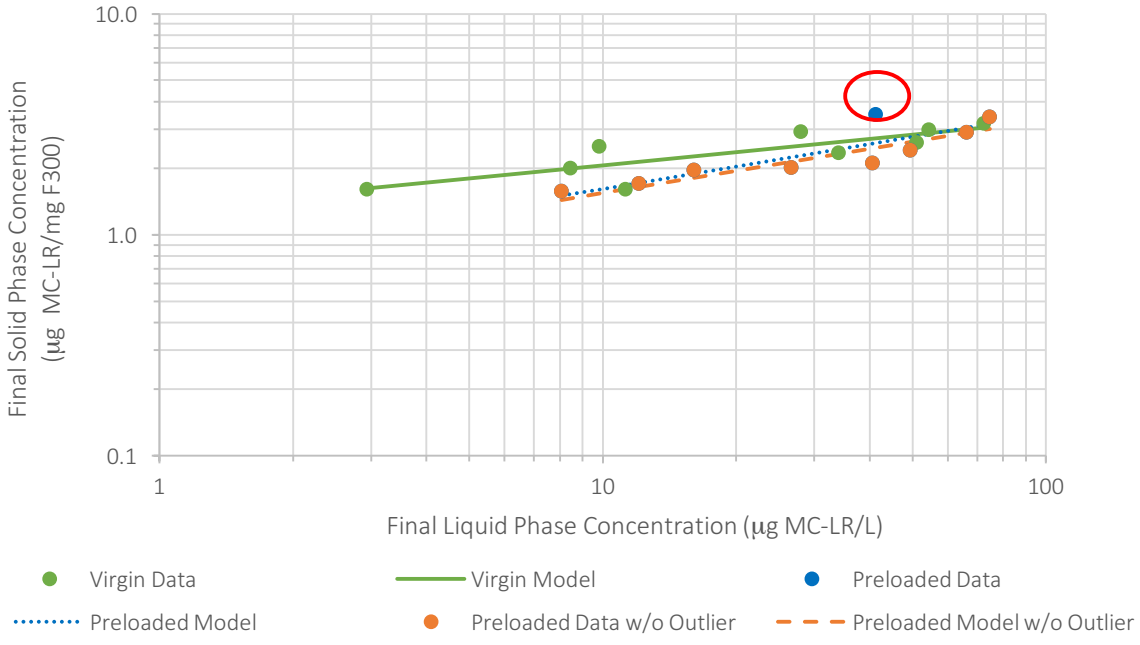

Figure 3.9. Preloaded and Virgin F300 Isotherms for MC-LR

Table 3.5. Freundlich isotherm parameters for the adsorption of MC-LR on virgin and preloaded F300 in ultrapure water including 95% confidence intervals

Carbon	K_f (μg MC-LR/mg GAC)(μg MC-LR/L)$^{-1/n}$	1/n	SSE
Virgin F300	1.29 *(0.63-2.08)*	0.20 *(0.07-0.38)*	0.782
Preloaded F300	0.78 *(-0.01-1.62)*	0.32 *(0.15-0.78)*	1.287
Preloaded F300 w/o outlier	0.81 *(0.23-1.25)*	0.30 *(0.20-0.58)*	0.375

Plots of the residuals for each of the isotherms are shown in Appendix C. As is evident, there is no trend in residuals. The preloaded F300 isotherm does show the outlier clearly as an abnormal residual.

The Freundlich isotherm modelling parameters, K_F (adsorption coefficient) and 1/n (related to the curvature) are very closely related. K_F indicates the degree of adsorption that can be achieved, and higher values of K_F result in higher removals for the same 1/n values (Worch, 2012). The slope of the isotherm curve (on a log-log plot) relates to the 1/n parameter. Unlike K_F, no general statements about 1/n and adsorption quality can be made; at low concentration ranges 1/n values less than 1 show higher loading and are typically considered favourable (Worch, 2012). Since any changes in K_F directly impact 1/n, joint confidence regions, shown in figure Figure 3.10 were considered in place of the more common one-at-a-time confidence intervals (Yu, 2007). Joint confidence regions determine a space over which the two related parameters would fall, at the specified confidence level; where regions intersect it can be inferred that the parameters may not

be different at the selected confidence level. This was done using MATLAB in conjunction with code completed as per Yu (2007).

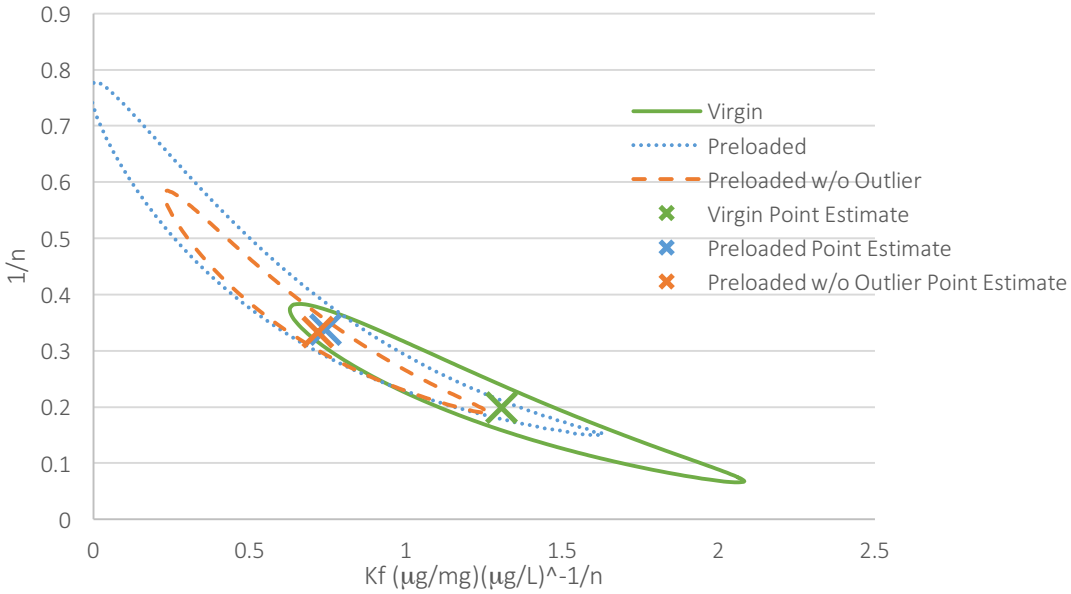

Figure 3.10. 95% Joint Confidence Regions for Freundlich Parameters

The virgin F300 has a higher K_F and a shallower slope (lower 1/n) than the preloaded F300. However, this finding is not significant at the 95% confidence interval since the banana-shaped ellipses of the joint confidence regions overlap. This means that the differences in the predicted values for each of the two parameters cannot be considered independently. Although individual confidence intervals provide only an indication in such situations, they are relatively wide here. From Figure 3.9, this can be seen to be due to both the relatively small number of data points and the considerable scatter in the data.

As an overall statement it could be said, based on the parameters for the Freundlich equation, that there is not a statistically significant difference between the virgin and

preloaded F300. However, this statement must be interpreted with caution, as differences may exist that cannot be detected at this level of confidence, given the data quality and experimental variability. The poor data quality affects the confidence regions by widening the regions where the parameters may exist. Table 3.6 shows estimated equilibrium solid phase MC-LR concentration for three target MC-LR liquid phase concentrations. As is evident from the overlapping confidence intervals on the predictions shown in Table 3.6, and Figure 3.11, these estimates are not significantly different at the 95% confidence level. Statistical method details are presented in Appendix E. There is indication, by the size of the joint confidence regions for the parameters, that differences may exist in the parameters which may be detected with improved data quality (which is to say tighter confidence regions).

Table 3.6 MC-LR predicted final solid phase concentration using various final aqueous concentrations (C) with 95% prediction intervals shown in brackets

Carbon	**C= 1 µg MC-LR/L**	**C = 10 µg MC-LR/L**	**C = 100 µg MC-LR/L**
	q_e (µg MC-LR/mg GAC)		
Virgin	1.31 *(0.26-2.36)*	2.06 *(0.81-3.32)*	3.26 *(1.59-4.93)*
Preloaded	0.74 *(-0.47-1.96)*	1.61 *(0.15-3.08)*	3.51 *(1.19-5.83)*
Preloaded w/o Outlier	0.72 *(-0.01-1.50)*	1.55 *(0.70-2.53)*	3.33 *(2.07-4.95)*

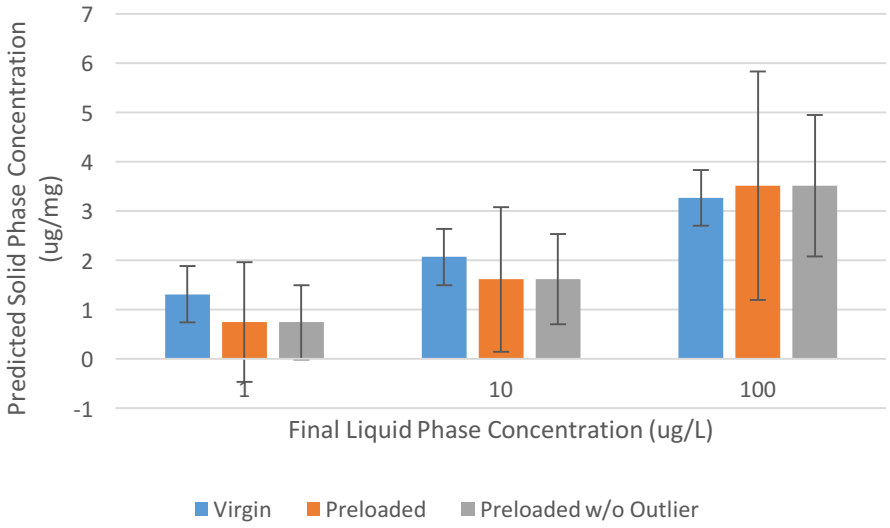

Figure 3.11 MC-LR predicted final solid phase concentration prediction using various final aqueous concentrations with 95% prediction intervals

The literature is very sparse in terms of similar isotherm studies on coal-based virgin carbon. Figure 3.12 presents a summary of similar isotherm studies on various carbons. Table 3.7 shows a comparison of virgin carbons from this work and others. Mohamed et al. (1999) completed an isotherm study using F300 (12x30 mesh) and a range of other carbons; in that study, multiple and unknown variants of microcystin were extracted from two species of cyanobacteria. The ELISA method was used to quantify the concentration, and since the ELISA method is generally considered a semi-quantitative method there are some concerns regarding its accuracy that will not be discussed in detail here. In addition, it's not clear how the approximately 80 variants of microcystin might interfere and if the ELISA method would capture all of these variants. However, the experiment time was only 7 days and there are no data presented to assure that equilibrium was achieved within 7 days. Based on the results obtained as part of this work, the experiment time would not

have been long enough for equilibrium to have been reached and hence, the study by Mohamed et al. (1999) likely underestimated the MC-LR removal compared to this thesis (i.e. shows lower capacity as evident from Figure 3.12) for the coal-based F300 and likely also for the other carbons investigated. All carbons examined by Mohamed et al. (1999) are shown in Figure 3.12 for comparison. Also presented in the literature is a study on a custom made mixed adsorbent made from bamboo charcoal and chitosan; it was not clear what the grain size was for this product, and only a 6-8 hour equilibrium time was required (as shown by the kinetic results presented in their paper) (Zhang et al., 2011). This bamboo product appears to be potentially superior to the F300 examined in this work, as shown by its high capacity for MC-LR in Figure 3.12. However, without statistical analysis (which was not provided by those authors) this difference cannot be confirmed to be significant.

Studies that compare virgin and preloaded GAC for MC-LR removal are even scarcer; Figure 3.13 shows a summary of the available studies compared with this work. Ho and Newcombe (2007) examined virgin and preloaded Picazine for the removal of MC-LR and determined that virgin was better able to remove MC-LR, due to the prior adsorption of NOM by the preloaded carbon; and this was quantified using the Freundlich isotherm as presented in Table 3.7 and Figure 3.13. The difference in adsorptive capacity between the virgin and preloaded carbon in the Ho and Newcombe (2007) study was much greater than in the present study. Reasons for this could be the nature of the preloading and type of carbon used.

Julio (2011) looked briefly at preloading Norit carbon with tannic acid, with the justification that tannic acid represents the portion of the NOM which is of similar size to MC-LR and would compete for the same adsorption sites and therefore would best represent NOM preloading and competition from NOM. The author also found that following preloading, a negative isotherm slope was reported, which was not the case in this study. No isotherm equations were presented by Julio (2011) for the preloaded carbon.

Table 3.7. Available literature on Freundlich isotherms for MC-LR adsorption

Carbon	K_f	1/n	C_o (μg/L)	GAC_i (mg/L)	Matrix	Ref
Virgin F300	1.306 $(\mu g/mg)(L/\mu g)^{-1/n}$	0.199	100	10-90	Autoclaved ultrapure water (Milli-Q)	This work
Preloaded F300	0.742 $(\mu g/mg)(L/\mu g)^{-1/n}$	0.337				
Preloaded (w/o outlier)	0.718 $(\mu g/mg)(L/\mu g)^{-1/n}$	0.333				
F300 12x30 mesh (Coal-based)	0.5129 $(\mu g/mg)(L/\mu g)^{-1/n}$	0.36	2000	100-500	DI water	Mohamed et al., 1999
Darco 12 x 30 mesh (wood-based)	0.5012 $(\mu g/mg)(L/\mu g)^{-1/n}$	0.36				
PCB 12 x 30 mesh (coconut-based)	0.3311 $(\mu g/mg)(L/\mu g)^{-1/n}$	0.44				
HOA 12 x 40 mesh (coal-based)	0.126 $(\mu g/mg)(L/\mu g)^{-1/n}$	0.57				
Bamboo charcoal & chitosan	1.7519 mg/g $(L/\mu g)^{-1/n}$	0.2948	0.1-7.5	15	DI water	Zhang et al., 2011
Virgin Picazine	2.202 $(mg/g)(L/\mu g)^{-1/n}$	0.205	100	not reported	Treated reservoir water prior to chlorination	Ho and Newcombe, 200
Preloaded Picazine	0.396 $(mg/g)(L/\mu g)^{-1/n}$	0.313				

Note: The initial concentration was altered to suit the fitting parameter to prevent conversion errors.
C_o = initial concentration
GAC_i = applied GAC dose
DI = deionized water

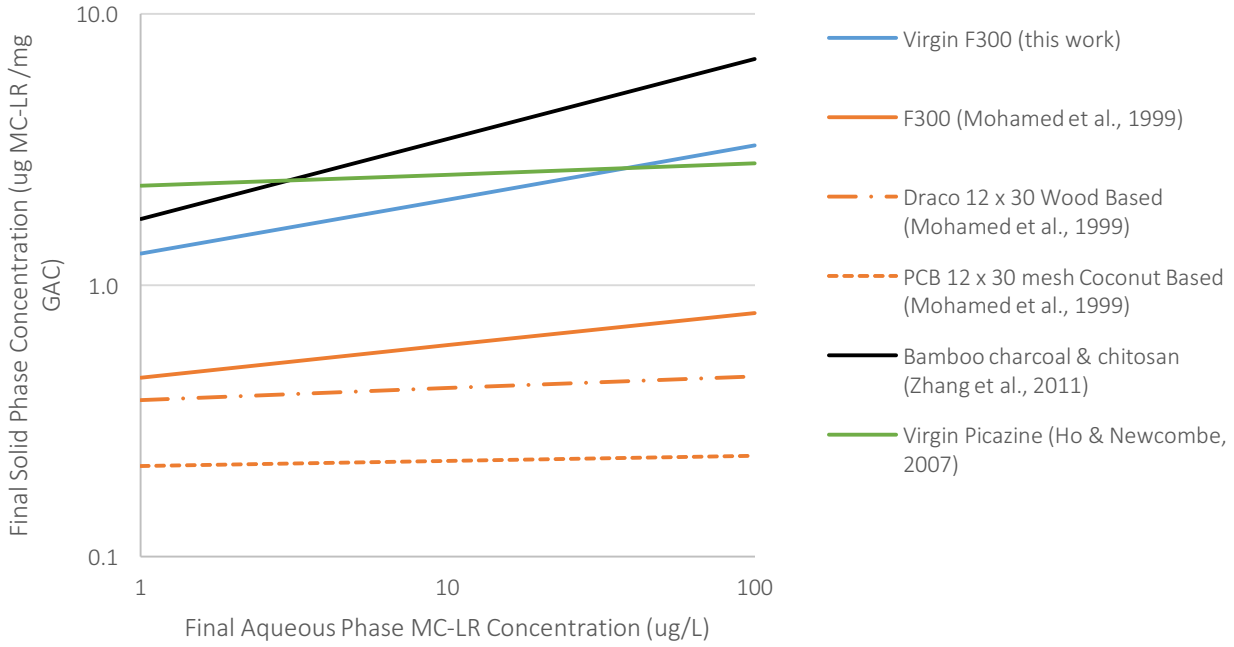

Figure 3.12. Available literature on the virgin Freundlich isotherms compared with this work

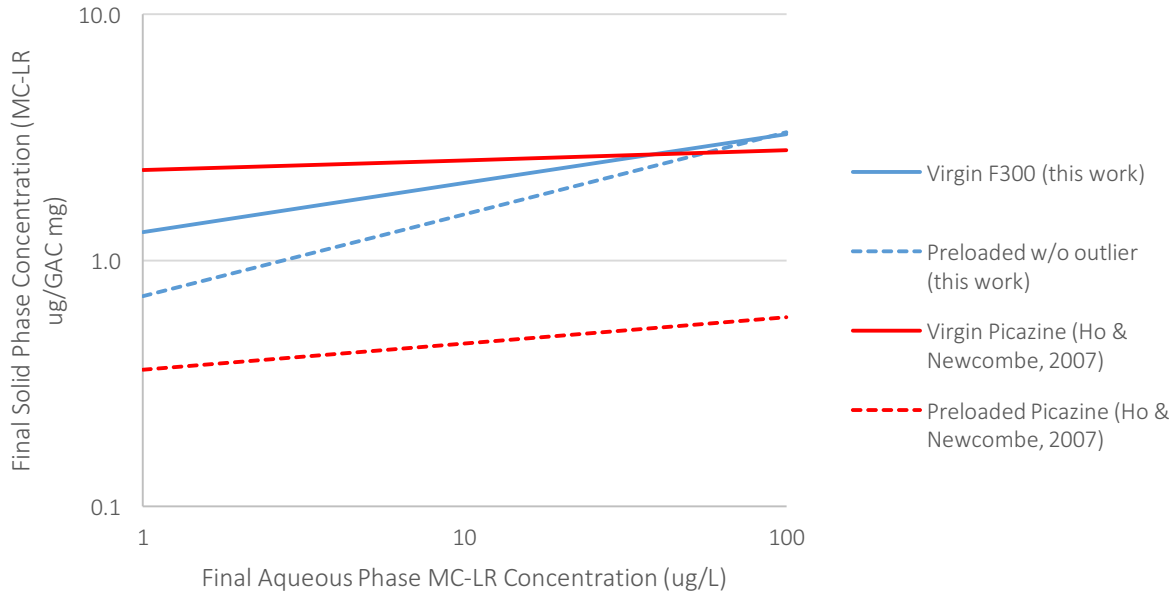

Figure 3.13 Available literature comparing virgin and preloaded Freundlich isotherms compared with this work

3.5 Conclusions

In order to simulate one season of use, virgin F300 GAC was preloaded using filter effluent from a full-scale drinking water treatment plant operating on Lake Ontario. The duration of preloading (seven weeks) was dictated by the historical presence of the taste and odour compounds geosmin and 2-methylisoborneol (secondary cyanobacterial metabolites), and although not predictive of MC-LR occurrence, serve to identify the seasonal period for cyanobacterial bloom occurrence.

The virgin and preloaded F300 carbons were then subject to the bottle point method for analysis of MC-LR kinetics and capacity. The virgin carbon reached equilibrium after 18 days. The preloaded carbon reached equilibrium after 49 days. Pseudo-first and –second order rate expressions were considered to model the removal of MC-LR over time. Both pseudo-first and -second order kinetic models were considered, and the data quality and fit between the models was generally similar. For both carbons, data acquired at lower carbon doses were less reliable, due to experimental variability impacting the removal at the lower F300 doses. The preloaded carbon adsorbed MC-LR more slowly than the virgin carbon; which may result from the blockage of adsorption sites during preloading.

At equilibrium, the Freundlich isotherms were used to model the data following non-linear regression. Although the virgin carbon appeared to have higher equilibrium capacity, the Freundlich parameters were not statistically significant at the 95% confidence level. This was evidenced by the overlapping joint confidence regions for the two parameters. At lower liquid phase equilibrium concentrations (less than

approximately 50 µg/L) it appeared that higher preloaded carbon dosages would be required to achieve a given liquid phase concentration, although a statistically significant difference could not be demonstrated at the 95% confidence level. One season of preloading was not sufficient to exhaust the carbon capacity for MC-LR adsorption.

In conclusion, F300 is well able to remove MC-LR through adsorption. The kinetics of adsorption slow following one season of preloading. One season of preloading appeared to decrease the removal of MC-LR at the lower F300 dosage, although this was not significate at the 95% confidence levels.

4 A Comparison of GAC Storage Techniques for the Removal of Microcystin-LR

4.1 Summary

Following preloading with Lake Ontario water, a typical coal-based granular activated carbon was taken out of service and stored under four different conditions; drained and kept in a high moisture content (HMC) environment, drained and kept in a low moisture content (LMC) environment, completely immersed in Lake Ontario water (submerged), and immersed in saline water. An operational control was maintained at the full-scale water treatment plant to simulate a GAC contactor which remained in operation throughout the year. Following storage for selected intervals, bottle point studies were conducted in ultra-pure water to evaluate the kinetics and equilibrium capacity (isotherms) of the stored carbons and the operational control for MC-LR removal. The salt storage showed the fastest kinetics, 41 day equilibrium, while the GAC submerged in water showed the slowest kinetics, 57 day equilibrium. All stored carbons and the operational control removal rates were best approximated by pseudo-first order kinetics. As expected, the control was impacted by the continuous loading, and had diminished capacity for MC-LR after the 8-month test period. The remainder of the storage methods showed improvements relative to the operational control in terms of capacity at equilibrium. The LMC condition appeared to be the most effective strategy to preserve the GAC's capacity for MC-LR removal from one season to the next. When compared with the virgin and preloaded GAC discussed in Chapter 3, the LMC storage was the only storage method to show no significant change in isotherm parameters (i.e. no change in

adsorption equilibrium capacity). In conclusion, there is a benefit in terms of capacity being maintained from taking GAC off-line and storing it between seasonal cyanotoxin occurrences compared to leaving the GAC in service. The LMC storage condition appeared to retain the most MC-LR capacity and the highest rate of removal.

4.2 Introduction

MC-LR occurs in temperate regions seasonally, when summer temperatures and nutrient loading provide ideal conditions for cyanobacterial bloom formation (Fogg, 1968; Paerl & Fulton, 2006; Paerl & Huisman, 2008; Paerl, 1988; Reynolds, 1987; Steinberg & Hartmann, 1988; Wood et al., 2006). This is true in the North American Great Lakes region, where a valuable drinking water resource can be seasonally impacted (Dyble et al., 2008; Rinta-Kanto et al., 2005; Watson at al., 2008). With the progression of climate change, cyanobacterial bloom formation and seasonal presence of the associated cyanotoxins such as MC-LR are increasing (Paerl & Huisman, 2008, 2009; Paerl & Paul, 2012; Wiedner et al., 2007).

Activated carbon is effective for the removal of MC-LR to below drinking water targets through adsorption, and this has been discussed in detail in Chapters 2 and 3. With ongoing usage, the nonspecific capacity of the GAC diminishes, as target and non-target compounds (NOM) are adsorbed, which are present at much higher concentrations than the target compound (Crittenden et al., 2012; Worch, 2012). During intermittent loading, desorption can be observed when the target contaminant is no longer present in the influent (Corwin & Summers, 2011).

Taking GAC out of service and storing it between seasonal events may preserve capacity of the GAC for the target compound, by limiting the exposure of the GAC to the non-target background NOM during the portion of the year when it is unlikely that MC-LR will be present. How and if GAC should be stored to best preserve, or restore, capacity for organic contaminant removal remains uninvestigated as this has not been reported to-date in the current literature. However, Wang et al. (2014) examined the seasonal changes in the invertebrate community of filter beds in China; several methods of invertebrate elimination were examined to reduce the population, which swelled during warmer temperatures. They found that a 20 g/L salt rinse was most effective at reducing invertebrate population, while air drying the media was more economical (Wang et al., 2014). Backwashing with and without chlorine was also investigated. Wang et al. (2014) focused on the invertebrate community, and did not evaluate how the properties of the adsorptive media changed with the treatments.

The objective of this study was to determine whether there are benefits in terms of kinetics and equilibrium capacity to be obtained from the storage of GAC between uses for seasonal contaminants, in particular for the drinking water regulated cyanotoxin MC-LR.

4.3 Materials and Methods

4.3.1 Materials

Virgin and preloaded F300 were prepared as described in section 3.3.1. Chemicals and materials were also as described in section 3.3.1.

4.3.2 Carbon Storage

Following preloading, the F300 was stored for 8 months. All of the GAC was removed from the preloading set up (described in 3.3.2), mixed and divided according to ASTM C702/C702M-11 (Standard Practice for Reducing Sample of Aggregate to Testing Size) to ensure a representative sample (ASTM International, 2011). The carbon was divided into 5 lots (including 4 storage methods and an operational control) and prepared for storage as described below.

Four storage conditions were tested using lots of the preloaded carbon over an 8-month period. The submerged storage contained the preloaded F300, immersed in post filtration water from the full-scale Lake Ontario plant. The water was changed monthly. The full-scale plant water was taken upstream of the preloading set up, and therefore contained an initial chlorine residual of 1.2 mg/L on average. The high moisture content (HMC) storage was intended to simulate the bottom of a drained full scale filter, and was stored as is. The moisture content of the HMC storage was initially found to be 54%, and remained approximately constant throughout the duration of storage. The low moisture content storage (LMC), which was intended to simulate the top portion of a drained filter, used a lot from the GAC removed from the preloading column which was dried at 50°C for 24 hours to a final moisture content of 43% and stored. Moisture contents were determined according to ASTM D2867-09, Standard Test Method for Moisture In Activated Carbon (ASTM International, 2013). Finally, a lot of preloaded GAC was immersed in dechlorinated post-filtration water from the full-scale Lake Ontario plant containing 20 g/L sodium chloride, similar to the work of Wang et al. (2014) in

investigating the seasonal invertebrate filter bed changes. The GAC remained immersed in this solution for the duration of the 8-month storage period (no water changes).

Following storage preparation, two 250 mL bottles were filled with approximately 150 mL of GAC per each storage method (the carbon was stored in duplicate). The bottles were capped securely with Teflon® lined lids. The bottles were stored in the dark at room temperature. Each bottle was shaken weekly to ensure the media remained homogeneous; although full scale filters would not be shaken, this ensured a representative sample could be obtained.

Samples were taken bimonthly to monitor for biological activity (through ATP analysis) and to ensure that limited changes in moisture content were occurring. Prior to sampling, the bottles were well mixed. Half the sample volume (approximately 50 mL) was removed from each of the duplicates, and mixed well prior to ATP and moisture content analysis. The remaining sample was then freeze-dried for point of zero change, kinetic, and isotherm analyses. Freeze-drying was completed as per Andrews (1990). Samples were placed in glass vials, covered with foil, pierced several times to allow for ventilation, and covered with a lint free tissue (using an elastic band) to prevent the sample from escaping. The freeze dried carbon was capped securely and stored in a desiccator prior to usage.

4.3.3 Operational Control

An operational control column was maintained in continuous operation following full-scale filtration of Lake Ontario water (Figure 4.1 and 4.2). The operational control was operated at the same hydraulic loading rate, 5 $m^3/h/m^2$ (5 m/h) as the full-scale filters.

The chlorine removal columns, described in Chapter 3, remained in operation. The operational control was intended to determine the effects of continued NOM loading onto GAC, if it were to remain in operation year around, rather than be stored offline. The control column was fully emptied bimonthly, and mixed completely before a sample was taken. The remainder of the sampling procedure was as per the previous section.

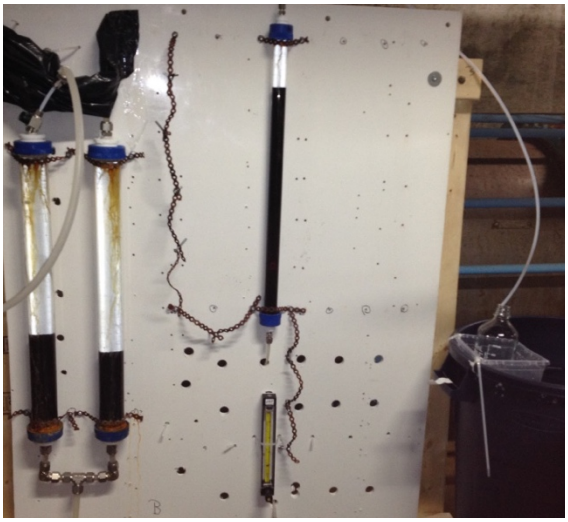

Figure 4.1 Continuous operation control at the fullscale drinking water treatment facility

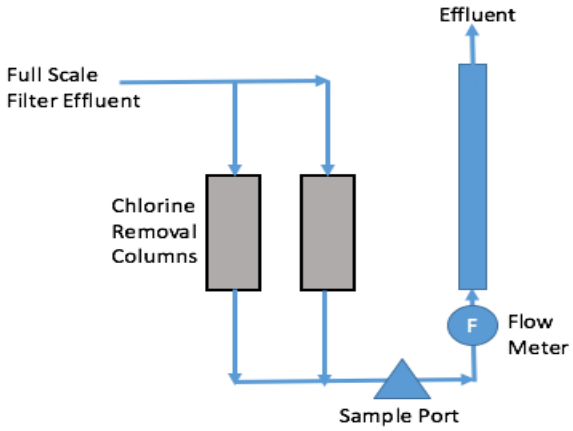

Figure 4.2 Continuous operation control schematic

4.3.4 Analytical Methods

MC-LR was quantified by LC-MS/MS as described in section 3.3.6. TOC and DOC were quantified as described in section 3.3.4. NOM was quantified by LC-OCD 3.3.5.

The chlorine residual was determined by the Region of Durham staff as by amperomeric titration.

ATP concentrations were determined using the LuminUltra Deposit and Surface Analysis test kit (LuminUltra Technologies Ltd., Fredericton, New Brunswick, Canada).

4.4 Results

4.4.1 Carbon Storage Monitoring

4.4.1.1 Biological Activity Monitoring

The activity of biomass in the stored carbon samples was determined through ATP analysis bimonthly (Figure 4.3). Over the 8-month storage period, only the on-site continuously operated control was in the beginning phases of biological activity (as defined by Pharand et al., (2014)) This indicates that the predominant removal mechanism in the stored samples remained as adsorption and that biomass did not interfere substantially with adsorption sites (positively or negatively).

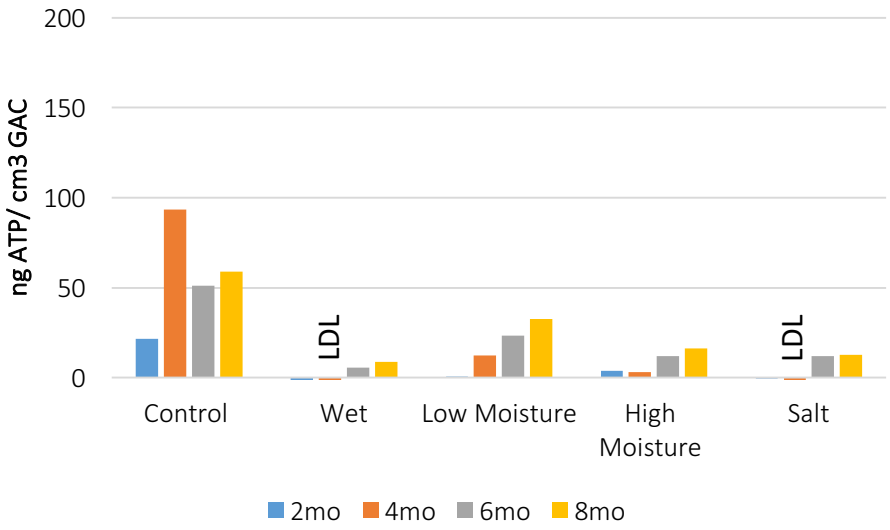

Figure 4.3 ATP monitoring of stored carbons and the operational control over an 8-month period

4.4.1.2 Moisture Content Changes

Throughout the 8-month study, the GAC was sampled bimonthly to monitor for any changes in moisture content in the LMC and HMC samples.

The HMC storage initially had a moisture content of 59%. Over the course of the storage period the moisture content decreased to 44%, and again this change is suspected to result from opening the bottles to sample. The LMC storage initially had a moisture content of 43%, and this decreased to 41% over the course of the study. The slightly elevated LMC ATP levels could be due to the increased availability of oxygen compared to the other storage techniques.

4.4.2 Continuous Operation Control Monitoring

The operational control was in operation for a total of 44 weeks, including the preloading period. Ongoing water quality analysis, including TOC, DOC and NOM by LC-OCD was conducted. Table 4.1 shows the average influent NOM as determined by LC-OCD. Influent TOC and DOC remained low, as the preloading setup was located downstream of the full-scale filters. Upwards of 90% DOC breakthrough was observed over the course of the control operation (Figure 4.4). The largest NOM fraction identified by LC-OCD was humics, and a similar removal trend was observed during the control operation for this fraction (Figure 4.5).

Table 4.1. Average concentration of NOM fractionation of influent water (post-filtration water from full-scale plant) as determined by LC-OCD

NOM Fraction	***mg C/L***
DOC	2.18
Biopolymers	0.24
Humics	1.14
Building Block	0.27
LMW Neutrals	0.32
LMW Acids	0.01

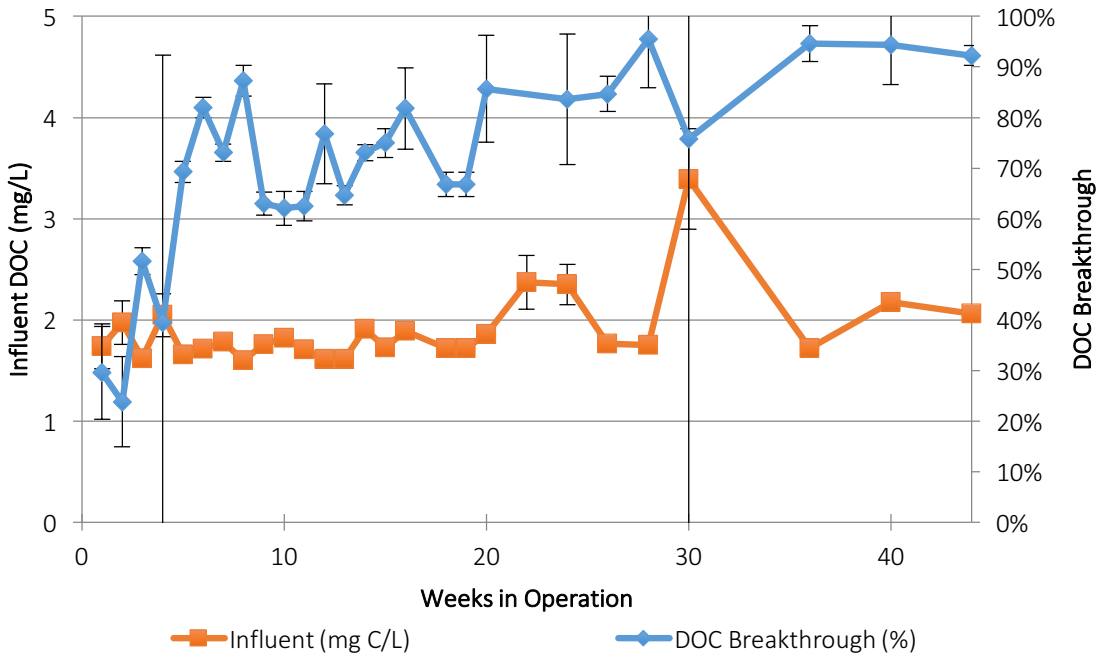

Figure 4.4 DOC % breakthrough of continuous operation control over 8-month period (n= 6). Error bars relate to duplicate samples with 3 injections each for a total of 6 measurements per point.

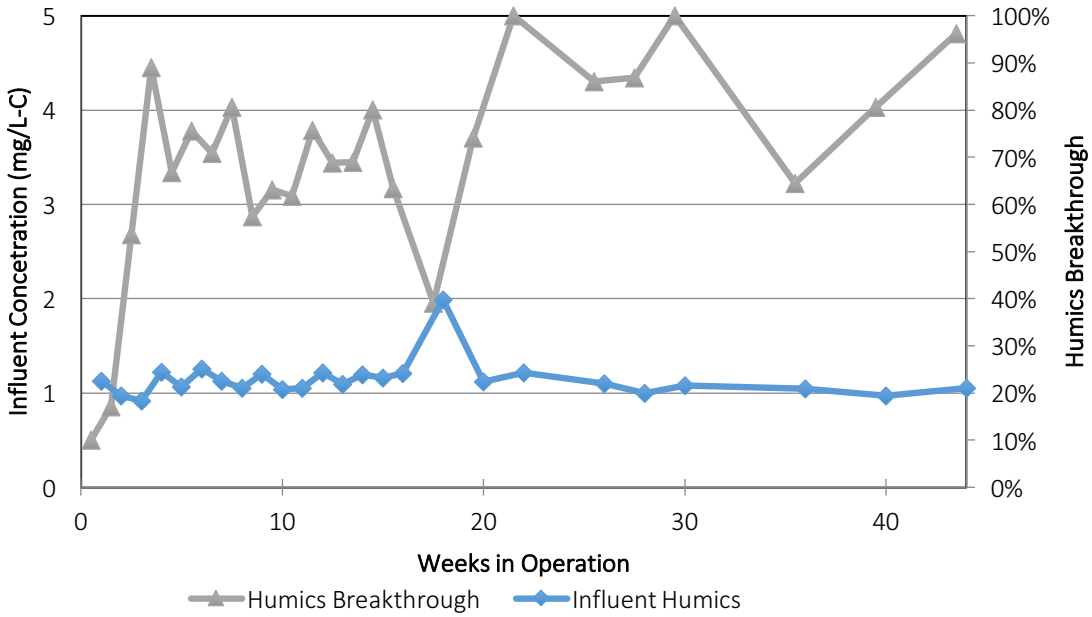

Figure 4.5 Humics % breakthrough of continuous operation control over 8-month period (n = 1)

Additional NOM, TOC and DOC data is presented in Appendix B.

4.4.3 Carbon Characteristics

For each of the stored carbons, the point of zero charge was determined (Table 4.2). The pH_{PZC} of the GAC of all the storage methods was neutral, ranging from 6.6 – 6.9. Following preloading, the pH_{PZC} decreased from 10.2 to 7.2, as NOM was adsorbed, revealing that the surface charge of the carbon was effectively neutralized during preloading. It does not appear that any of the storage methods altered the pH_{PZC} of the F300 compared to the preloaded carbon.

Table 4.2 The pH_{PZC} of the stored F300

Carbon	pH_{PZC}
Virgin	10.2
Preloaded	7.2
Operation Control	6.6
High Moisture Content	6.8
Low Moisture Content	6.9
Salt	6.9
Submerged	6.9

4.5 Kinetics

The MC-LR removal kinetic results for the various storage methods and the operational control are shown in Figure 4.6 and Table 4.3. The salt storage samples reached equilibrium (less than 1% change in percent removal) after 41 days, and displayed the fastest kinetics. The submerged storage method displayed the slowest kinetics, and reached equilibrium after 57 days.

For all samples, the removal of MC-LR increased with increasing GAC dose. The highest dose (approximately 90 mg/L) not surprisingly led to the highest removal. The LMC and

the submerged storage methods displayed the highest removal. As expected, the continuous operation control removed the least MC-LR, as a result of the continuous exposure to NOM. At the highest dose, the salt treatment performed similarly to the HMC storage; however, at the lowest dose no MC-LR removal was observed.

Table 4.3 Kinetics of F300 following storage

Storage Method	Time to Equilibrium	GAC Dose (mg/L)	% MC-LR Removal
Operation Control	43 days	11.6	30
		54.4	56
		91.2	66
HMC	44 days	10.8	12
		50.8	60
		91.2	90
LMC	43 days	11.8	29
		47.6	74
		91.0	97
Submerged	57 days	11.4	15
		53.2	82
		92.0	97
Salt	41 days	11.4	0
		51.0	58
		93.0	88

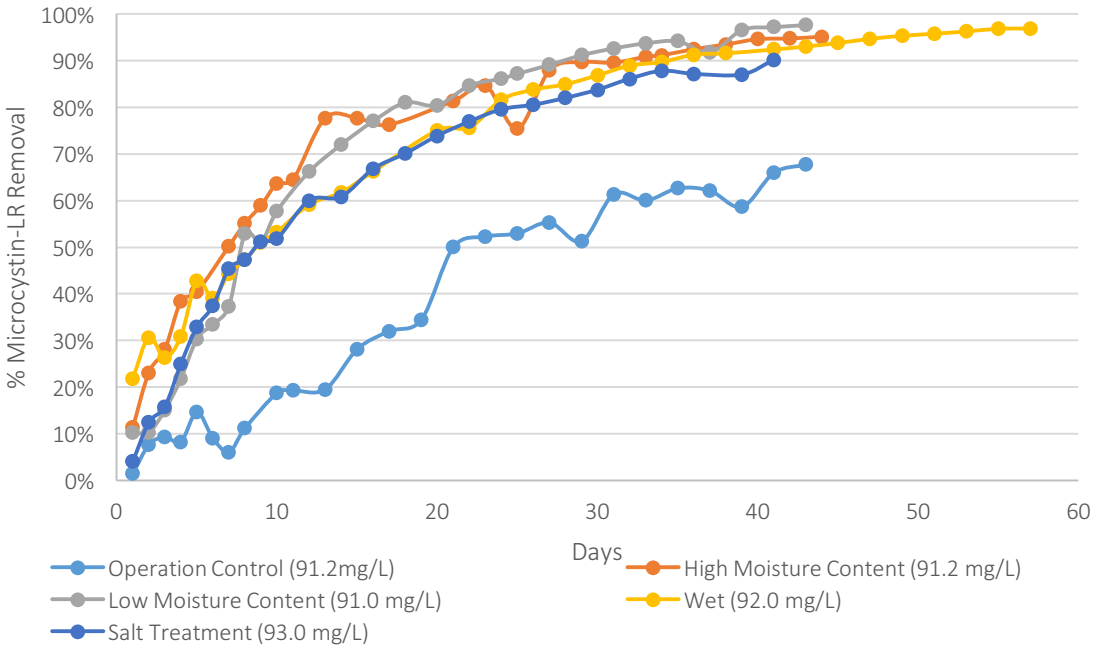

Figure 4.6 Kinetics of the highest carbon dose of the stored carbons

All of the stored carbons and the operational control displayed slower kinetics than the virgin F300 (Discussed in chapter 3). The carbon stored under submerged conditions displayed slower kinetics than the preloaded F300 discussed in Chapter 3. The remaining storage methods and the operational control reached equilibrium faster than the preloaded F300.

In order to further evaluate the kinetics of MC-LR removal, pseudo kinetic equations were applied, as described in Chapter 3. Both pseudo-first and -second order kinetics equations were considered (Ho & McKay, 1999; Lagergren, 1898). Non-linear regression was used to determine the kinetic parameters through the least sum of squared errors method. The limitations of the equations are discussed in Chapter 3

Table 4.4 Pseudo- first and -second order analysis of kinetic data

			Pseudo-First Order			Pseudo-Second Order		
Carbon	Dose (mg/L)	$q_{e\ observed}$ (μg/mg)	k_1 ($days^{-1}$)	$q_{e\ predicted}$ (μg/mg)	SSE	k_2 (mg/μg/ days)	$q_{e\ predicted}$ (μg/mg)	SSE
Operational Control	11.6	1.04	5.18E-05	456.54	6.09	1.00E+00	0.38	10.80
	54.4	0.92	1.13E-02	2.55	0.05	2.65E-03	3.45	0.04
	91.2	0.66	1.40E-02	1.57	0.07	2.62E-03	2.89	0.07
HMC	10.8	1.26	3.02E-01	1.54	2.78	4.47E-01	1.61	2.40
	50.8	1.34	7.12E-02	1.35	0.05	3.41E-02	1.81	0.04
	91.2	1.09	1.23E-01	1.05	0.04	1.04E-01	1.28	0.03
LMC	11.8	2.11	3.56E-02	2.83	10.39	4.37E-03	4.79	10.49
	47.6	1.57	4.42E-02	1.80	0.37	1.11E-02	2.75	0.39
	91.0	1.20	8.56E-02	1.23	0.03	4.61E-02	1.63	0.06
Submerged	11.4	0.87	9.76E-01	0.00	8.57	8.98E-01	0.00	8.57
	53.2	1.41	2.83E-02	1.77	0.57	6.41E-03	2.84	0.57
	92.0	0.98	7.65E-02	0.95	0.60	6.61E-02	1.19	0.56
Salt	11.4	0.40	5.80E-05	0.00	12.18	1.66E-03	0.00	12.18
	51.0	1.11	6.01E-02	1.02	1.28	2.73E-02	1.53	1.33
	93.0	0.90	8.92E-02	0.90	0.01	6.89E-02	1.18	0.01

.

At the lowest carbon doses, both kinetic models generally fail to predict the removal of MC-LR due to poor data quality (high SSE). This is likely due to the limited overall removal observed at the low doses, which amplified any variability in experimentation (both equipment and human). The considerable scatter (including negative q_e values) is evident in Figure 4.7 to 4.10

The operational control at the middle and highest F300 doses have similar fits when the SSE are considered, and the rate constants are consistent (Figure 4.7). At the lowest carbon dose the pseudo-first order model fails to predict the equilibrium MC-LR solid phase concentration. At the middle and highest carbon doses the pseudo-first order model better predicts final MC-LR solid phase concentration. It should be noted that the final experimental MC-LR solid phase concentration was defined at less than 1% change in percent removal and therefore may not be representative of true equilibrium if the rate of change slowed dramatically.

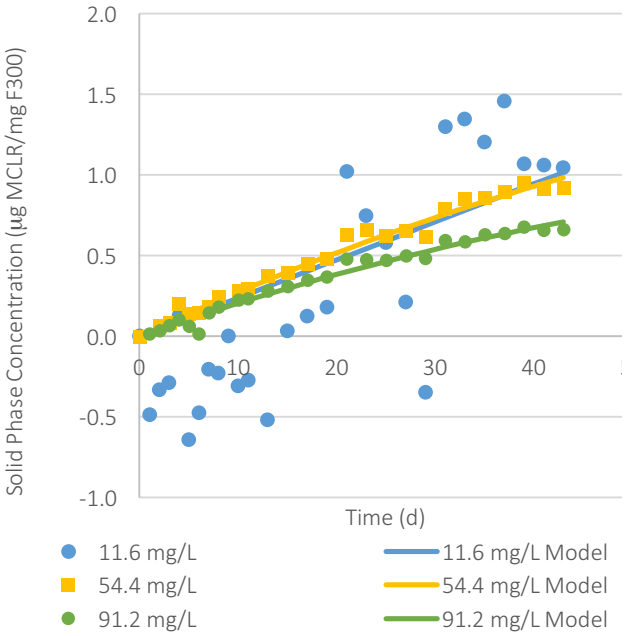

Figure 4.7a Pseudo-First Order Kinetics for Continuous Operational Control

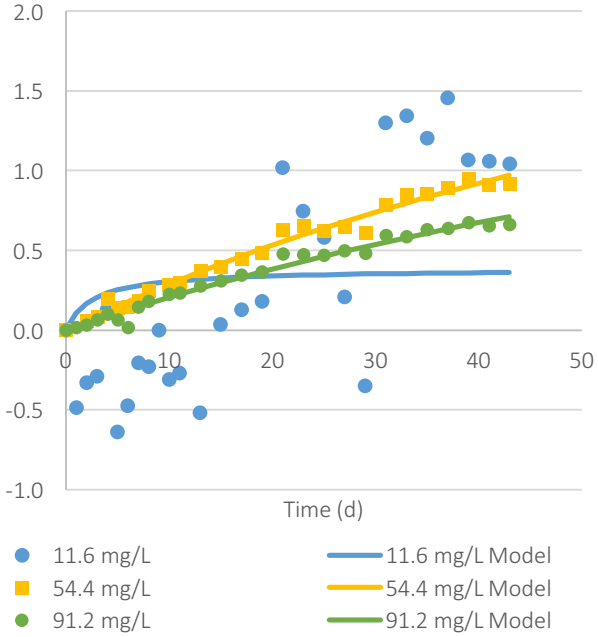

Figure 4.7b Pseudo-Second Order Kinetics for Continuous Operational Control

For HMC storage kinetics the SSE was quite similar for both models at a given carbon dose and the fits are visually quite similar (Figure 4.8). The equilibrium solid phase concentration was better predicted by the pseudo-first order model. Both the models show some variability in terms of the rate constants.

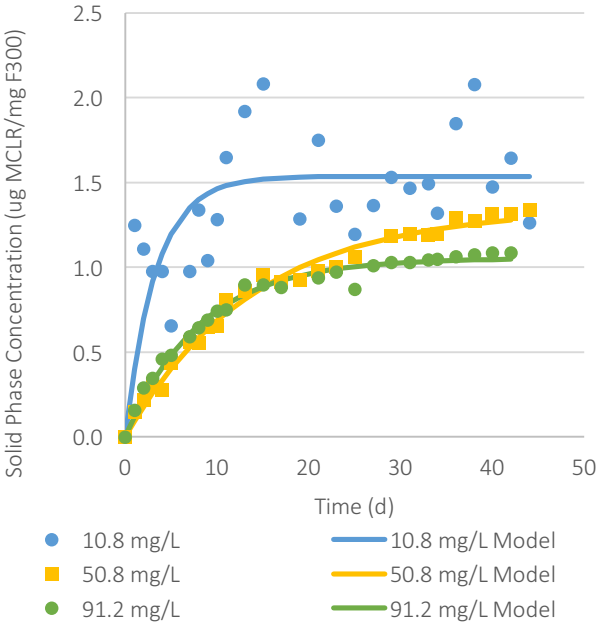

Figure 4.8a Pseudo-First Order Kinetics for High Moisture Content Storage

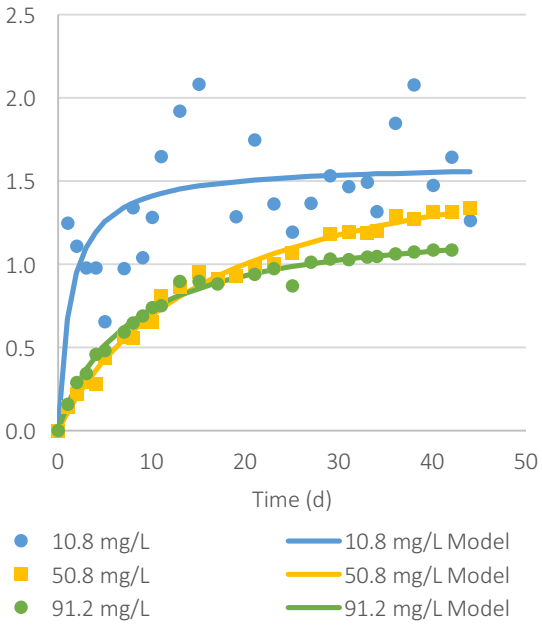

Figure 4.8b Pseudo-Second Order Kinetics for High Moisture Content Storage

The fits of the two models were quite similar for the LMC storage (Table 4.4 and Figure 4.9), with increasing data quality (lower SSE) with increasing carbon dose from 11.8 to 91.0 mg/L. The equilibrium MC-LR solid phase concentration was better predicted by the pseudo-first order kinetics. One outlier was observed in the data, likely caused by experimental error, which was not removed from analysis.

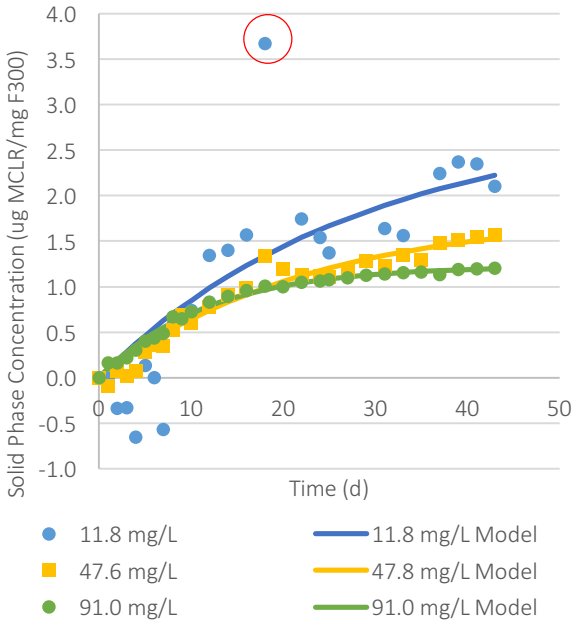

Figure 4.9a Pseudo-First Order Kinetics for Low Moisture Content Storage

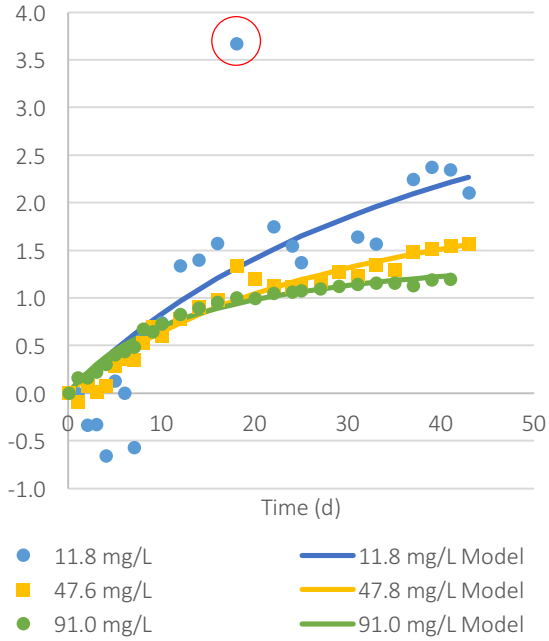

Figure 4.9b Pseudo-Second Order Kinetics for Low Moisture Content Storage

The submerged storage also showed a similar degree of fit by the two models in terms of the SSE. The lowest F300 dose showed limited removal over time; initially the data quality is quite poor due to experimental variation, the final data points do show some limited removal which is poorly predicted by the model. The middle and higher F300 dose equilibrium MC-LR solid phase concentration is better predicted by the pseudo-first order model.

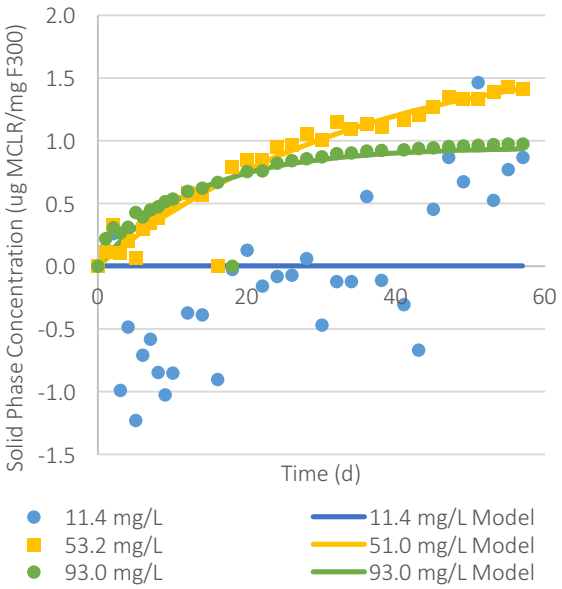

Figure 4.10a Pseudo-First Order Kinetics for Submerged Storage

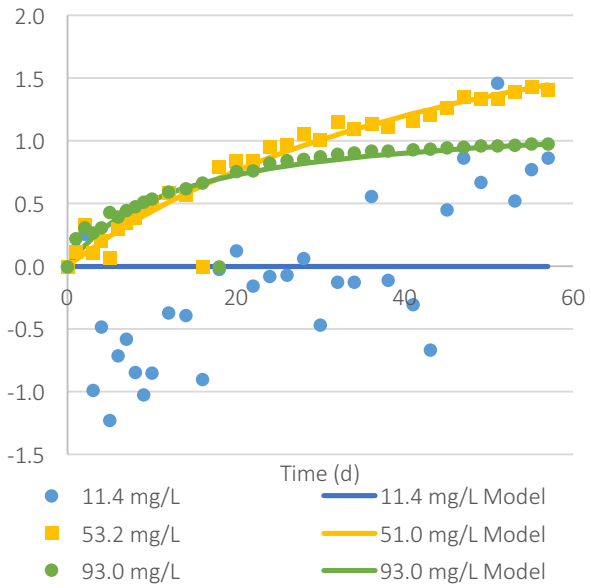

Figure 4.10b Pseudo-Second Order Kinetics for Submerged Storage

A similar trend for the salt storage as per the submerged storage was observed in terms of the lowest F300 dose. Both models showed similar data quality in terms of the SSE; the pseudo-first order model showed marginally better predictions of the observed final solid phase concentration.

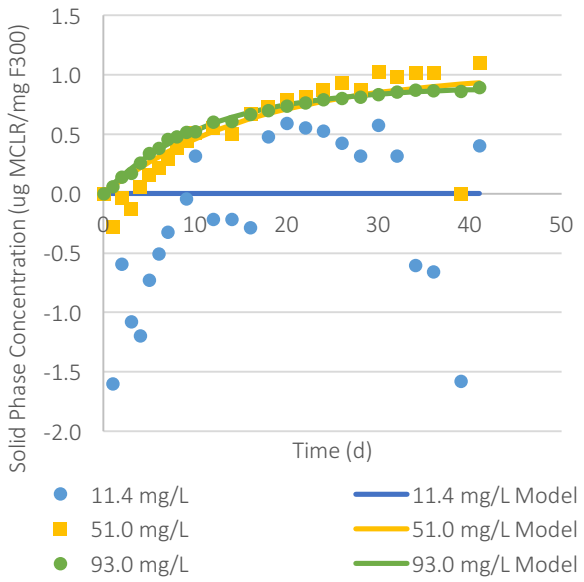

Figure 4.11a Pseudo-First Order Kinetics for Salt Storage

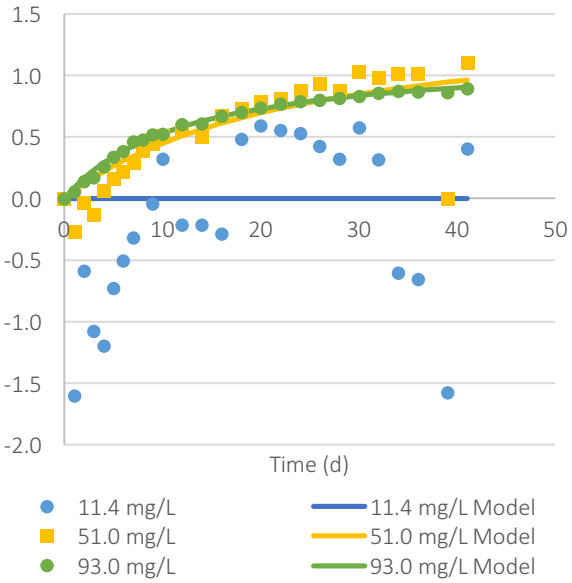

Figure 4.11b Pseudo-Second Order Kinetics for Salt Storage

Overall, both models were similar in terms of data quality (SSE). The pseudo-first order model was generally more predictive of the equilibrium MC-LR solid phase concentration. The lower F300 dose showed poor data quality, which is a function of the data quality and experimental variability. Additional details and data are shown in Appendix D.

When compared with the preloaded carbon (Chapter 3), the kinetic rate constants were of similar magnitude. This indicates that the rate of removal for the stored and preloaded carbon was similar, and no changes to the kinetics occurred during storage. The virgin rate constants were generally higher, indicating that the rate of the removal of MC-LR was higher than the stored carbon, which is supported by the shorter equilibrium time

observed for the virgin F300. For all data sets, neither the pseudo-first nor –second order model proved to be more predictive of the data sets.

4.5.1 Isotherms

Freundlich isotherms were developed for all stored carbon once equilibrium was reached, using the methodology detailed in Chapter 3, and results are presented in Figure 4.12 to 4.15 and Table 4.5. Non–linear least squared regression was used to determine the isotherm parameters, with the SSE being included as a measure of fit. Data points considered to be outliers are circled in red.

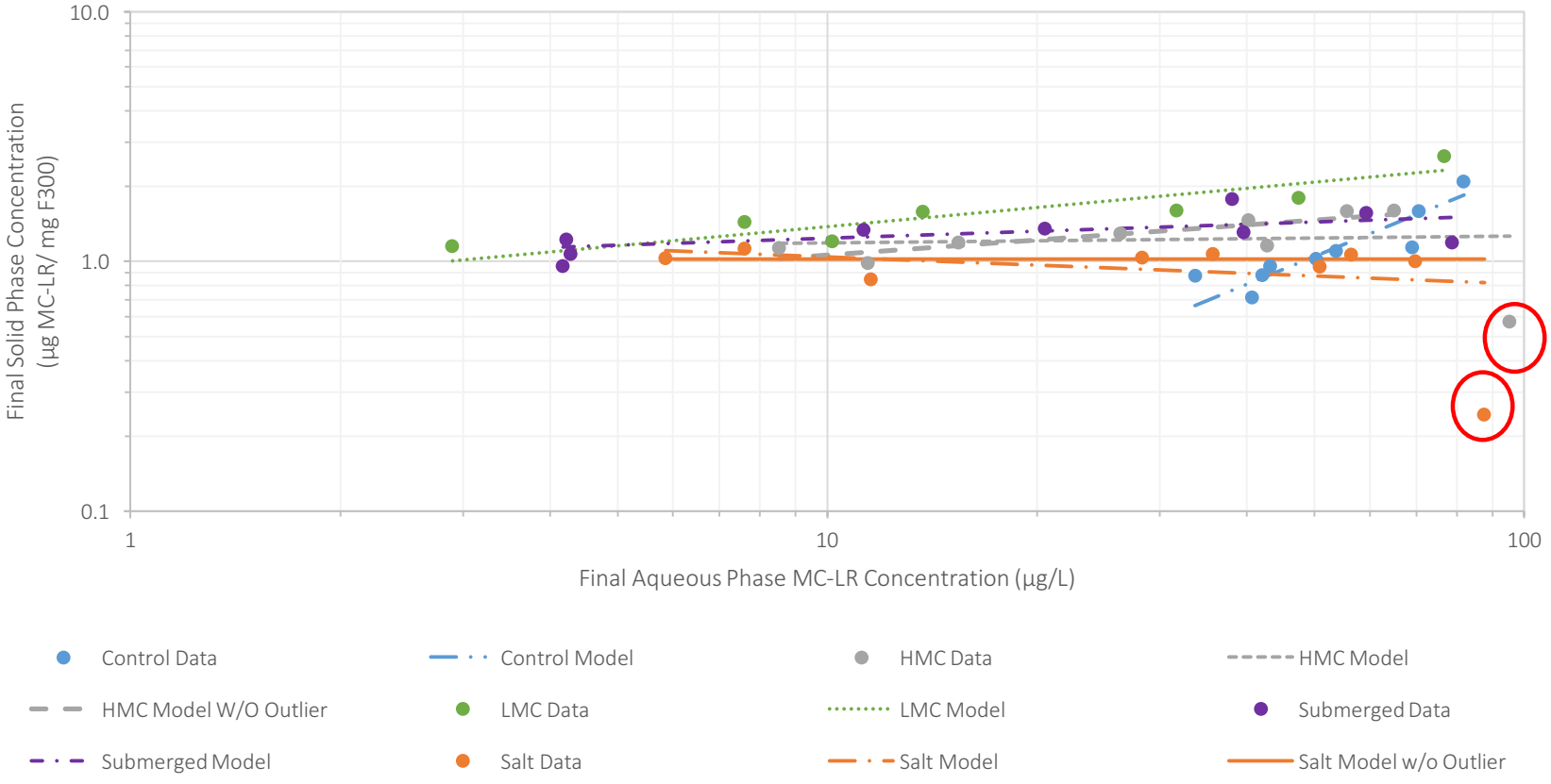

Figure 4.12 Isotherm data and Freundlich model for all stored F300. Outliers are circled in red.

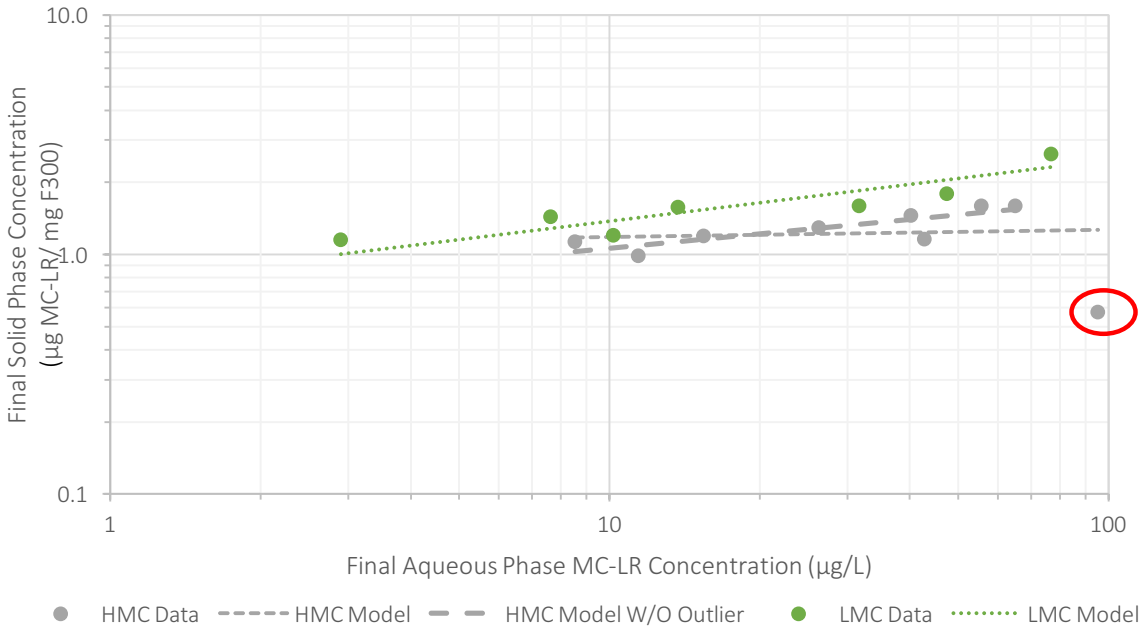

Figure 4.13 Freundlich isotherm data and model for HMC and LMC Stored F300 experiments, with outlier circled in red

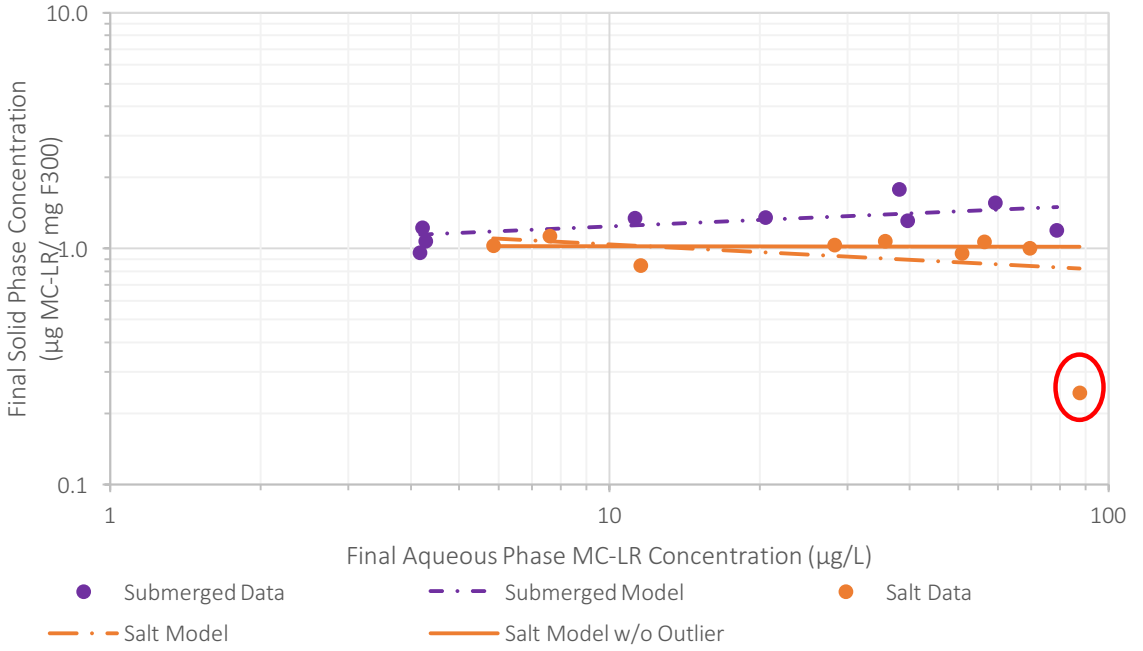

Figure 4.14 Freundlich isotherm data and model for submerged and salt stored F300, with outlier circled in red

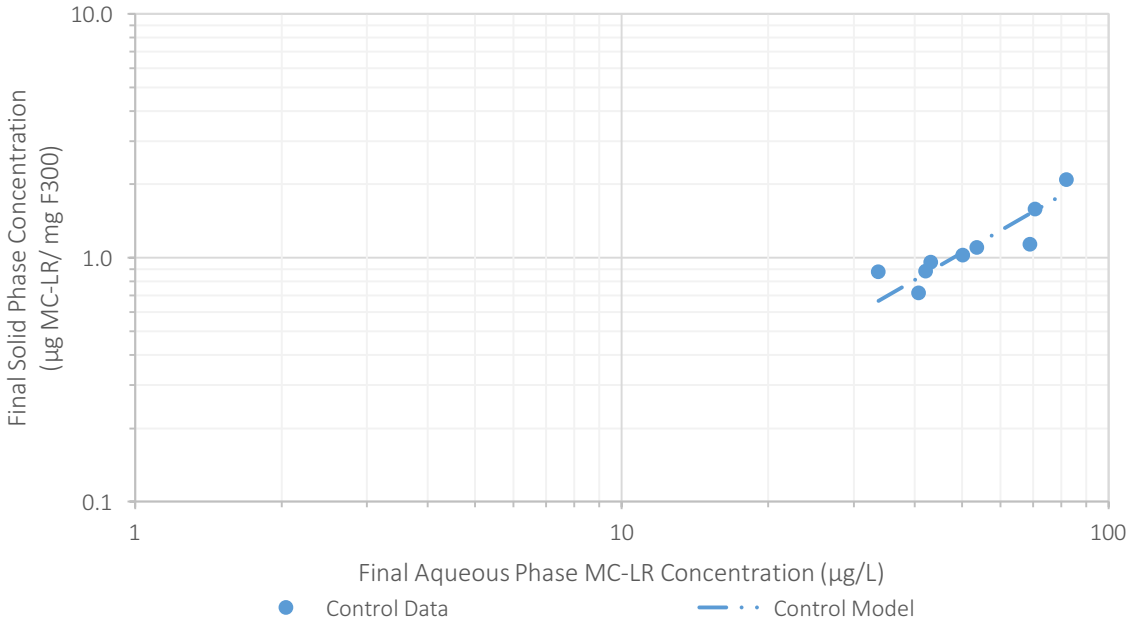

Figure 4.15 Freundlich isotherm data and model for continuous operational control

Table 4.5 Freundlich isotherm parameters determined using non-linear regression (95% confidence level in brackets)

Storage	Kf (µg/mg)(µg/L)$^{-1/n}$	1/n	SSE
Control	0.01 *(-0.02-0.04)*	1.15 *(0.93-3.21)*	0.27
HMC	*1.13 (-0.28-2.63)*	*0.02 (-0.19-0.62)*	0.82
HMC w/o outlier	*0.67 (0.27-1.11)*	*0.20 (0.06-0.43)*	0.11
LMC	0.77 *(0.24-1.39)*	0.25 *(0.09-0.51)*	0.31
Submerged	1.00 *(0.53-1.50)*	0.09 *(-0.03-0.26)*	0.31
Salt	1.34 *(-0.09-2.80)*	-0.11 *(-0.33-0.36)*	0.49
Salt w/o outlier	1.01 *(0.41-1.69)*	0.00 (-0.15-0.23)	0.05

In order to compare the isotherms at the 95% significance level, joint confidence regions were established for all storage methods using MATLAB®, as described in Chapter 3 and shown in Figure 4.16. The limits of these joint confidence regions (JCRs) are presented in Table 4.5 as the 95% confidence limits. The JCRs better depict the limits of related parameters than the more traditional one at a time confidence intervals (Yu, 2007). As is evident from the JCRs in Figure 4.16, the continuous operational control isotherm is distinct from all of the storage methods at the 95% confidence level. This indicates that there is a difference created by taking a GAC contactor offline and storing during the non-cyanobacteria portion of the year. Adsorptive capacity is apparent from the isotherms shown in Figure 4.12. It is clear that the isotherm for the control overlaps the other isotherms in the concentration range for which data for the control are available. The trend of the control isotherm would suggest, however, that at lower liquid phase equilibrium concentrations, the solid phase concentration on the control carbon would be lower. This would indicate that it would be less effective than any of the other carbons at achieving lower liquid phase concentrations. In other words, it would appear that the various storage procedures of the carbon have an advantage.

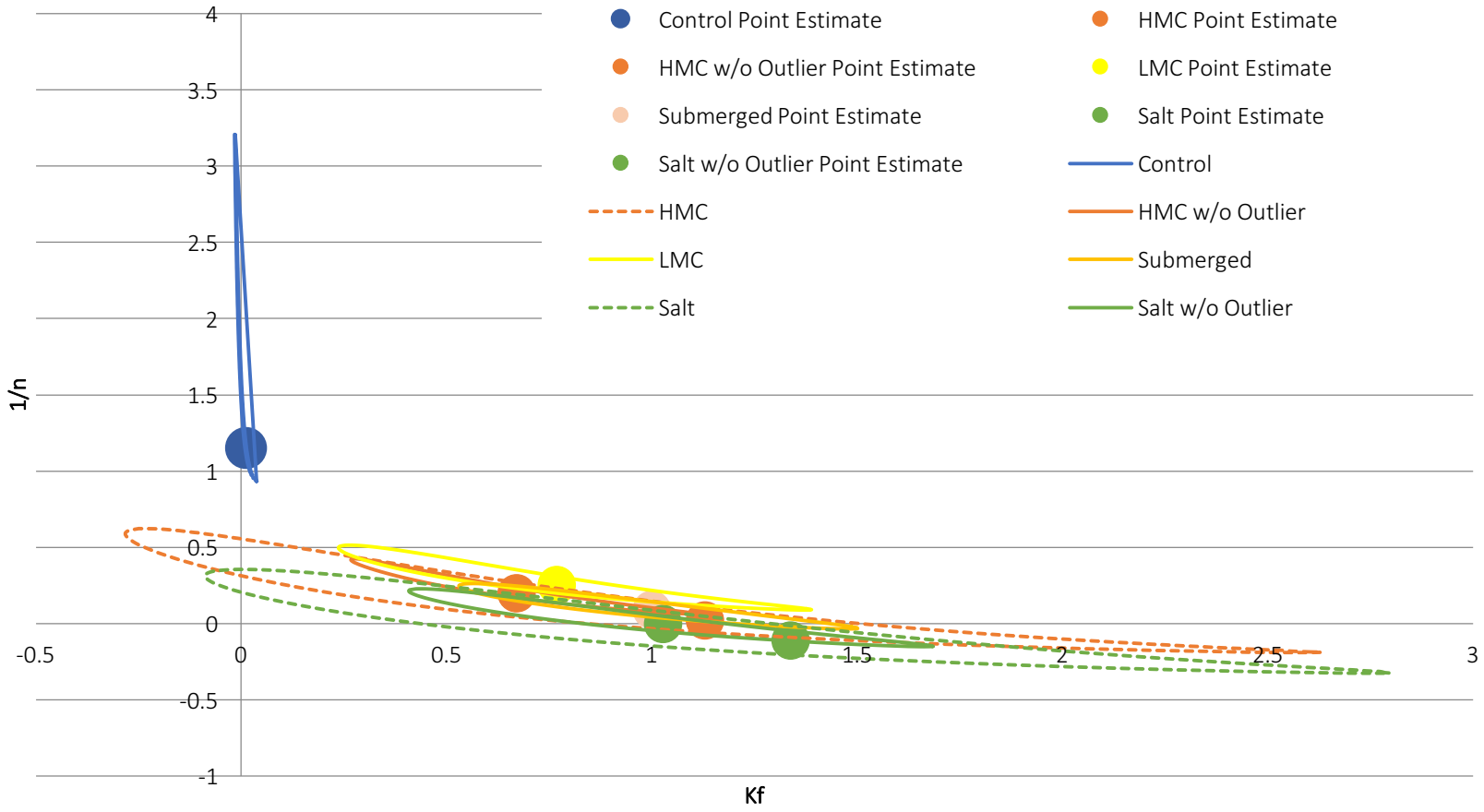

Figure 4.16 Joint confidence regions (95%) for stored F300

The storage methods confidence regions are clumped tightly; to better visualize any differences Figure 4.12 shows only the storage methods, with outliers and the operational control excluded. At this level, it is apparent that only the joint confidence regions for the LMC and salt storages are statistically different from each other, as all other confidence regions intersect.

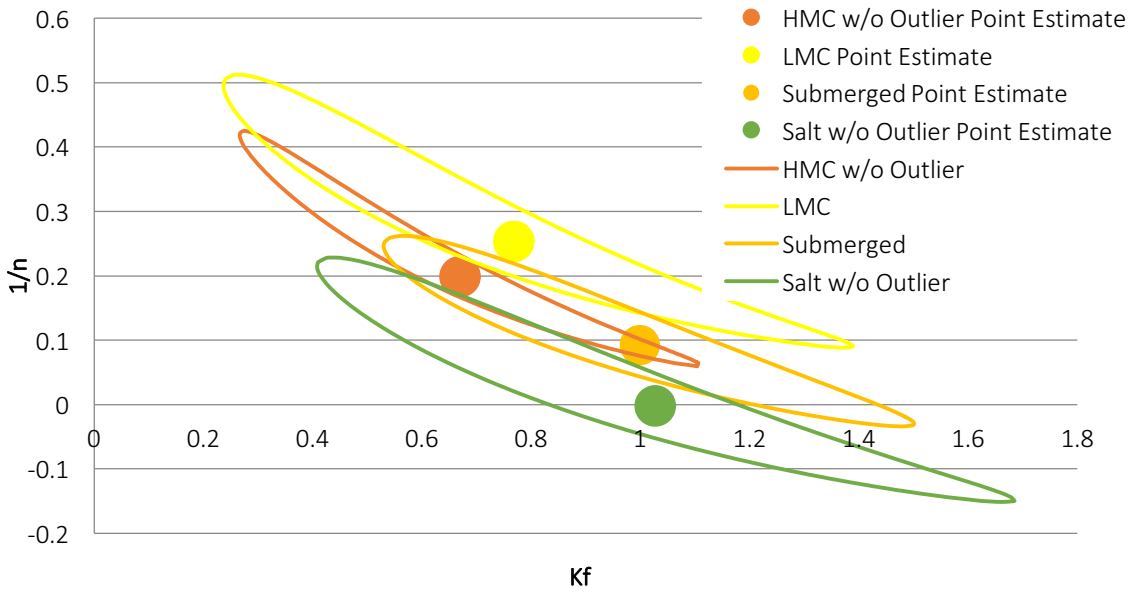

Figure 4.17 Comparison of joint confidence regions for storage methods (excluding outliers)

In order to further conceptualize this, Table 4.6 and Figure 4.18 shows the corresponding predicted solid phase concentration at various aqueous phase concentrations. Without considering outliers, at the lowest aqueous MC-LR concentration the salt treatment shows the highest solid phase concentration and the control shows the lowest. At the middle aqueous MC-LR phase concentration, the LMC shows the highest solid phase

concentration, and the control shows the lowest. At the highest aqueous MC-LR phase concentration, the LMC again shows the highest solid phase concentration, and the salt storage shows the lowest. This indicates that at the higher concentrations, the LMC storage will outperform the other storage methods. Due to the slope of the isotherm (namely 1/n) this does not hold for all concentrations, and the salt storage will dominate at the low end of the aqueous concentration spectrum. When the 95% prediction intervals are considered, it can be seen that there are no differences in the predicted solid phase concentrations due to the overlapping regions. This must be considered with caution, as there may be differences in the treatment which are not detectable at the 95% confidence level.

Table 4.6 Predicted equilibrium solid phase concentration for various equilibrium aqueous concentrations of MC-LR (C) with 95% prediction intervals shown in brackets

Carbon	**C= 1 µg/L**	**C = 10 µg/L**	**C = 100 µg/L**
	q_e (µg MC-LR/mg GAC)		
Control	0.01 (-0.51-0.53)	0.16 (-0.36-0.69)	2.32 (1.16-3.48)
HMC	1.11 (-0.23-2.44)	1.19 (-0.20-2.57)	1.27 (-0.17-2.71)
HMC w/o Outlier	0.67 (0.22-1.12)	1.06 (0.52-1.60)	1.68 (0.96-2.39)
LMC	0.77 (0.14-1.40)	1.38 (0.61-2.14)	2.47 (1.38-3.56)
Submerged	1.00 (0.25-1.75)	1.24 (0.40-2.08)	1.53 (0.58-2.48)
Salt	1.34 (0.14-1.40)	1.04 (0.61-2.14)	0.81 (1.38-3.56)
Salt w/o Outlier	1.03 (0.14-1.40)	1.02 (0.61-2.14)	1.02 (1.38-3.56)

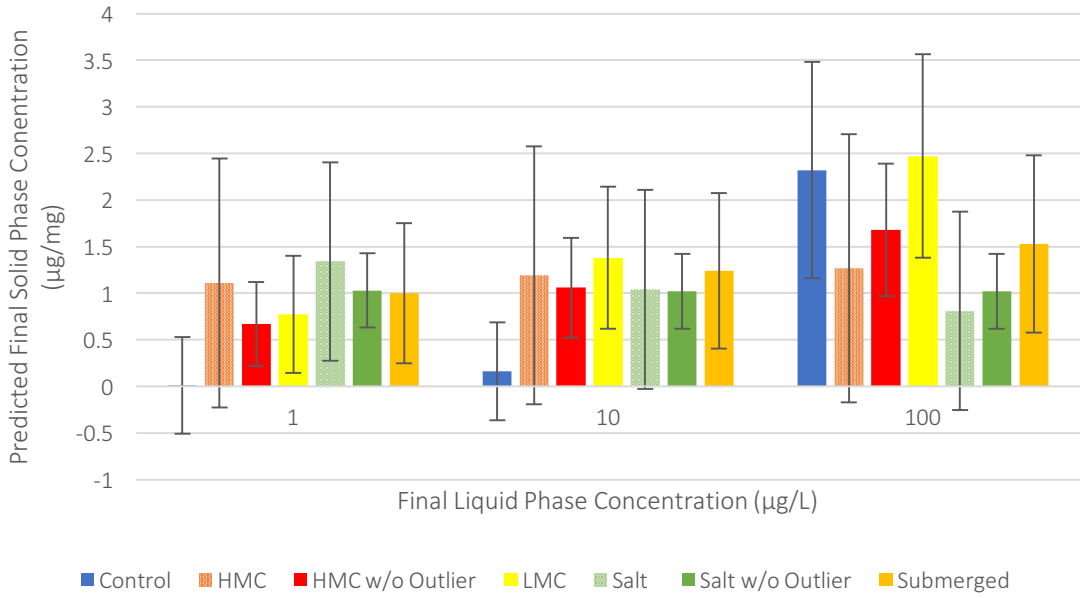

Figure 4.18 Predicted final MC-LR solid phase concentration with 95% prediction intervals

4.5.1.1 Comparison with Preloaded and Virgin F300 Isotherms

The virgin and preloaded F300, discussed in Chapter 3, are compared with the storage methods using the Freundlich isotherm in Figure 4.19. Figure 4.20 shows a comparison of the 95% joint confidence regions for the Freundlich isotherm parameters. The continuous operational control does not cross into the banana shaped joint confidence regions, and is therefore distinct from the virgin and preloaded isotherm parameters at the 95% confidence level. In order to further examine the storage methods, Figure 4.21 examines the joint confidence regions excluding the continuous operation control and the outliers. At the 95% confidence level, the virgin, preloaded and LMC stored carbon JCRs are not distinct. Although capacity cannot be directly determined simply by examining the

Freundlich parameters, the results suggest that the storage of the F300 under LMC conditions provides a benefit in terms of equilibrium capacity. The HMC, submerged and salt storage isotherm parameters are different from the virgin and preloaded at the 95% confidence level. Based on the fitted isotherm parameters and table 4.6, at higher concentrations the LCM could outperform the remaining storage techniques for the removal of MC-LR, although the prediction intervals indicated that this difference is not statistically significant with the available data set. Additional data from future experiments might be able to demonstrate a statistically significant difference.

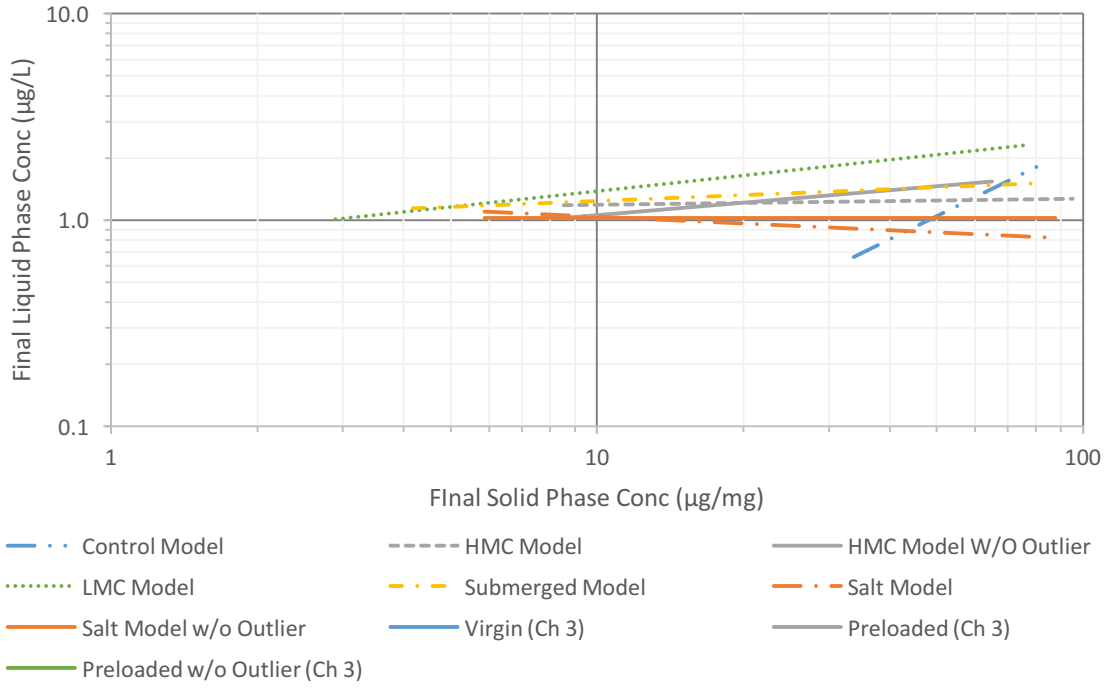

Figure 4.19 Comparison of virgin and preloaded Freundlich isotherm models with storage methods

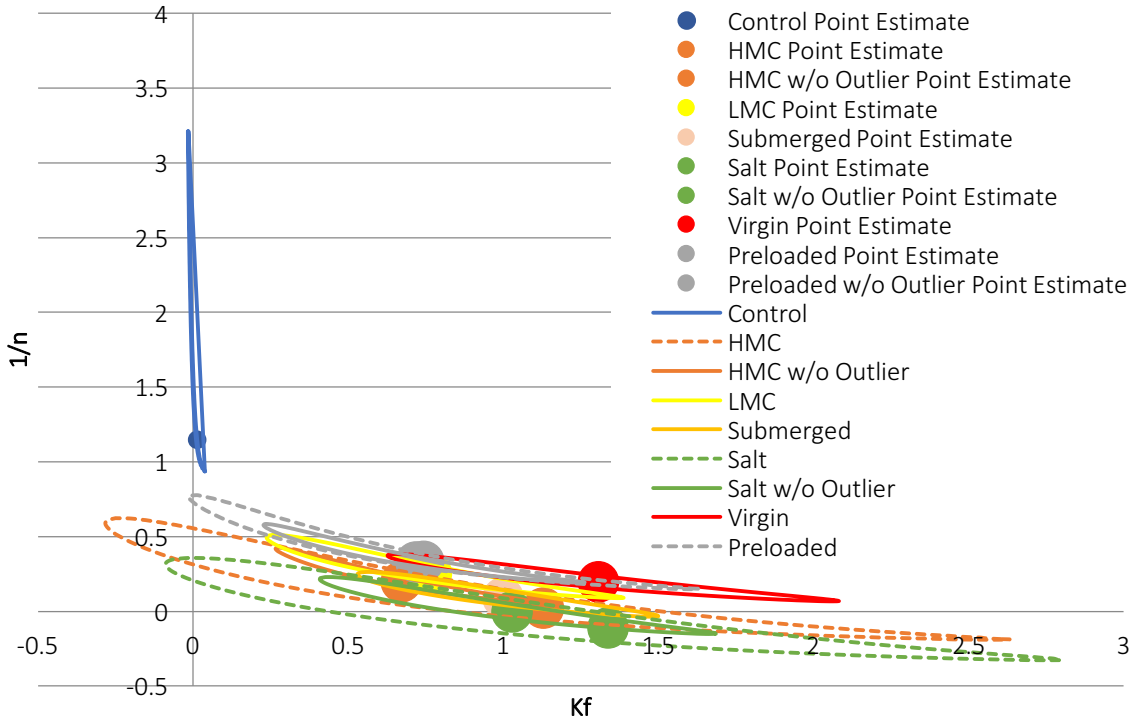

Figure 4.20 Freundlich isotherm parameter 95% joint confidence regions

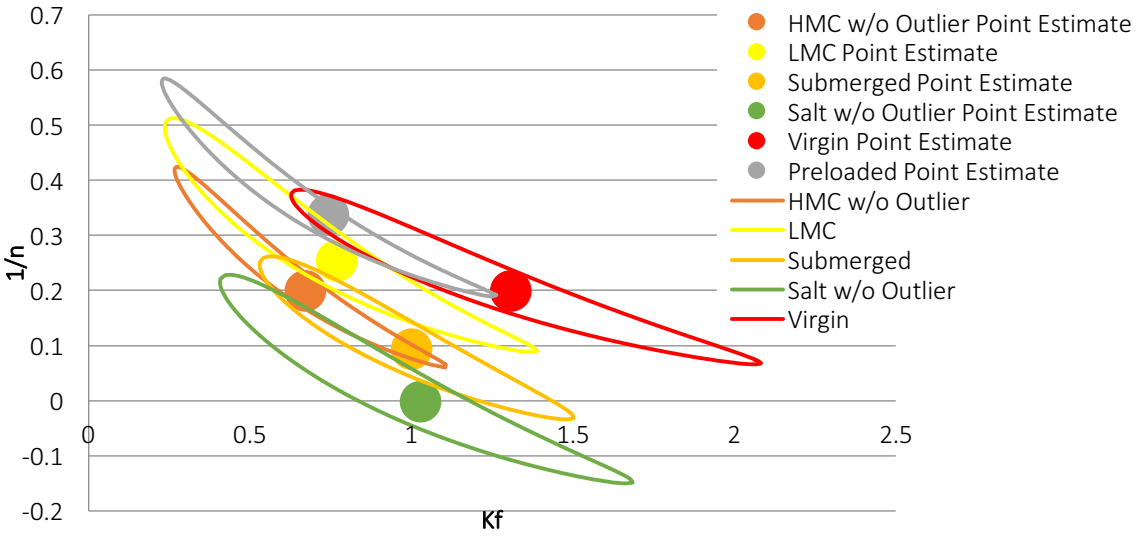

Figure 4.21 Joint confidence regions (95%) for the stored, virgin and preloaded F300, excluding the control and outliers

4.6 Conclusions

The preloaded carbon discussed in Chapter 3 was stored under four different conditions, while a control continued in operation in parallel to simulate a GAC contactor which remained in operation year-round. The stored carbon was sampled bimonthly and monitored for moisture content and biomass (ATP). Limited changes in moisture content were observed, indicating that the storage vessels were properly sealed. ATP analysis indicated that only the control was in the beginning stages of being biologically active. The continuous operation control was monitored for TOC, DOC and NOM. The average influent DOC was 2.18 mg/L and upwards of 90% DOC breakthrough was observed. Humics were the largest contributor to NOM, and a similar breakthrough trend was observed compared to DOC.

Following the 8-month storage period, the GAC was freeze-dried and bottle point kinetic and isotherm studies were conducted, in addition to surface charge analysis (pH_{PZC}). The surface charge of all GACs stored using 4 distinct methods further converged, to between a pH_{PZC} of 6.6-6.9 which was similar to the preloaded GAC. The salt storage displayed the fastest MC-LR kinetics, and reached equilibrium after 41 days; the submerged storage displayed the slowest kinetics and reached equilibrium after 57 days. Pseudo-first order kinetics better modelled the removal of MC-LR over time at the higher GAC doses. There was benefit in terms of equilibrium capacity to be gained from taking the GAC off line and storing it, under any of the conditions considered, during the non-MC-LR portion of the year when compared to the continuous operation control. All of the stored GACs

parameters were statistically different from the operational control. The stored carbons would likely be better able to remove MC-LR at typical concentration ranges, based on the Freundlich isotherms parameters. At the 95% confidence level, the LMC storage outperformed the salt treatment at high concentration ranges when the parameters (JCR) are considered. There was no statistical difference between the HMC, submerged, and salt storage Freundlich parameters. As well, there was no statistical difference between the HMC, submerged, and the LMC storage conditions when the Freundlich parameters (JCRs) are considered. When the broader prediction intervals are considered, there was no significant difference in any of the predicted solid phase concentrations when considering various liquid phase concentrations. This finding indicates that non-detectable differences may be present, due to the data quality.

When compared with the virgin and preloaded F300 there was no statistical difference with the LMC storage, indicating that the equilibrium capacity is preserved during storage under the LMC conditions. The remainder of the storage techniques were different from the virgin and preloaded at the 95% confidence level and showed decreased removal for MC-LR.

5 Conclusions and Recommendations

A detailed literature review was conducted to examine the properties and removal mechanisms for MC-LR on a seasonal basis. GAC was selected as a promising treatment technology for the removal of MC-LR, for application on a seasonal basis. Calgon F300 was selected as a commonly used GAC in the study region, and preloaded to simulate one season of use using post-filtration water from the Region of Durham Drinking Water Treatment Facility on Lake Ontario. During the MC-LR free portion of the year the GAC was stored under four conditions for eight (8) months: submerged in filtered Lake Ontario water, in a 20 g/L salt solution, low moisture content, and high moisture content representing the top and bottom of a drained contactor, respectively. In order to simulate a GAC contactor remaining in operation, an operational pilot contactor control remained in operation at the full-scale plant, at the same hydraulic loading rate as an existing full-scale anthracite/sand filter at the plant. The virgin, preloaded, stored, and operational control F300 were assessed for biological activity (ATP), surface charge (pH_{PZC}), kinetics of MC-LR removal and equilibrium capacity for MC-LR by generating Freundlich isotherms. These studies were conducted in ultrapure water. The conclusions from this work are summarized below, along with recommendations for future work. MC-LR was quantified using LC-MS/MS with direct injection.

5.1 Virgin and Preloaded F300 for the Removal of MC-LR

- Using the bottle point method, virgin F300 reached equilibrium after 18 days. Preloaded F300 GAC displayed much slower kinetics for MC-LR removal than virgin F300, and reached equilibrium after 49 days.
- Both pseudo-second and –first order kinetics described MC-LR removal by virgin and preloaded F300 over time. Generally, the virgin F300 MC-LR removal kinetics were marginally better predicted by the pseudo-second order model. The preloaded MC-LR removal kinetics were marginally better predicted by the pseudo-first order model. For both model a poor fit was observed at the lower GAC doses, due to experimental variability.
- The virgin F300 appeared to have a higher capacity than the preloaded F300 for the removal of MC-LR. However, at the 95% confidence level, there was no statistical change in isotherm parameters between the virgin and preloaded F300; there was no statistically significant loss of capacity following preloading. This was somewhat unexpected and may be attributable to the fact that only one season of preloading was conducted, and the adsorption sites used for MC-LR were not significantly filled.
- The virgin F300 pH_{PZC} was 10.2. Following preloading, the surface charge of the F300 was reduced to 7.2. The implication of this was that any benefit from the high pH_{PZC}, for example attraction of negatively charged NOM, is negated following one season of preloading.

5.2 The Storage of Preloaded F300 and the Removal of MC-LR

- There was benefit in terms of equilibrium capacity to be gained from taking the GAC off-line and storing it, under all of the conditions considered, during the MC-LR free portion of the year when compared to the continuous operation control.
- When compared with the virgin and preloaded F300 there was no statistical difference with the low moisture content storage, indicating that the equilibrium capacity is preserved during storage under the low moisture content conditions. The remainder of the storage techniques were different from the virgin and preloaded at the 95% confidence level.
- Of the stored carbons, the salt storage displayed the fastest kinetics for MC-LR removal, and reached equilibrium after 41 days; the submerged storage displayed the slowest kinetics and reached equilibrium after 57 days. All of the stored carbon performed similarly in terms of kinetics.
- Pseudo-first and –second order kinetic models were both examined. The pseudo-first order model was generally more predictive of the equilibrium MC-LR solid phase concentration. At the lowest carbon doses the data quality was generally poor as there may only be three grains of GAC. With very small doses, problems affecting one or more grains are magnified as there are insufficient grains to smooth out problems with even one grain (different levels of inactivation, grains sticking to glassware above or below the water line, etc.).

- There was no statistical difference between the high moisture content storage, submerged, and salt storage in terms of Freundlich isotherm parameters. As well, there was no statistical difference between the high moisture content, submerged, and the low moisture content storage conditions. This indicates that these storage methods would perform similarly, as the equilibrium parameters are not unique at the 95% confidence level.
- Low level biological activity was observed in the operational control GAC contactor (as quantified by ATP). However, there was little evidence of biological activity under the remaining storage conditions, even in the submerged condition, where water was replaced monthly.
- The pH_{PZC} for all of the stored F300 samples remained neutral and ranged from 6.6-6.9, similar to the preloaded carbon before storage.

5.3 Recommendations for Future Work

Over the course of this work, several recommendations for future work were identified including:

- In order to further evaluate MC-LR removal over time and better compare to a full-scale contactor or filter containing GAC, column tests and pilot set ups should be utilized to acquire site-specific data. This will allow for more detailed breakthrough models to be developed.
- When GAC is used to remove MC-LR on a seasonal basis, desorption of MC-LR may occur. The desorption of MC-LR during storage should be evaluated. In addition,

the amount of desorption occurring when the GAC is brought back into service should be evaluated.

- In order to further evaluate how a full-scale GAC contactor will perform, the water to be treated should be used as the feed to bench- or pilot-scale setups to accurately assess competition effects. This will determine the reduction in MC-LR removal due to the competition of NOM with MC-LR for adsorption sites.
- Additional investigations are recommended to evaluate other seasonally occurring compounds, including other cyanotoxins and taste and odour compounds.
- Additional investigations and comparison with other commonly used GACs, are needed as the literature is sparse on well-developed isotherm studies.

References

Acero, J. L., Rodriguez, E., & Meriluoto, J. (2005). Kinetics of reactions between chlorine and the cyanobacterial toxins microcystins. *Water Research*, *39*(8), 1628–1638.

Andrews, R. C. (1990). *Removal of Low Concentrations of Chlorination By-Products using Activated Carbon*. University of Alberta.

ASTM International. (2011). *Standard Practice for Reducing Samples of Aggregate to Testing Size*. *C702/C702M-11*.

ASTM International. (2013). Standard Test Methods for Moisture in Activated Carbon, D2687-09 (Reapproved 2008).

Calgon Carbon. (2012). *Filtrasorb ® 300 [Product Bulletin]*.

Carey, C. C., Ibelings, B. W., Hoffmann, E. P., Hamilton, D. P., & Brookes, J. D. (2012). Eco-physiological adaptations that favour freshwater cyanobacteria in a changing climate. *Water Research*, *46*(5), 1394–1407.

Carmichael, W. W. (1992). Cyanobacteria secondary metabolites - the cyanotoxins. *Journal of Applied Bacteriology*, *72*, 445–459.

Carter, M. C., Weber, W. J. J., & Olmstead, K. P. (1992). Effects of Background Dissolved Organic Matter on TCE Adsorption by GAC. *Journal of American Water Works Assosiation*, *84*, 81–91.

Chen, J. J., & Yeh, H. H. (2005). The mechanisms of potassium permanganate on algae removal. *Water Research*, *39*(18), 4420–4428.

Cheng, P., Ge, F., Liu, X., Zeng, X., & Chen, B. (2015). Coagulation performance and floc

properties of *Microcystis aeruginosa* in the presence of humic acid. *Water Science & Technology: Water Supply*, *15*(2), 339.

City of Toledo Department of Public Utilities. (2014). Microcystin Event Preliminary Screening. Toledo.

Coral, L. A., Zamyadi, A., Barbeau, B., Bassetti, F. J., Lapolli, F. R., & Prévost, M. (2013). Oxidation of Microcystis aeruginosa and Anabaena flos-aquae by ozone: Impacts on cell integrity and chlorination by-product formation. *Water Research*, *47*(9), 2983–2994.

Corwin, C. J., & Summers, R. S. (2011). Adsorption and desorption of trace organic contaminants from granular activated carbon adsorbers after intermittent loading and throughout backwash cycles. *Water Research*, *45*(2), 417–26.

Cousins, I. T., Bealing, D. J., James, H. A., & Sutton, A. (1996). Biodegradation of microcystin-LR by indigenous mixed bacterial populations. *Water Research*, *30*(2), 481–485.

Crittenden, J. C., Trussell, R. R., Hand, D. W., Howe, K. J., & Tchodanoglous, G. (2012). *MWH's Water Treatment: Principals and Design* (Third). Hoboken: John Wiley & Sons, Inc.

De Maagd, P. G. J., Hendriks, A. J., Seinen, W., & Sijm, D. T. H. M. (1999). pH-dependent hydrophobicity of the cyanobacteria toxin microcystin-LR. *Water Research*, *33*(3), 677–680.

DeVries, S. L., Liu, W., Wan, N., Zhang, P., & Li, X. (2012). Biodegradation of MIB,

geosmin and microcystin-LR in sand columns containing Taihu lake sediment. *Water Science and Technology: Water Supply*, *12*(5), 691–698.

Droste, R. L. (1997). *Theory and practice of water and wastewater treatment*. Hoboken: John Wiley & Sons, Inc.

Dyble, J., Fahnenstiel, G. L., Litaker, R. W., Millie, D. F., & Tester, P. A. (2008). Microcystin concentrations and genetic diversity of Microcystis in the lower Great Lakes. *Environmental Toxicology*, *23*(4), 507–516.

Falconer, I. R. (2005). Is there a human health hazard from microcystins in the drinking water supply? *Acta Hydrochimica et Hydrobiologica*, *33*(1), 64–71.

Falconer, I. R., Beresford, A. M., & Runnegar, T. C. (1983). Evidence of liver damage by toxin from a bloom of the blue-green alga, Microcystis aeuginosa. *The Medical Journal of Australia*, *1*, 511–514.

Falconer, I. R., Runnegar, T. C., Buckley, T., Huyn, V. L., & Bradshaw, P. (1989). Using activated carbon to remove toxicity from drinking water containing cyanobacterial blooms. *Journal of American Water Works Assosiation*, 102–105.

Fawell, J. K., Hart, J., James, H. A., & Parr, W. (1993). Blue-green algae and their toxins - analysis, toxicity, treatment and environmental control. *Water Supply*, *11*(3/4), 109–121.

Fogg, G. E. (1968). The physiology of an algal nuisance. *Royal Society London*.

Francis, G. (1878). Poisonous Australian Lake.

Freundlich, H. (1926). *Solid and Capillary Chemistry*. London: Methuen & Co.

Gijsbertsen-Abrahamse, A. J., Schmidt, W., Chorus, I., & Heijman, S. G. J. (2006). Removal of cyanotoxins by ultrafiltration and nanofiltration. *Journal of Membrane Science*, *276*(1-2), 252–259.

Gillogly, T. E. T., Snoeyink, V. L., Vogel, J. C., Wilson, C. M., & Royal, E. P. (1999). Determining GAC bed life. *Journal of American Water Works Assosiation*, *91*(8), 98–110.

Gonzalez-Torres, A., Putnam, J., Jefferson, B., Stuetz, R. M., & Henderson, R. K. (2014). Examination of the physical properties of Microcystis aeruginosa flocs produced on coagulation with metal salts. *Water Research*, *60*, 197–209.

Health Canada. (2016). *Cyanobacterial Toxins in Drinking Water*.

Himberg, K., Keijola, A. M., Hiisvirta, L., Pyysalo, H., & Sivonen, K. (1989). The effect of water treatment processes on the removal of hepatotoxins from microcystis and oscillatoria cyanobacteria: a laboratory study. *Water Research*, *23*(8), 979–984.

Ho, L., Lambling, P., Bustamante, H., Duker, P., & Newcombe, G. (2011). Application of powdered activated carbon for the adsorption of cylindrospermopsin and microcystin toxins from drinking water supplies. *Water Research*, *45*(9), 2954–2964.

Ho, L., Meyn, T., Keegan, A., Hoefel, D., Brookes, J., Saint, C. P., & Newcombe, G. (2006). Bacterial degradation of microcystin toxins within a biologically active sand filter. *Water Research*, *40*(4), 768–774.

Ho, L., & Newcombe, G. (2007). Evaluating the adsorption of microcystin toxins using

granular activated carbon (GAC). *Journal of Water Supply: Research and Technology - AQUA*, *56*(5), 281–291.

Ho, L., Onstad, G., Gunten, U. Von, Rinck-Pfeiffer, S., Craig, K., & Newcombe, G. (2006). Differences in the chlorine reactivity of four microcystin analogues. *Water Research*, *40*(6), 1200–1209.

Ho, L., Sawade, E., & Newcombe, G. (2012). Biological treatment options for cyanobacteria metabolite removal - A review. *Water Research*, *46*(5), 1536–1548.

Ho, Y. S., & McKay, G. (1999). Pseudo-second order model for sorption processes. *Process Biochemistry*, *34*(5), 451–465.

Hoffmann, J. R. H. (1976). Removal of Microcystis in Water Purification Processes. *Water SA*.

Huang, W.-J., Cheng, B.-L., & Cheng, Y.-L. (2007). Adsorption of microcystin-LR by three types of activated carbon. *Journal of Hazardous Materials*, *141*(1), 115–122.

Huber, S. A., Balz, A., Abert, M., Pronk, W. 2011. Characterisation of aquatic humic and non-humic matter with size-exclusion chromatography – organic carbon detection – organic nitrogen detection (LC-OCD-OND).

IPCC. (2013). *Summary for Policymakers. In: Climate Change 2013: The Physical Science Basis. Contribution of Working Group I to the Fifth Assessment Report of the Intergovernmental Panel on Climate Change*. Cambridge, United Kingdon and New York, NY, USA.

Izaguirre, G., & Taylor, W. (2004). A guide to geosmin-and MIB-producing cyanobacteria

in the United States. *Water Science & Technology*, *49*(9), 19–24.

Jochimsen, E. M., Carmichael, W. W., An, J., Cardo, D. M., Cookson, S. T., Holmes, C. E. M., Jarvis, W. R. (1998). Liver Failure and Death After Exposure To Microcystins at a Hemodialysis Center in Brazil. *Water*, *338*(13), 873–878.

Julio, M. de F. de J. L. (2011). *Carbon key-properties for microcystin adsorption in drinking water treatment: Structure or surface chemistry ?* Universidade Nova De Lisboa.

Keijola, a. M., Himberg, K., Esala, a. L., Sivonen, K., & Hiis-Virta, L. (1988). Removal of cyanobacterial toxins in water treatment processes: Laboratory and pilot-scale experiments. *Toxicity Assessment*, *3*(5), 643–656.

Knappe, D. R. U., Snoeyink, V. L., Roche, P., Prados, M. J., & Bourbigot, M.-M. (1999). Atrazine removal by preloaded GAC. *Journal of American Water Works Assosiation*, *91*(10), 97–109.

Kull, T. P. J., Sjövall, O. T., Tammenkoski, M. K., Backlund, P. H., & Meriluoto, J. A. O. (2006). Oxidation of the cyanobacterial hepatotoxin microcystin-LR by chlorine dioxide: Influence of natural organic matter. *Environmental Science and Technology*, *40*(5), 1504–1510.

Lagergren, S. Y. (1898). *Zur Theorie der sogenannten Adsorption Geloster Stoffe*. Stockholm.

Lambert, T. W., Holmes, C. F., & Hrudey, S. E. (1996). Adsorption of microcystin-LR by activated carbon and removal in full scale water treatment. *Water Research*, *30*(6),

1411–1422.

Liu, I., Lawton, L. a., Bahnemann, D. W., Liu, L., Proft, B., & Robertson, P. K. J. (2009). The photocatalytic decomposition of microcystin-LR using selected titanium dioxide materials. *Chemosphere*, *76*(4), 549–553.

MacKintosh, C., Beattie, K. A., Klumpp, S., Cohen, P., & Codd, G. A. (1990). Cyanobacterial microcystin-LR is a potent and specific inhibitor of protein phosphatases 1 and 2A from both mammals and higher plants. *FEBS Letters*, *264*(2), 187–192.

McMlure, A., & Megonnell, N. (2001). Filtering out carbon myths: The facts are essential in choosing the right carbon for the job [Technical Pages]. *Water Technology*, *24*(2), 58–62.

Mohamed, Z. A., Carmichael, W. W., An, J., & El-Sharouny, H. M. (1999). Activated carbon removal efficiency of microcystins in an aqueous cell extract of Microcystis aeruginosa and Oscillatoria tenuis strains isolated from Egyptian freshwaters. *Environmental Toxicology*, *14*(1), 197–201.

National Oceanic and Atmospheric Administration. (2016). *Experimental Lake Erie Harmful Algal Bloom Bulletin*.

Newcombe, G., Cook, D., Brooke, S., Ho, L., & Slyman, N. (2003). Treatment options for microcystin toxins: similarities and differences between variants. *Environmental Technology*, *24*(3), 299–308.

Nicholson, B. C., Rositano, J., & Burch, M. D. (1994). Destruction of cyanobacterial

peptide hepatotoxins by chlorine and chloramine. *Water Research*, *28*(6), 1297–1303.

O'Neil, J. M., Davis, T. W., Burford, M. A., & Gobler, C. J. (2012). The rise of harmful cyanobacteria blooms: The potential roles of eutrophication and climate change. *Harmful Algae*, *14*, 313–334.

Onstad, G. D., Strauch, S., Meriluoto, J., Codd, G. A., & Von Gunten, U. (2007). Selective oxidation of key functional groups in cyanotoxins during drinking water ozonation. *Environmental Science and Technology*, *41*(12), 4397–4404.

Ontario. (2006). *Technical Support Document for Ontario Drinking Water Standards , Objectives and Guidelines*.

Paerl, H. W. (1988). Nuisance phytoplankton blooms in coastal, estuarine, and inland water. *Limnology and Oceanography*, *33*(2), 823–847.

Paerl, H. W., & Fulton, R. S. I. (2006). *Ecology of Harmful Cyanobateria*. *Ecological Studies* (Vol. 189). Berlin Heidelberg.

Paerl, H. W., & Huisman, J. (2008). Blooms like it hot. *Science (New York, N.Y.)*, *320*(5872), 57–58.

Paerl, H. W., & Huisman, J. (2009). Climate change: A catalyst for global expansion of harmful cyanobacterial blooms. *Environmental Microbiology Reports*, *1*(1), 27–37.

Paerl, H. W., & Paul, V. J. (2012). Climate change: Links to global expansion of harmful cyanobacteria. *Water Research*, *46*(5), 1349–1363.

Pharand, L., Dyke, M. I. V. A. N., Anderson, W. B., & Huck, P. M. (2014). Assessment of

biomass in drinking water biofilters by adenosine triphosphate. *American Water Works Association*, (October), 433–444.

Randtke, S. J., & Snoeyink, V. L. (1983). Evaluating GAC adsorptive capacity. *Journal of American Water Works Assosiation*, *75*(8), 406–413.

Reynolds, C. S. (1987). The response of phytoplankton communities to changing lake environments. *Swiss Journal of Hydrology*, *49*(2), 220–236.

Ribau Teixeira, M., & Rosa, M. J. (2006). Neurotoxic and hepatotoxic cyanotoxins removal by nanofiltration. *Water Research*, *40*(15), 2837–2846.

Rice, E.W., Baird, R.B., Eaton, A.D., Clesceri, L. S. (Ed.). (2012). *Standard Methods for the Examination of Water and Wastewater* (22nd ed.). American Public Health Association.

Rinta-Kanto, J. M., Ouellette, A. J. A., Boyer, G. L., Twiss, M. R., Bridgeman, T. B., & Wilhelm, S. W. (2005). Quantification of toxic Microcystis spp. during the 2003 and 2004 blooms in western Lake Erie using quantitative real-time PCR. *Environmental Science and Technology*, *39*(11), 4198–4205.

Rodríguez, E., Onstad, G. D., Kull, T. P. J., Metcalf, J. S., Acero, J. L., & von Gunten, U. (2007). Oxidative elimination of cyanotoxins: Comparison of ozone, chlorine, chlorine dioxide and permanganate. *Water Research*, *41*(15), 3381–3393.

Rositano, J., Newcombe, G., Nicholson, B., & Sztajnbok, P. (2001). Ozonation of nom and algal toxins in four treated waters. *Water Research*, *35*(1), 23–32.

Schopf, J. W. (2006). Fossil evidence of Archaean life. *Philosophical Transactions of the*

Royal Society of London. Series B, Biological Sciences, *361*(1470), 869–885.

Sontheimer, H, Crittenden, J.C., Summers, R.S.. 1988. Activated carbon for water treatment. DVGW- Forschungsstelle, Engler-Bunte-Institut, Universitat Karlsruhe (TH), p. 1-722.

Sorlini,Steinberg, C. E. W., & Hartmann, H. M. (1988). Planktonic bloom-forming Cyanobacteria and the eutrophication of lakes and rivers. *Freshwater Biology*, *20*, 279–287.

Summers, R.S. 1986. Activated carbon adsorption of humic substances: Effect of molecular size and heterodispersity. PhD thesis, Department of Civil Engineering, Stanford University.

Svrcek, C., & Smith, D. W. (2004). Cyanobacteria toxins and the current state of knowledge on water treatment options: a review. *Journal of Environmental Engineering and Science*, *3*(3), 155–185.

Teixeira, M. R., & Rosa, M. J. (2006). Comparing dissolved air flotation and conventional sedimentation to remove cyanobacterial cells of Microcystis aeruginosa. Part II. The effect of water background organics. *Separation and Purification Technology*, *52*, 84–94.

Tsuji, K., Watanuki, T., Kondo, F., Watanabe, M. F., Suzuki, S., Nakazawa, H., Harada, K. (1994). Stability of microcystins from cyanobacteria: Effect of light on decomposition and isomerization. *Environmental Science and Technology*, *28*, 173–177.

U.S. EPA. (2015). *Drinking Water Health Advisory for the Cyanobacterial Microcystin Toxins*.

United Nations, Development of Economic and Social Affairs, P. D. (2015). *World population prospects: The 2015 revision, key findings and advance tables*. *Working Paper No. ESA.P.WP.241*.

Vlad, S. (2015). *Treatment of the Cyanotoxin Anatoxin-a via Activated Carbon Adsorption*. University of Waterloo.

Wang, Q., You, W., Li, X., Yang, Y., & Liu, L. (2014). Seasonal changes in the invertebrate community of granular activated carbon filters and control technologies. *Water Research*, *51*, 216–27.

Watson, S. B., Ridal, J., & Boyer, G. L. (2008). Taste and odour and cyanobacterial toxins: impairment, prediction, and management in the Great Lakes. *Canadian Journal of Fisheries and Aquatic Sciences*, *65* (April 2016), 1779–1796.

Welker, M., & Steinberg, C. (1999). Indirect photolysis of cyanotoxins: One possible mechanism for their low persistence. *Water Research*, *33*(5), 1159–1164.

Westrick, J. A., Szlag, D. C., Southwell, B. J., & Sinclair, J. (2010). A review of cyanobacteria and cyanotoxins removal/inactivation in drinking water treatment. *Analytical and Bioanalytical Chemistry*, *397*(5), 1705–14.

Wheeler, R. E., Lackey, J. B., & Schott, S. (1942). A Contribution of the Toxicity of Algae. *Public Health Reports*, *57*(45), 1695–1701.

Wiedner, C., Rucker, J., Bruggemann, R., & Nixdorf, B. (2007). Climate change affects

timing and size of populations of an invasive cyanobacterium in temperate regions. *Oecologia*, *152*(3), 473–484.

Wood, S. A., Holland, P. T., Stirling, D. J., Briggs, L. R., Sprosen, J., Ruck, J. G., & Wear, R. G. (2006). Survey of cyanotoxins in New Zealand water bodies between 2001 and 2004. *New Zealand Journal of Marine and Freshwater Research*, *40*(4), 585–597.

Worch, E. (2012). *Adsorption technology in water treatment*. Germany: De Gruyter.

World Health Organization. (1999). *Toxic cyanobacteria in water: A guide to public health consequences, monitoring and management*. (I. Chorus & J. Bartram, Eds.). E & FN Spon.

World Health Organization. (2011). *Management of Cyanobacteria in Drinking Water Supplies : Information for regulators and water suppliers*.

World Health Organization. (2011). *Guidelines for Drinking-water Quality: Fourth Edition*. *World Health Organization*.

Xagoraraki, I., Harrington, G. W., Zulliger, K., Zeier, B., Krick, W., Karner, D. A., Westrick, J. (2006). Inactivation Kinetics of the Cyanobacterial Toxin Microcystin-LR by Free Chlorine. *Journal of Environmental Engineering*, *132*(7), 818–823.

Yu, Z. (2007). Analysis of Selected Pharmaceuticals and Endocrine Disrupting Compounds and their Removal by Granular Activated Carbon in Drinking Water Treatment. PhD Theis. University of Waterloo.

Zamyadi, A., Dorner, S., Sauvé, S., Ellis, D., Bolduc, A., Bastien, C., & Prévost, M. (2013). Species-dependence of cyanobacteria removal efficiency by different drinking

water treatment processes. *Water Research*, *47*(8), 2689–2700.

Zhang, H., Huang, Q., Ke, Z., Yang, L., Wang, X., & Yu, Z. (2012). Degradation of microcystin-LR in water by glow discharge plasma oxidation at the gas-solution interface and its safety evaluation. *Water Research*, *46*(19), 6554–6562.

Zhang, H., Zhu, G., Jia, X., Ding, Y., Zhang, M., Gao, Q., Xu, S. (2011). Removal of microcystin-LR from drinking water using a bamboo-based charcoal adsorbent modified with chitosan. *Journal of Environmental Sciences*, *23*(12), 1983–1988.

Zhang, M., Duan, H., Shi, X., Yu, Y., & Kong, F. (2012). Contributions of meteorology to the phenology of cyanobacterial blooms: Implications for future climate change. *Water Research*, *46*(2), 442–452.

Appendix A LC-MS/MS Calibration Examples and QA/QC

QA/QC Procedure:

Calibrate at the start of every run

Inject a mid-level calibration standard (50 μg/L) the more frequency of once per run or every 10% of samples

Example Calibration Run:

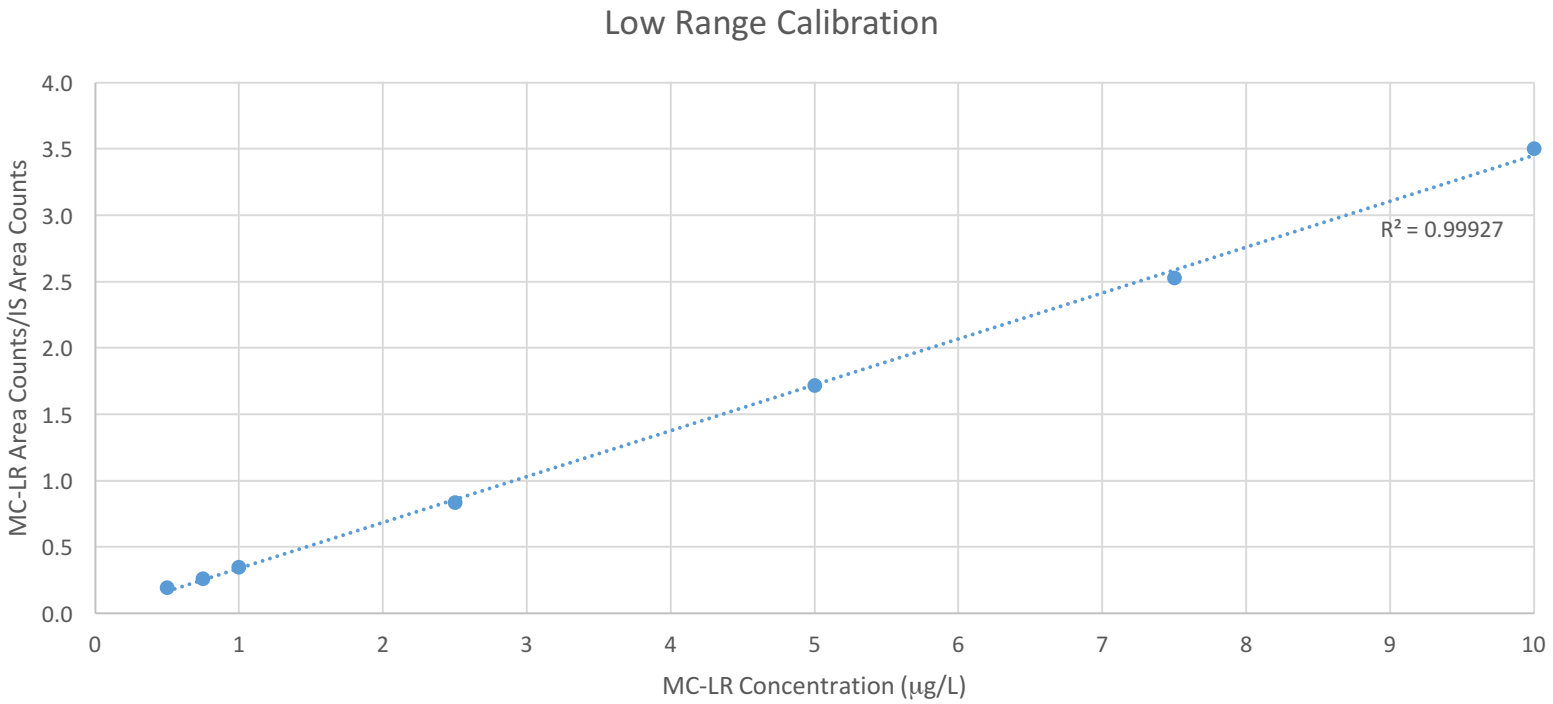
Low Range Calibration
MC-LR Area Counts/IS Area Counts
MC-LR Concentration (µg/L)
R² = 0.99927
0.0
0.5
1.0
1.5
2.0
2.5
3.0
3.5
4.0
0
1
2
3
4
5
6
7
8
9
10

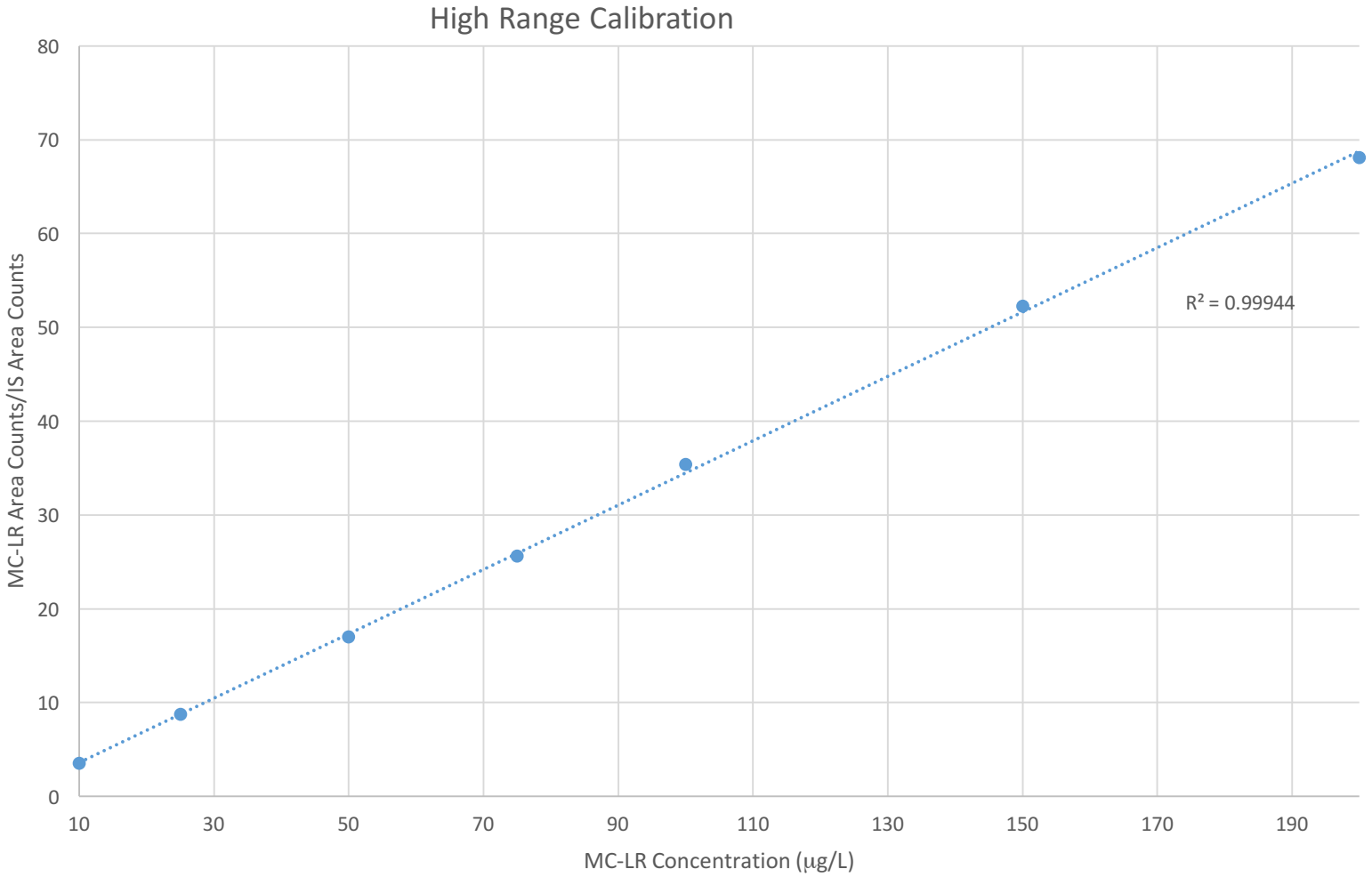
High Range Calibration
MC-LR Area Counts/IS Area Counts
MC-LR Concentration (µg/L)
R² = 0.99944
0
10
20
30
40
50
60
70
80
10
30
50
70
90
110
130
150
170
190

Example QA/QC Results:

Virgin and Preloaded (Run together)

Run Date	Reported Concentration (μg/L)						
2016-04-20	48.3	40.5					
2016-04-26	54.8	69.7*	59.5*	59.9*			
2016-05-04	47.8	40.2	46.2	48.9	48.8	51.0	52.1
2015-05-05		48.9	50.8	53.7			
2016-05-15	49.9	50.5	51.1	53.3	52.1	51.0	53.0
2016-05-16	49.4	50.9					
2016-05-17	51.4	51.2	53.2	53.0	53.0	53.7	
2016-05-18	52.6	52.2	52.4				
2016-06-07	51.8	53.5	53.4	53.4	53.0	53.4	
2016-06-08	50.6	50.9	51.9				

* Samples re-injected in a later run

Operational Control

Run Date	Reported Concentration (μg/L)					
2016-06-16	52.8	52.8	53.8	54.8	56.1	55.1
2016-06-24	50.1	51.6	50.6	53.7		
2016-07-02	72.5*					
2016-07-11	53.2	50.1	53.1			

2016-07-25	50.2	51.3	50.5			

* Samples re-injected in a later run

Wet Storage

Run Date	Reported Concentration (μg/L)				
2016-07-02	49.7	51.8			
2016-07-08	48.4	48.4	50.2	51.3	52.6
2016-07-21	51.7	49.9	49.4	55.4	

Salt Storage

Run Date	Reported Concentration (μg/L)			
2016-07-02	49.7	51.8	52.9	
2016-07-08	52.8	51.9	48.3	48.4
2016-07-21	51.6	52.4	47.9	51.7

Low Moisture Content Storage

Run Date	Reported Concentration (μg/L)				
2016-06-03	52.6	55.8	56.0	55.5	
2016-06-08	54.6				
2016-06-11	51.3	50.4			
2016-06-12	52.8	54.3	55.6	57.2	54.9

High Moisture Content Storage

Run Date	Reported Concentration (μg/L)					
2016-06-24	53.9	56.8	57.1	55.4	54.6	56.6
2016-06-30	51.5	52.2				
2016-07-13	50.2	52.0	51.9	52.4		
2016-07-14	52.8	51.6	50.7			

Appendix B NOM, TOC and DOC Data

	DOC (mg/L)						TOC (mg/L)					
	A		*B*		*C*		*A*		*B*		*C*	
WK#	*AVE*	*STDEV*	*AVE*	*STDEV*	*AVE*	*STDEV*	*AVE*	*STDEV*	*AVE*	*STDEV*	*AVE*	*STDEV*
1	1.74	0.22	0.82	0.02	0.51	0.02	2.11	0.02	0.79	0.01	0.54	0.01
2	1.97	0.22	0.28	0.78	0.47	0.04	1.65	0.08	1.35	0.01	0.56	0.11
3	1.62	0.06	1.37	0.02	0.84	0.02	1.68	0.11	1.36	0.02	0.84	0.02
4	2.05	0.21	2.09	0.15	0.81	1.28	1.60	0.03	1.44	0.04	1.13	0.09
5	1.66	0.04	1.63	0.02	1.15	0.03	1.65	0.05	1.63	0.03	1.14	0.03
6	1.71	0.03	1.65	0.04	1.40	0.04	1.76	0.12	1.63	0.04	1.39	0.05
7	1.78	0.03	1.74	0.04	1.30	0.02	1.77	0.04	1.81	0.05	1.33	0.08
8	1.60	0.05	1.52	0.04	1.40	0.05	1.61	0.03	1.58	0.04	1.63	0.14
9	1.76	0.05	1.77	0.16	1.11	0.02	1.81	0.09	1.89	0.05	1.07	0.03
10	1.83	0.07	1.87	0.05	1.13	0.05	1.83	0.06	1.96	0.14	1.10	0.06
11	1.71	0.06	1.65	0.05	1.07	0.04	1.76	0.13	1.66	0.07	1.03	0.04
12	1.61	0.05	1.59	0.02	1.24	0.24	1.65	0.04	1.59	0.02	1.15	0.17
13	1.61	0.05	1.57	0.05	1.04	0.02	1.63	0.04	1.65	0.04	1.01	0.03
14	1.91	0.03	1.72	0.06	1.40	0.02	2.03	0.11	1.72	0.04	1.37	0.07
15	1.73	0.05	1.98	0.33	1.30	0.05	1.75	0.06	2.19	0.21	1.57	0.36
16	1.89	0.04	1.63	0.05	1.55	0.19	1.92	0.02	1.63	0.02	1.66	0.10
18	1.72	0.06	1.67	0.04	1.15	0.01	1.77	0.02	1.65	0.03	1.13	0.01
19	1.72	0.06	1.67	0.04	1.15	0.01	1.77	0.02	1.65	0.03	1.13	0.01
20	1.86	0.04	2.15	0.17	1.60	0.26	1.87	0.03	1.92	0.04	1.40	0.12
22	2.37	0.27	3.64	0.27	4.98	2.51	1.92	0.04	1.94	0.05	1.72	0.33
24	2.35	0.20	1.97	0.14	1.97	0.24	1.68	0.06	1.91	0.26	1.38	0.07
26	1.77	0.05	1.67	0.04	1.50	0.07	1.76	0.05	1.67	0.05	1.47	0.07
28	1.75	0.06	2.02	0.48	1.67	0.23	1.73	0.14	1.76	0.04	1.38	0.02

30	3.39	0.49	5.83	0.60	2.57	3.61	1.75	0.01	1.86	0.09	1.65	0.20
36	1.72	0.04	2.16	0.45	1.63	0.08	1.70	0.07	2.68	0.88	1.99	0.25
40	2.18	0.06	2.44	0.40	2.05	0.18	2.18	0.07	2.71	0.71	2.15	0.17
44	2.06	0.03	2.11	0.13	1.90	0.04	2.11	0.03	2.24	0.21	1.90	0.01

A= Influent (from full scale filtration)
B = Effluent from chlorine removal columns (influent to preloading set up)
C = Final effluent from set up

WK#	DOC	HOC	CDOC	Biopolymers	Humics	Building Blocks	LMW Neutrals	LMW Acids	Contamination
	ppm-C	*ppb-C*	*ppb-C*	*ppb-C*	*ppm-c*	*ppb-C*	*ppb-C*	*ppb-C*	*ppb-C*
1	2.126	80	2045	186	1.12	187	547	0	388
2	2.541	411	2130	218	0.97	276	667	0	569
3	2.052	346	1706	194	0.92	357	236	0	130
4	2.952	63	2890	209	1.22	302	944	215	905
5	1.826	92	1735	220	1.07	231	216	0	0
6	1.892	-100	1992	236	1.26	213	286	0	0
7	2.028	179	1849	282	1.12	230	212	0	0
8	1.912	131	1781	258	1.06	275	192	0	0
9	2.054	193	1860	210	1.21	221	225	0	0
10	2.529	779	1750	246	1.04	254	215	0	0
11	2.213	518	1694	188	1.05	250	204	0	0
12	1.902	61	1841	245	1.21	170	210	0	0
13	1.857	-18	1875	244	1.09	269	271	0	0
14	2.019	14	2005	338	1.20	247	223	0	0
15	2.245	194	2051	266	1.16	263	360	0	0
16	1.968	7	1961	237	1.21	288	227	0	0
18	4.808	1053	3754	644	1.99	706	413	0	0
20	2.051	120	1931	307	1.12	289	213	0	0
22	4.748	2364	2384	275	1.21	221	673	0	0
26	1.952	147	1805	198	1.10	247	258	0	0
28	1.778	114	1663	180	1.00	277	210	0	0
30	1.669	41	1627	144	1.08	212	188	0	0
36	1.871	151	1719	158	1.05	273	242	0	0
40	1.823	108	1715	142	0.969	317	287	0	0

44	1.71	113	1597	95	1.055	203	244	0	0

Appendix C Isotherm Data

Virgin F300

C_o (μg/L)	C_f (μg/L)	GAC (mg/L)	$X_{Calculated}$ (μg/mg)	X_{model} (μg/mg)	$\varepsilon_i 2$	ε_i
107.336	72.282	11.000	3.187	3.059	0.0163	0.128
107.336	54.433	17.800	2.972	2.891	0.0065	0.081
107.336	50.951	21.600	2.610	2.854	0.0592	-0.243
107.336	27.954	27.200	2.918	2.533	0.1489	0.386
107.336	34.050	31.200	2.349	2.634	0.0812	-0.285
107.336	9.822	38.800	2.513	2.057	0.2081	0.456
107.336	8.438	49.600	1.994	1.996	0.0000	-0.002
107.336	11.246	60.000	1.602	2.113	0.2618	-0.512
107.336	2.932	65.000	1.606	1.617	0.0001	-0.011
				SUM	0.7821	
				1/n	0.199	
				K	1.306	

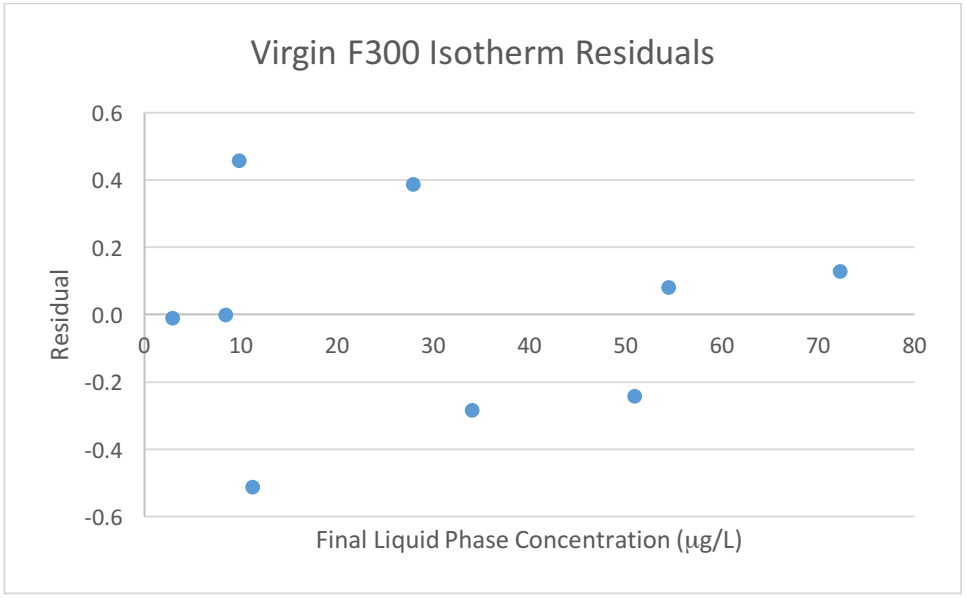
Virgin F300 Isotherm Residuals
Residual
0.6
0.4
0.2
0.0
-0.2
-0.4
-0.6
0
10
20
30
40
50
60
70
80
Final Liquid Phase Concentration (µg/L)

Preloaded

C_o (μg/L)	C_f (μg/L)	GAC (mg/L)	$X_{Calculated}$ (μg/mg)	X_{model} (μg/mg)	$\varepsilon_i 2$	ε_i
113.266	74.551	11.400	3.396	3.2	0.0472	0.217
113.266	66.168	16.200	2.907	3.1	0.0213	-0.146
113.266	41.236	20.600	3.497	2.6	0.7985	0.894
113.266	49.382	26.600	2.402	2.8	0.1330	-0.365
113.266	40.567	34.400	2.113	2.6	0.2260	-0.475
113.266	26.577	43.000	2.016	2.2	0.0522	-0.228
113.266	16.042	49.800	1.952	1.9	0.0035	0.059
113.266	12.046	59.400	1.704	1.7	0.0002	-0.015
113.266	8.074	67.000	1.570	1.5	0.0047	0.069
				SUM	1.2866	
				1/n	0.337	
				K	0.742	

Preloaded w/o Outlier

C_o (μg/L)	C_f (μg/L)	GAC (mg/L)	$X_{Calculated}$ (μg/mg)	X_{model} (μg/mg)	$\varepsilon_i 2$	ε_i
113.266	74.551	11.400	3.396	3.0	0.1441	0.380
113.266	66.168	16.200	2.907	2.9	0.0001	0.008
113.266	49.382	26.600	2.402	2.6	0.0521	-0.228
113.266	40.567	34.400	2.113	2.5	0.1224	-0.350
113.266	26.577	43.000	2.016	2.1	0.0153	-0.124
113.266	16.042	49.800	1.952	1.8	0.0207	0.144
113.266	12.046	59.400	1.704	1.6	0.0036	0.060

113.266	8.074	67.000	1.570	1.4	0.0172	0.131
				SUM	0.3753	
				1/n	0.333	
				K	0.718	

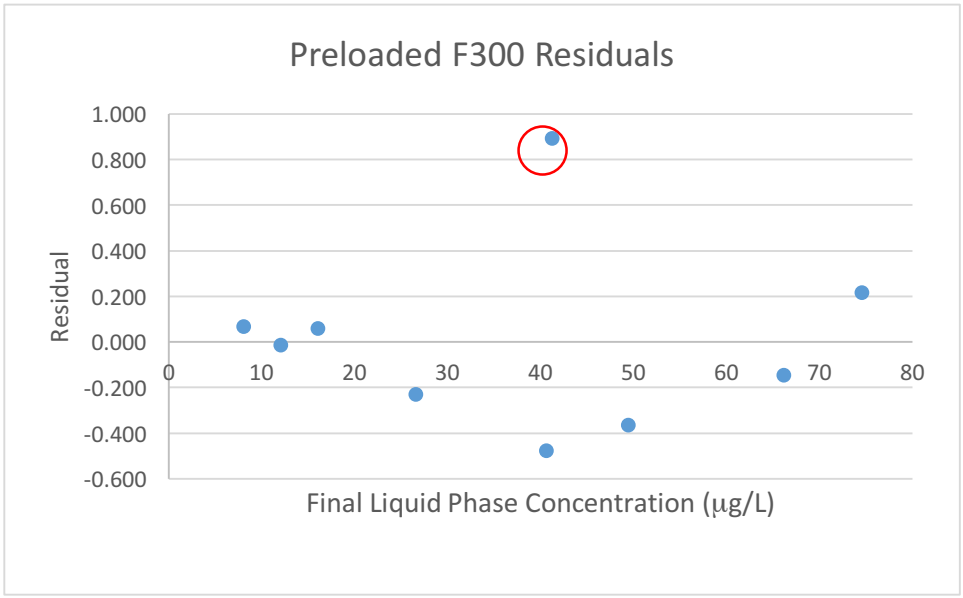

HMC

C_o (μg/L)	C_f (μg/L)	GAC (mg/L)	$X_{Calculated}$ (μg/mg)	X_{model} (μg/mg)	$\varepsilon_i 2$	ε_i
101.51	95.295	10.8	0.575	1.266	0.477	-0.691
101.51	65.004	22.8	1.601	1.252	0.122	0.349
101.51	55.657	28.8	1.592	1.246	0.120	0.346
101.51	40.215	42	1.459	1.234	0.051	0.225
101.51	42.788	50.8	1.156	1.237	0.007	-0.081
101.51	26.310	58.2	1.292	1.219	0.005	0.073
101.51	15.439	72.2	1.192	1.200	0.000	-0.008
101.51	8.531	82.2	1.131	1.180	0.002	-0.049
101.51	11.437	91.2	0.988	1.190	0.041	-0.202
				SSE	0.824	
				1/n	0.029	
				K	1.108	

HMC w/o Outlier

C_o (μg/L)	C_f (μg/L)	GAC (mg/L)	$X_{Calculated}$ (μg/mg)	X_{model} (μg/mg)	$\varepsilon_i 2$	ε_i
101.51	65.004	22.8	1.601	1.540	0.0037	0.061
101.51	55.657	28.8	1.592	1.493	0.0097	0.099
101.51	40.215	42	1.459	1.400	0.0036	0.060
101.51	42.788	50.8	1.156	1.417	0.0682	-0.261
101.51	26.310	58.2	1.292	1.286	0.0000	0.006
101.51	15.439	72.2	1.192	1.156	0.0013	0.036
101.51	8.531	82.2	1.131	1.027	0.0108	0.104

101.51	11.437	91.2	0.988	1.089	0.0103	-0.101
				SSE	0.108	
				1/n	0.200	
				K	0.670	

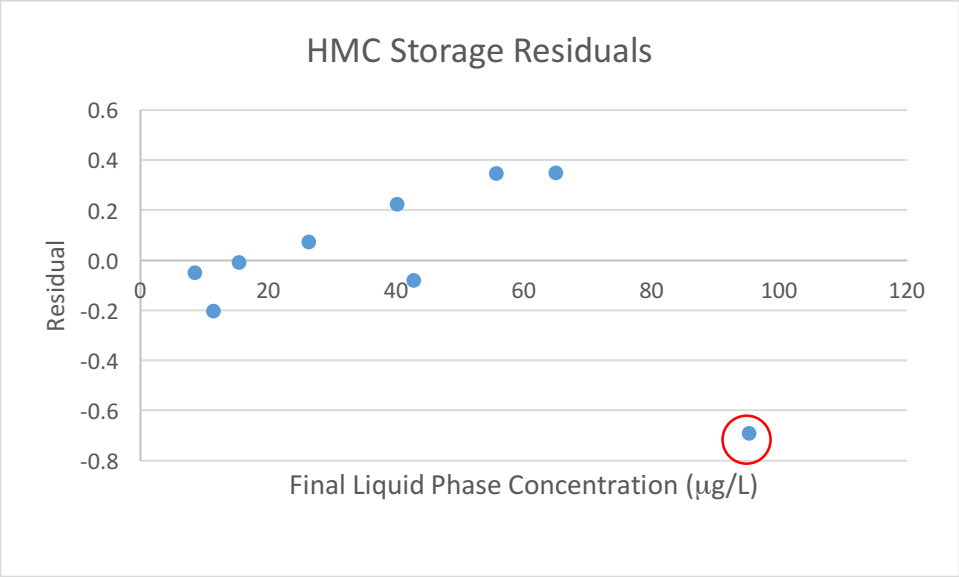

LMC

C_o (μg/L)	C_f (μg/L)	GAC (mg/L)	$X_{Calculated}$ (μg/mg)	X_{model} (μg/mg)	$\varepsilon_i 2$	ε_i
107.79	76.713	11.8	2.633	2.311	0.104	0.322
107.79	47.415	33.6	1.797	2.046	0.062	-0.249
107.79	31.676	47.6	1.599	1.846	0.061	-0.248
107.79	13.704	59.6	1.579	1.493	0.007	0.086
107.79	7.615	69.8	1.435	1.286	0.022	0.149
107.79	10.170	81	1.205	1.384	0.032	-0.179
107.79	2.897	91	1.153	1.006	0.021	0.146
				SSE	0.310	
				1/n	0.254	
				K	0.768	

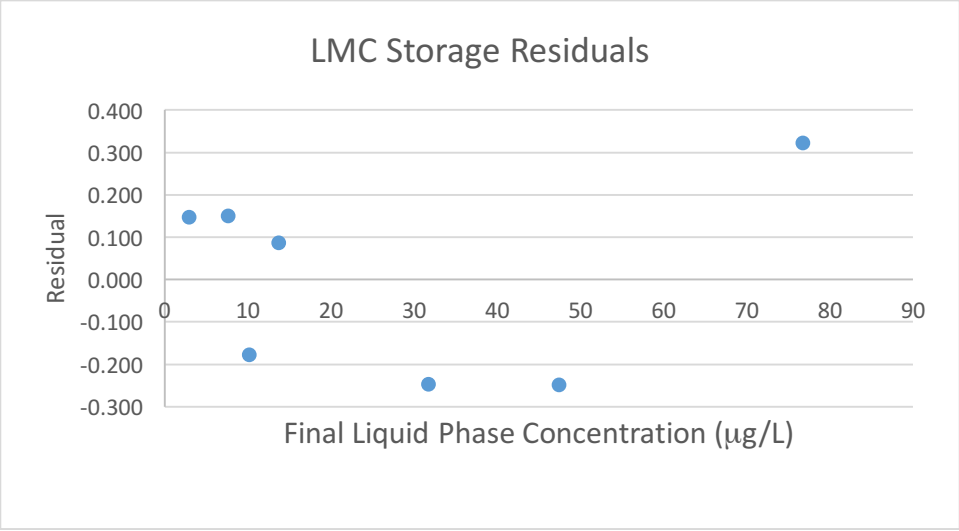

Submerged

C_o (μg/L)	C_f (μg/L)	GAC (mg/L)	$X_{Calculated}$ (μg/mg)	X_{model} (μg/mg)	$\varepsilon_i 2$	ε_i
92.44	78.859	11.4	1.192	1.501	0.095	-0.309
92.44	59.306	21.2	1.563	1.461	0.010	0.102
92.44	38.080	30.6	1.777	1.403	0.140	0.374
92.44	39.565	40.4	1.309	1.408	0.010	-0.099
92.44	20.533	53.2	1.352	1.325	0.001	0.027
92.44	11.271	60.6	1.339	1.253	0.007	0.086
92.44	4.219	72	1.225	1.145	0.007	0.081
92.44	4.283	82.2	1.073	1.146	0.005	-0.074
92.44	4.175	92	0.959	1.143	0.034	-0.184
				SSE	0.3092	
				1/n	0.092	
				K	1.002	

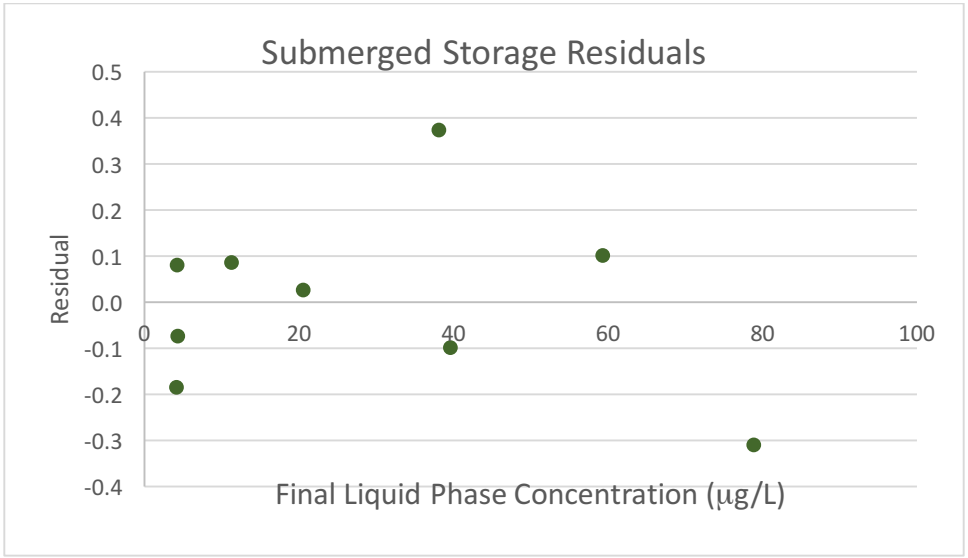
Submerged Storage Residuals
0.5
0.4
0.3
0.2
0.1
0.0
-0.1
-0.2
-0.3
-0.4
Residual
0
20
40
60
80
100
Final Liquid Phase Concentration (µg/L)

Salt

C_o (μg/L)	C_f (μg/L)	GAC (mg/L)	$X_{Calculated}$ (μg/mg)	X_{model} (μg/mg)	$\varepsilon_i 2$	ε_i
90.4	87.6	11.4	0.244	0.820	0.332	-0.576
90.4	69.7	20.6	1.004	0.841	0.027	0.163
90.4	56.5	31.8	1.066	0.861	0.042	0.205
90.4	50.9	41.4	0.954	0.871	0.007	0.083
90.4	35.7	51	1.072	0.905	0.028	0.167
90.4	28.3	60	1.035	0.928	0.011	0.107
90.4	11.6	93	0.848	1.024	0.031	-0.176
90.4	7.6	73.4	1.128	1.072	0.003	0.056
90.4	5.9	82.2	1.028	1.103	0.006	-0.074
				SSE	0.4868	
				1/n	-0.1093	
				K	1.338	

Salt w/o Outlier

C_o (μg/L)	C_f (μg/L)	GAC (mg/L)	$X_{Calculated}$ (μg/mg)	X_{model} (μg/mg)	$\varepsilon_i 2$	ε_i
90.4	69.707	20.6	1.004	1.0204	0.000	-0.016
90.4	56.505	31.8	1.066	1.0207	0.002	0.045
90.4	50.897	41.4	0.954	1.0208	0.004	-0.067
90.4	35.716	51	1.072	1.0213	0.003	0.051
90.4	28.295	60	1.035	1.0217	0.000	0.013
90.4	11.784	93	0.845	1.0229	0.032	-0.178

90.4	7.609	73.4	1.128	1.0235	0.011	0.104
90.4	5.9	82.2	1.028	1.0239	0.000	0.004
				SSE	0.0520	
				1/n	-0.001	
				K	1.026	

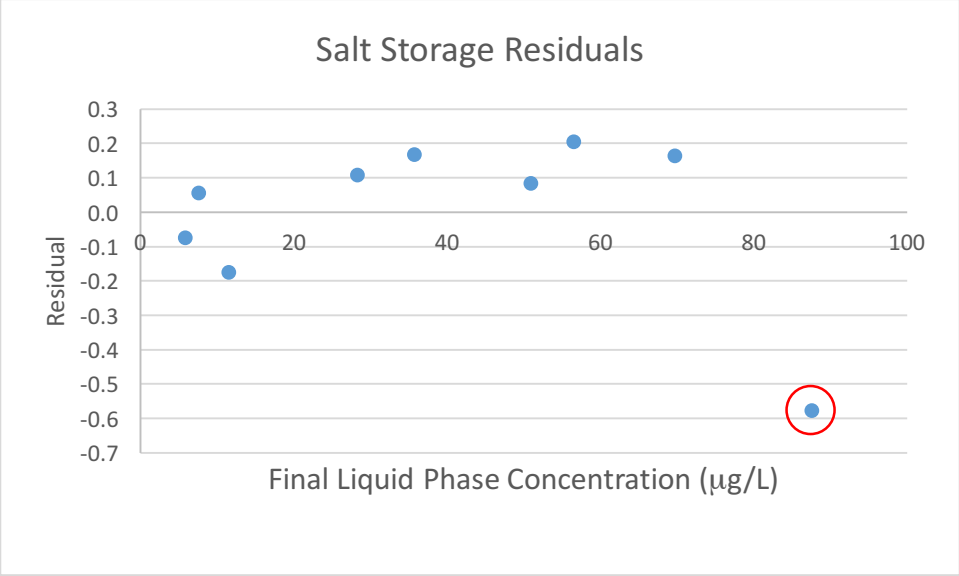

Continuous Operational Control

C_o (μg/L)	C_f (μg/L)	GAC (mg/L)	$X_{Calculated}$ (μg/mg)	X_{model} (μg/mg)	$\varepsilon_i 2$	ε_i
106.14	70.566	22.4	1.588	1.556	0.001	0.032
106.14	53.696	47.6	1.102	1.136	0.001	-0.034
106.14	43.176	65.6	0.960	0.884	0.006	0.076
106.14	81.899	11.6	2.090	1.847	0.059	0.243
106.14	69.012	32.6	1.139	1.517	0.143	-0.378
106.14	50.250	54.4	1.027	1.052	0.001	-0.025
106.14	42.067	72.6	0.883	0.858	0.001	0.025
106.14	33.699	82.6	0.877	0.664	0.045	0.213
106.14	40.723	91.2	0.717	0.826	0.012	-0.109
				SSE	0.2678	
				1/n	1.152	
				K	0.012	

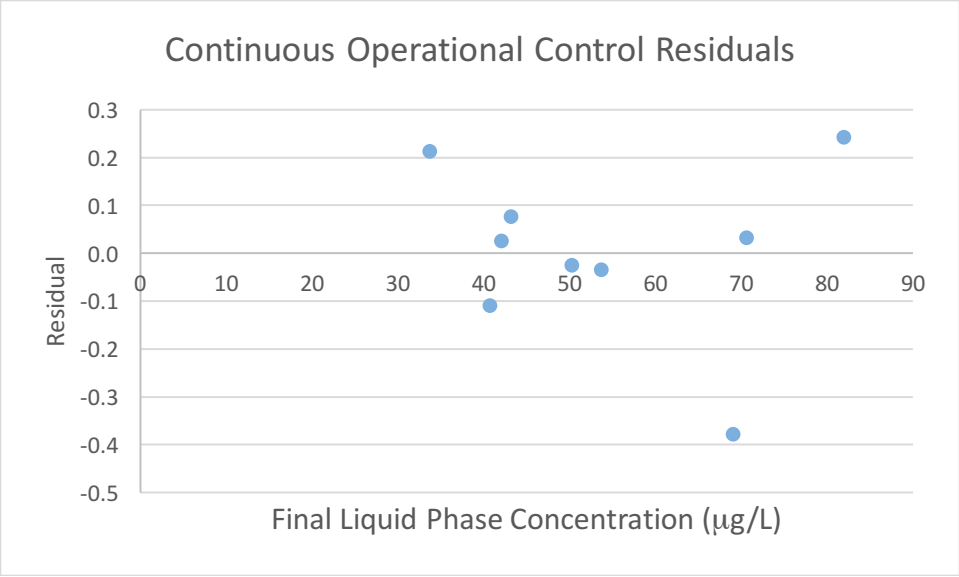
Continuous Operational Control Residuals
Residual
0.3
0.2
0.1
0.0
-0.1
-0.2
-0.3
-0.4
-0.5
0
10
20
30
40
50
60
70
80
90
Final Liquid Phase Concentration (µg/L)

Appendix D Kinetic Data

Pseudo First Order Kinetics

Virgin F300

	V2A = 11.0 mg/L			V2E = 31.2 mg/L			V2I = 65.0 mg/L		
Model Fitting Parameters	k	0.051		k	0.245		k	0.624	
	qe	6.881	(μg/mg)	qe	2.479	(μg/mg)	qe	1.625	(μg/mg)
	SSE	3.653		SSE	0.430		SSE	0.097	
t (days)	q_t(μg/mg)	q_t (model) (μg/mg)	$Error^2$	q_t(μg/mg)	q_t (model) (μg/mg)	$Error^2$	q_t(μg/mg)	q_t (model) (μg/mg)	$Error^2$
0	0.00	0.00	0.00	0.00	0.00	0.00	0.00	0.00	0.00
1	-0.20	0.34	0.30	0.40	0.54	0.02	0.69	0.75	0.00
2	1.41	0.67	0.54	1.18	0.96	0.05	1.36	1.16	0.04
3	1.21	0.98	0.05	1.60	1.29	0.10	1.35	1.38	0.00
4	2.18	1.28	0.82	1.71	1.55	0.02	1.39	1.49	0.01
5	1.37	1.56	0.03	1.72	1.75	0.00	1.48	1.55	0.01
6	1.63	1.82	0.04	1.76	1.91	0.02	1.53	1.59	0.00
7	1.45	2.08	0.39	1.82	2.03	0.05	1.54	1.60	0.00
8	1.96	2.32	0.13	1.93	2.13	0.04	1.52	1.61	0.01
9	1.91	2.54	0.40	1.93	2.21	0.08	1.60	1.62	0.00
10	2.74	2.76	0.00	2.26	2.27	0.00	1.63	1.62	0.00
12	4.04	3.16	0.77	2.48	2.35	0.02	1.68	1.62	0.00
14	3.84	3.52	0.10	2.52	2.40	0.01	1.69	1.63	0.00
16	3.85	3.85	0.00	2.51	2.43	0.01	1.70	1.63	0.01

18	3.87	4.15	0.08	2.55	2.45	0.01	1.71	1.63	0.01

Preloaded F300

	P2A = 11.4 mg/L			P2E= 34.4 mg/L			P2I = 67.0 mg/L		
Model Fitting Parametes	k	0.018		k	0.0290		k	0.0555	
	q_e	5.134	(μg/mg)	q_e	2.7082	(μg/mg)	q_e	1.6072	(μg/mg)
	SSE	9.953		SSE	1.5768		SSE	0.1651	
t (days)	q_t(μg/mg)	q_t (model) (μg/mg)	$Error^2$	q_t(μg/mg)	q_t (model) (μg/mg)	$Error^2$	q_t(μg/mg)	q_t (model) (μg/mg)	$Error^2$
0	0.00	0.00	0.00	0.00	0.00	0.00	0.00	0.00	0.00
1	-0.11	0.09	0.04	0.15	0.08	0.00	-0.08	0.09	0.03
2	1.23	0.18	1.09	0.59	0.15	0.19	0.35	0.17	0.03
3	0.67	0.27	0.16	0.56	0.23	0.11	0.31	0.25	0.00
4	0.98	0.36	0.39	0.71	0.30	0.17	0.41	0.32	0.01
5	-0.18	0.45	0.40	0.24	0.37	0.01	0.30	0.39	0.01
6	-0.15	0.53	0.47	0.09	0.43	0.12	0.38	0.46	0.01
7	-0.17	0.62	0.63	0.33	0.50	0.03	0.44	0.52	0.01
8	0.13	0.70	0.33	-0.19	0.56	0.57	0.52	0.58	0.00
9	-0.69	0.78	2.14	0.34	0.62	0.08	0.48	0.63	0.02
10	0.67	0.86	0.04	0.67	0.68	0.00	0.65	0.68	0.00
12	1.89	1.01	0.77	1.05	0.80	0.07	0.87	0.78	0.01
14	1.81	1.16	0.43	0.92	0.90	0.00	0.93	0.87	0.00
16	0.81	1.30	0.24	0.95	1.01	0.00	0.91	0.95	0.00
18	0.57	1.44	0.76	0.89	1.10	0.04	0.96	1.02	0.00
20	2.47	1.57	0.81	1.33	1.19	0.02	1.12	1.08	0.00
24	1.84	1.82	0.00	1.41	1.36	0.00	1.25	1.18	0.00

26	1.99	1.94	0.00	1.61	1.43	0.03	1.31	1.23	0.01
28	2.20	2.06	0.02	1.64	1.51	0.02	1.35	1.27	0.01
30	3.12	2.17	0.91	1.84	1.57	0.07	1.38	1.30	0.01
32	2.14	2.27	0.02	1.64	1.64	0.00	1.33	1.33	0.00
34	2.52	2.38	0.02	1.77	1.70	0.00	1.35	1.36	0.00
36	2.76	2.47	0.08	1.83	1.75	0.01	1.38	1.39	0.00
39	2.49	2.62	0.02	1.86	1.83	0.00	1.41	1.42	0.00
41	2.72	2.71	0.00	1.89	1.88	0.00	1.44	1.44	0.00
43	2.95	2.79	0.02	1.89	1.93	0.00	1.44	1.46	0.00
45	2.78	2.88	0.01	1.87	1.97	0.01	1.46	1.47	0.00
47	2.93	2.96	0.00	1.98	2.01	0.00	1.46	1.49	0.00
49	2.77	3.04	0.07	1.95	2.05	0.01	1.47	1.50	0.00
52	2.82	3.15	0.10	2.02	2.11	0.01	1.49	1.52	0.00

HMC

	HA = 10.8 mg/L			HE = 50.8 mg/L			HI = 91.2 mg/L		
Model Fitting Parameters	k	0.302		k	0.0712		k	0.1228	
	qe predicated	1.537	(μg/mg)	qe	1.3455	(μg/mg)	qe	1.0530	(μg/mg)
	SSE	2.783		SSE	0.0540		SSE	0.0385	
t (days)	q_t(μg/mg)	q_t (model) (μg/mg)	$Error^2$	q_t(μg/mg)	q_t (model) (μg/mg)	$Error^2$	q_t(μg/mg)	q_t (model) (μg/mg)	$Error^2$
0	0.00	0.000	0.000	0.00	0.000	0.000	0.00	0.000	0.000
1	1.25	0.400	0.717	0.15	0.092	0.003	0.16	0.122	0.001
2	1.11	0.696	0.171	0.22	0.179	0.002	0.29	0.229	0.004
3	0.98	0.915	0.004	0.29	0.259	0.001	0.35	0.324	0.000
4	0.98	1.077	0.010	0.28	0.333	0.003	0.46	0.409	0.003
5	0.66	1.197	0.291	0.44	0.403	0.001	0.48	0.483	0.000
6									
7	0.98	1.351	0.140	0.56	0.528	0.001	0.59	0.607	0.000
8	1.34	1.400	0.004	0.56	0.584	0.001	0.65	0.659	0.000
9	1.04	1.435	0.156	0.65	0.637	0.000	0.69	0.704	0.000
10	1.28	1.462	0.032	0.65	0.685	0.001	0.74	0.745	0.000
11	1.65	1.482	0.028	0.81	0.731	0.006	0.75	0.780	0.001
13	1.92	1.507	0.172	0.86	0.812	0.002	0.90	0.840	0.003
15	2.08	1.521	0.317	0.96	0.883	0.005	0.90	0.886	0.000
17				0.91	0.944	0.001	0.88	0.922	0.002
19	1.29	1.532	0.060	0.93	0.998	0.005			

21	1.75	1.535	0.046	0.98	1.044	0.004	0.94	0.973	0.001
23	1.36	1.536	0.030	1.00	1.084	0.007	0.98	0.991	0.000
25	1.20	1.536	0.116	1.07	1.119	0.003	0.87	1.004	0.017
27	1.37	1.537	0.030				1.01	1.015	0.000
29	1.53	1.537	0.000	1.18	1.175	0.000	1.03	1.023	0.000
31	1.47	1.537	0.005	1.20	1.198	0.000	1.03	1.030	0.000
33	1.50	1.537	0.002	1.19	1.217	0.001	1.04	1.035	0.000
34	1.32	1.537	0.048	1.20	1.226	0.001	1.05	1.037	0.000
36	1.85	1.537	0.097	1.29	1.242	0.002	1.06	1.040	0.000
38	2.08	1.537	0.293	1.27	1.256	0.000	1.07	1.043	0.001
40	1.47	1.537	0.004	1.32	1.268	0.002	1.09	1.045	0.002
42	1.64	1.537	0.011	1.32	1.278	0.001	1.09	1.047	0.002
44	1.26	1.537	0.074	1.34	1.287	0.003			

LMC

	LA = 11.8 mg/L			LE = 47.6 mg/L			LI = 91.0 mg/L		
Model Fitting Parameters	k	0.036		k	0.0442		k	0.0856	
	qe predicated	2.834	(μg/mg)	qe	1.8001	(μg/mg)	qe	1.2293	(μg/mg)
	SSE	10.388		SSE	0.3689		SSE	0.0322	
t (days)	q_t(μg/mg)	q_t (model) (μg/mg)	$Error^2$	q_t(μg/mg)	q_t (model) (μg/mg)	$Error^2$	q_t(μg/mg)	q_t (model) (μg/mg)	$Error^2$
0	0.00	0.000	0.000	0.00	0.000	0.000	0.00	0.00	0.00
1	-0.01	0.099	0.011	-0.09	0.078	0.028	0.17	0.10	0.00
2	-0.34	0.195	0.283	0.08	0.152	0.006	0.17	0.19	0.00
3	-0.33	0.287	0.377	0.02	0.224	0.042	0.22	0.28	0.00
4	-0.65	0.376	1.062	0.08	0.292	0.046	0.30	0.36	0.00
5	0.13	0.462	0.109	0.29	0.357	0.005	0.40	0.43	0.00
6	0.00	0.545	0.297	0.36	0.419	0.003	0.44	0.49	0.00
7	-0.57	0.625	1.425	0.35	0.479	0.017	0.49	0.55	0.00
8	0.58	0.703	0.015	0.53	0.536	0.000	0.67	0.61	0.00
9	0.66	0.777	0.014	0.69	0.591	0.010	0.65	0.66	0.00
10	0.74	0.849	0.012	0.61	0.643	0.001	0.73	0.71	0.00
12	1.34	0.986	0.127	0.78	0.741	0.002	0.83	0.79	0.00
14	1.40	1.113	0.083	0.91	0.831	0.006	0.90	0.86	0.00
16	1.57	1.231	0.116	0.98	0.913	0.005	0.96	0.92	0.00
18	3.67	1.341	5.417	1.34	0.988	0.124	1.00	0.97	0.00
20				1.20	1.057	0.020	1.00	1.01	0.00

22	1.75	1.540	0.043	1.13	1.120	0.000	1.05	1.04	0.00
24	1.55	1.629	0.007	1.12	1.177	0.003	1.07	1.07	0.00
25	1.37	1.671	0.089	1.12	1.204	0.008	1.08	1.08	0.00
27				1.17	1.255	0.007	1.10	1.11	0.00
29				1.28	1.301	0.000	1.13	1.13	0.00
31	1.64	1.895	0.065	1.23	1.343	0.013	1.14	1.14	0.00
33	1.57	1.959	0.155	1.35	1.382	0.001	1.16	1.16	0.00
35	1.28	2.019	0.548	1.29	1.417	0.015	1.16	1.17	0.00
37	2.25	2.076	0.029	1.48	1.449	0.001	1.13	1.18	0.00
39	2.37	2.128	0.060	1.51	1.479	0.001	1.19	1.19	0.00
41	2.35	2.176	0.030	1.55	1.506	0.002	1.20	1.19	0.00
43	2.11	2.221	0.013	1.57	1.531	0.002	1.20	1.20	0.00

Submerged

	WA = 11.4 mg/L			WE = 53.2 mg/L			WI = 92.0 mg/L		
Model Fitting Parameters	k	0.976		k	0.0283		k	0.0765	
	qe predicated	0.000	(μg/mg)	qe	1.7655	(μg/mg)	qe	0.9450	(μg/mg)
	SSE	8.568		SSE	0.5704		SSE	0.6011	
t (days)	q_t(μg/mg)	q_t (model) (μg/mg)	$Error^2$	q_t(μg/mg)	q_t (model) (μg/mg)	$Error^2$	q_t(μg/mg)	q_t (model) (μg/mg)	$Error^2$
0	0.00	0.00	0.00	0.00	0.000	0.000	0.00	0.000	0.000
1	0.14	0.00	0.02	0.12	0.049	0.005	0.22	0.070	0.023
2	0.26	0.00	0.07	0.33	0.097	0.055	0.31	0.134	0.031
3	-0.99	0.00	0.97	0.11	0.144	0.001	0.27	0.194	0.005
4	-0.48	0.00	0.23	0.20	0.189	0.000	0.31	0.249	0.004
5	-1.22	0.00	1.50	0.07	0.233	0.027	0.43	0.300	0.017
6	-0.71	0.00	0.50	0.30	0.276	0.001	0.40	0.348	0.002
7	-0.58	0.00	0.33	0.35	0.318	0.001	0.45	0.392	0.003
8	-0.84	0.00	0.71	0.39	0.358	0.001	0.48	0.433	0.002
9	-1.02	0.00	1.05	0.47	0.397	0.005	0.52	0.470	0.002
10	-0.85	0.00	0.72	0.51	0.436	0.006	0.54	0.505	0.001
12	-0.37	0.00	0.14	0.58	0.509	0.006	0.60	0.568	0.001
14	-0.39	0.00	0.15	0.57	0.578	0.000	0.62	0.621	0.000
16	-0.90	0.00	0.81	0.00	0.644	0.414	0.67	0.667	0.000
18	-0.02	0.00	0.00	0.79	0.705	0.008	0.00	0.707	0.499
20	0.13	0.00	0.02	0.85	0.764	0.007	0.76	0.741	0.000

22	-0.16	0.00	0.02	0.85	0.819	0.001	0.76	0.770	0.000
24	-0.08	0.00	0.01	0.95	0.871	0.006	0.82	0.794	0.001
26	-0.07	0.00	0.00	0.97	0.920	0.002	0.84	0.816	0.001
28	0.06	0.00	0.00	1.05	0.967	0.008	0.86	0.834	0.000
30	-0.47	0.00	0.22	1.01	1.011	0.000	0.88	0.850	0.001
32	-0.12	0.00	0.01	1.15	1.053	0.010	0.90	0.863	0.001
34	-0.12	0.00	0.01	1.09	1.092	0.000	0.90	0.875	0.001
36	0.56	0.00	0.31	1.14	1.129	0.000	0.92	0.885	0.001
38	-0.11	0.00	0.01	1.11	1.164	0.003	0.92	0.893	0.001
41	-0.30	0.00	0.09	1.16	1.213	0.002	0.93	0.904	0.001
43	-0.67	0.00	0.44	1.21	1.243	0.001	0.94	0.910	0.001
45	0.45	0.00	0.21	1.27	1.272	0.000	0.95	0.915	0.001
47	0.87	0.00	0.75	1.35	1.299	0.002	0.95	0.919	0.001
49	0.67	0.00	0.45	1.34	1.325	0.000	0.96	0.923	0.001
51	1.46	0.00	2.14	1.33	1.349	0.000	0.97	0.926	0.002
53	0.53	0.00	0.28	1.40	1.372	0.001	0.97	0.929	0.002
55	0.77	0.00	0.60	1.43	1.394	0.001	0.98	0.931	0.002
57	0.87	0.00	0.75	1.41	1.414	0.000	0.98	0.933	0.002

Salt

	SA = 11.4 mg/L			SE = 51.0 mg/L			SI = 93.0 mg/L		
Model Fitting Parameters	k	0.000		k	0.0601		k	0.0892	
	qe predicated	0.000	(μg/mg)	qe	1.0182	(μg/mg)	qe	0.8993	(μg/mg)
	SSE	12.179		SSE	1.2782		SSE	0.0078	
t (days)	q_t(μg/mg)	q_t (model) (μg/mg)	$Error^2$	q_t(μg/mg)	q_t (model) (μg/mg)	$Error^2$	q_t(μg/mg)	q_t (model) (μg/mg)	$Error^2$
0	0.00	0.00	0.00	0.00	0.000	0.000	0.00	0.000	0.000
1	-1.60	0.00	2.56	-0.27	0.059	0.110	0.06	0.077	0.000
2	-0.59	0.00	0.35	-0.04	0.115	0.023	0.14	0.147	0.000
3	-1.07	0.00	1.15	-0.13	0.168	0.088	0.17	0.211	0.001
4	-1.20	0.00	1.43	0.06	0.218	0.024	0.26	0.270	0.000
5	-0.73	0.00	0.53	0.16	0.264	0.011	0.34	0.324	0.000
6	-0.51	0.00	0.26	0.22	0.308	0.008	0.38	0.373	0.000
7	-0.32	0.00	0.10	0.29	0.350	0.003	0.46	0.418	0.002
8	0.44	0.00	0.19	0.39	0.389	0.000	0.48	0.459	0.000
9	-0.04	0.00	0.00	0.45	0.425	0.000	0.52	0.496	0.000
10	0.32	0.00	0.10	0.51	0.460	0.003	0.52	0.531	0.000
12	-0.21	0.00	0.05	0.56	0.523	0.001	0.60	0.591	0.000
14	-0.21	0.00	0.05	0.51	0.579	0.006	0.61	0.641	0.001
16	-0.29	0.00	0.08	0.68	0.629	0.002	0.67	0.684	0.000
18	0.48	0.00	0.23	0.73	0.673	0.003	0.70	0.719	0.000
20	0.59	0.00	0.35	0.79	0.712	0.006	0.74	0.748	0.000

22	0.55	0.00	0.31	0.81	0.747	0.004	0.77	0.773	0.000
24	0.53	0.00	0.28	0.88	0.778	0.010	0.79	0.794	0.000
26	0.43	0.00	0.18	0.94	0.805	0.018	0.80	0.811	0.000
28	0.32	0.00	0.10	0.88	0.829	0.003	0.82	0.825	0.000
30	0.58	0.00	0.34	1.03	0.850	0.032	0.83	0.837	0.000
32	0.32	0.00	0.10	0.98	0.869	0.012	0.86	0.848	0.000
34	-0.60	0.00	0.37	1.02	0.886	0.017	0.87	0.856	0.000
36	-0.66	0.00	0.43	1.02	0.901	0.014	0.87	0.863	0.000
39	-1.57	0.00	2.48	0.00	0.920	0.847	0.87	0.872	0.000
41	0.40	0.00	0.16	1.11	0.932	0.031	0.90	0.876	0.000

Operational Control

	CD = 11.6 mg/L			CF = 54.4 mg/L			CI = 91.2 mg/L		
Model Fitting Parameters	k	0.000		k	0.0113		k	0.0140	
	qe predicated	456.536	(μg/mg)	qe	2.5507	(μg/mg)	qe	1.5723	(μg/mg)
	SSE	6.086		SSE	0.0451		SSE	0.0658	
t (days)	q_t(μg/mg)	q_t (model) (μg/mg)	$Error^2$	q_t(μg/mg)	q_t (model) (μg/mg)	$Error^2$	q_t(μg/mg)	q_t (model) (μg/mg)	$Error^2$
0	0.00	0.000	0.000	0.00	0.000	0.000		0.000	0.000
1	-0.49	0.024	0.260				0.02	0.022	0.000
2	-0.33	0.047	0.144	0.06	0.057	0.000	0.03	0.043	0.000
3	-0.29	0.071	0.131	0.08	0.085	0.000	0.06	0.064	0.000
4	0.13	0.095	0.001	0.20	0.113	0.007	0.10	0.085	0.000
5	-0.64	0.118	0.574	0.14	0.140	0.000	0.06	0.106	0.002
6	-0.47	0.142	0.380	0.15	0.167	0.000	0.02	0.126	0.012
7	-0.21	0.165	0.139	0.18	0.194	0.000	0.14	0.146	0.000
8	-0.23	0.189	0.177	0.25	0.221	0.001	0.18	0.166	0.000
9	0.00	0.213	0.045					0.186	0.034
10	-0.31	0.236	0.299	0.28	0.273	0.000	0.22	0.205	0.000
11	-0.27	0.260	0.283	0.29	0.298	0.000	0.23	0.224	0.000
13	-0.52	0.307	0.685	0.37	0.349	0.001	0.28	0.261	0.000
15	0.03	0.354	0.103	0.40	0.398	0.000	0.31	0.297	0.000
17	0.12	0.402	0.077	0.45	0.446	0.000	0.35	0.332	0.000
19	0.18	0.449	0.073	0.48	0.493	0.000	0.37	0.366	0.000

21	1.02	0.496	0.272	0.63	0.539	0.008	0.48	0.400	0.006
23	0.75	0.543	0.041	0.66	0.584	0.005	0.47	0.432	0.002
25	0.58	0.590	0.000	0.62	0.628	0.000	0.47	0.463	0.000
27	0.21	0.638	0.184	0.65	0.671	0.000	0.50	0.494	0.000
29	-0.35	0.685	1.070	0.61	0.713	0.010	0.48	0.524	0.002
31	1.30	0.732	0.320	0.79	0.754	0.001	0.59	0.552	0.002
33	1.34	0.779	0.320	0.85	0.794	0.003	0.59	0.580	0.000
35	1.20	0.826	0.141	0.85	0.834	0.000	0.63	0.608	0.001
37	1.46	0.874	0.339	0.89	0.872	0.000	0.64	0.634	0.000
39	1.07	0.921	0.021	0.95	0.909	0.002	0.68	0.660	0.000
41	1.06	0.968	0.008	0.91	0.946	0.001	0.66	0.685	0.001
43	1.04	1.015	0.001	0.92	0.982	0.004	0.66	0.710	0.002

Pseudo –Second Order Kinetics

Virgin F300

	V2A = 11.0 mg/L			V2E = 31.2 mg/L			V2I = 65.0 mg/L		
Model Fitting Parameters	k	2.80E-03		k	8.44E-02		k	4.82E-01	
	qe	11.389	(μg/mg)	qe	3.077	(μg/mg)	qe	1.819	(μg/mg)
	SSE	3.648		SSE	0.312		SSE	0.072	
t (days)	q_t(μg/mg)	q_t (model) (μg/mg)	$Error^2$	q_t (μg/mg)	q_t (model) (μg/mg)	$Error^2$	q_t (μg/mg)	q_t (model) (μg/mg)	$Error^2$
0	0.00	0.00	0.00	0.00	0.00	0.00	0.00	0.00	0.00
1	-0.20	0.35	0.30	0.40	0.63	0.06	0.69	0.85	0.02
2	1.41	0.68	0.52	1.18	1.05	0.02	1.36	1.16	0.04
3	1.21	0.99	0.05	1.60	1.35	0.07	1.35	1.32	0.00
4	2.18	1.29	0.80	1.71	1.57	0.02	1.39	1.42	0.00
5	1.37	1.57	0.04	1.72	1.74	0.00	1.48	1.48	0.00
6	1.63	1.83	0.04	1.76	1.87	0.01	1.53	1.53	0.00
7	1.45	2.08	0.40	1.82	1.98	0.03	1.54	1.56	0.00
8	1.96	2.31	0.13	1.93	2.08	0.02	1.52	1.59	0.00
9	1.91	2.54	0.40	1.93	2.15	0.05	1.60	1.61	0.00
10	2.74	2.75	0.00	2.26	2.22	0.00	1.63	1.63	0.00
12	4.04	3.15	0.79	2.48	2.33	0.02	1.68	1.66	0.00
14	3.84	3.52	0.10	2.52	2.41	0.01	1.69	1.68	0.00
16	3.85	3.85	0.00	2.51	2.48	0.00	1.70	1.70	0.00
18	3.87	4.15	0.08	2.55	2.53	0.00	1.71	1.71	0.00

Preloaded F300

	P2A = 11.4 mg/L			P2E= 34.4 mg/L			P2I = 67.0 mg/L		
Model Fitting Parameters	k	1.12E-03		k	4.29E-03		k	2.02E-02	
	qe predicated	9.154	(μg/mg)	qe	4.3444	(μg/mg)	qe	2.2272	(μg/mg)
	SSE	10.015		SSE	1.6156		SSE	0.2016	
t (days)	q_t(μg/mg)	q_t (model) (μg/mg)	$Error^2$	q_t(μg/mg)	q_t (model) (μg/mg)	$Error^2$	q_t(μg/mg)	q_t (model) (μg/mg)	$Error^2$
0	0.00	0.00	0.00	0.00	0.00	0.00	0.00	0.00	0.00
1	-0.11	0.09	0.04	0.15	0.08	0.00	-0.08	0.10	0.03
2	1.23	0.18	1.09	0.59	0.16	0.19	0.35	0.18	0.03
3	0.67	0.27	0.16	0.56	0.23	0.11	0.31	0.26	0.00
4	0.98	0.36	0.39	0.71	0.30	0.17	0.41	0.34	0.01
5	-0.18	0.45	0.40	0.24	0.37	0.02	0.30	0.41	0.01
6	-0.15	0.53	0.47	0.09	0.44	0.12	0.38	0.47	0.01
7	-0.17	0.61	0.62	0.33	0.50	0.03	0.44	0.53	0.01
8	0.13	0.69	0.32	-0.19	0.56	0.57	0.52	0.59	0.00
9	-0.69	0.77	2.13	0.34	0.62	0.08	0.48	0.64	0.03
10	0.67	0.85	0.03	0.67	0.68	0.00	0.65	0.69	0.00
12	1.89	1.00	0.78	1.05	0.79	0.07	0.87	0.78	0.01
14	1.81	1.15	0.44	0.92	0.90	0.00	0.93	0.86	0.00
16	0.81	1.29	0.23	0.95	1.00	0.00	0.91	0.93	0.00
18	0.57	1.42	0.74	0.89	1.09	0.04	0.96	1.00	0.00

20	2.47	1.56	0.84	1.33	1.18	0.02	1.12	1.05	0.00
24	1.84	1.81	0.00	1.41	1.34	0.00	1.25	1.16	0.01
26	1.99	1.92	0.00	1.61	1.42	0.04	1.31	1.20	0.01
28	2.20	2.04	0.02	1.64	1.49	0.02	1.35	1.24	0.01
30	3.12	2.15	0.94	1.84	1.56	0.08	1.38	1.28	0.01
32	2.14	2.26	0.02	1.64	1.62	0.00	1.33	1.31	0.00
34	2.52	2.36	0.02	1.77	1.69	0.01	1.35	1.35	0.00
36	2.76	2.47	0.08	1.83	1.74	0.01	1.38	1.38	0.00
39	2.49	2.61	0.02	1.86	1.83	0.00	1.41	1.42	0.00
41	2.72	2.71	0.00	1.89	1.88	0.00	1.44	1.44	0.00
43	2.95	2.80	0.02	1.89	1.93	0.00	1.44	1.47	0.00
45	2.78	2.89	0.01	1.87	1.98	0.01	1.46	1.49	0.00
47	2.93	2.97	0.00	1.98	2.03	0.00	1.46	1.51	0.00
49	2.77	3.06	0.09	1.95	2.07	0.01	1.47	1.53	0.00
52	2.82	3.18	0.13	2.02	2.14	0.01	1.49	1.56	0.00

HMC

	HA = 10.8 mg/L			HE = 50.8 mg/L			HI = 91.2 mg/L		
Model Fitting Parameters	k	0.447		k	0.0341		k	0.1044	
	qe predicated	1.605	(μg/mg)	qe	1.8113	(μg/mg)	qe	1.2793	(μg/mg)
	SSE	2.397		SSE	0.0417		SSE	0.0256	
t (days)	q_t(μg/mg)	q_t (model) (μg/mg)	$Error^2$	q_t(μg/mg)	q_t (model) (μg/mg)	$Error^2$	q_t(μg/mg)	q_t (model) (μg/mg)	$Error^2$
0	0.00	0.000	0.000	0.00	0.000	0.000	0.00	0.000	0.000
1	1.25	0.671	0.332	0.15	0.105	0.002	0.16	0.151	0.000
2	1.11	0.946	0.027	0.22	0.199	0.000	0.29	0.270	0.000
3	0.98	1.096	0.014	0.29	0.283	0.000	0.35	0.366	0.000
4	0.98	1.190	0.046	0.28	0.359	0.007	0.46	0.445	0.000
5	0.66	1.255	0.358	0.44	0.427	0.000	0.48	0.512	0.001
6									
7	0.98	1.339	0.131	0.56	0.546	0.000	0.59	0.618	0.001
8	1.34	1.367	0.001	0.56	0.599	0.002	0.65	0.661	0.000
9	1.04	1.390	0.122	0.65	0.647	0.000	0.69	0.698	0.000
10	1.28	1.409	0.016	0.65	0.691	0.001	0.74	0.732	0.000
11	1.65	1.425	0.050	0.81	0.732	0.006	0.75	0.761	0.000
13	1.92	1.450	0.222	0.86	0.806	0.003	0.90	0.812	0.007
15	2.08	1.469	0.378	0.96	0.871	0.007	0.90	0.853	0.002
17				0.91	0.927	0.000	0.88	0.888	0.000
19	1.29	1.496	0.043	0.93	0.978	0.002			

21	1.75	1.505	0.059	0.98	1.022	0.002	0.94	0.943	0.000
23	1.36	1.514	0.023	1.00	1.063	0.004	0.98	0.965	0.000
25	1.20	1.521	0.106	1.07	1.099	0.001	0.87	0.984	0.013
27	1.37	1.527	0.026				1.01	1.002	0.000
29	1.53	1.532	0.000	1.18	1.162	0.000	1.03	1.017	0.000
31	1.47	1.536	0.005	1.20	1.189	0.000	1.03	1.030	0.000
33	1.50	1.540	0.002	1.19	1.215	0.001	1.04	1.043	0.000
34	1.32	1.542	0.050	1.20	1.227	0.001	1.05	1.048	0.000
36	1.85	1.546	0.092	1.29	1.249	0.002	1.06	1.059	0.000
38	2.08	1.549	0.280	1.27	1.270	0.000	1.07	1.069	0.000
40	1.47	1.551	0.006	1.32	1.289	0.001	1.09	1.078	0.000
42	1.64	1.554	0.008	1.32	1.307	0.000	1.09	1.086	0.000
44	1.26	1.556	0.085	1.34	1.324	0.000			

LMC

	LA =11.8 mg/L			LE = 47.8 mg/L			LI = 91.0 mg/L		
Model Fitting Parameters	k	0.004		k	0.0111		k	0.0461	
	qe predicated	4.792	(μg/mg)	qe	2.7503	(μg/mg)	qe	1.6321	(μg/mg)
	SSE	10.487		SSE	0.3865		SSE	0.0576	
t (days)	q_t(μg/mg)	q_t (model) (μg/mg)	$Error^2$	q_t(μg/mg)	q_t (model) (μg/mg)	$Error^2$	q_t(μg/mg)	q_t (model) (μg/mg)	$Error^2$
0	0.00	0.000	0.000	0.00	0.000	0.000	0.00	0.000	0.00
1	-0.01	0.098	0.011	-0.09	0.081	0.029	0.17	0.114	0.00
2	-0.34	0.193	0.280	0.08	0.158	0.007	0.17	0.214	0.00
3	-0.33	0.283	0.372	0.02	0.231	0.045	0.22	0.301	0.01
4	-0.65	0.370	1.049	0.08	0.299	0.049	0.30	0.378	0.01
5	0.13	0.454	0.103	0.29	0.364	0.006	0.40	0.446	0.00
6	0.00	0.535	0.286	0.36	0.425	0.004	0.44	0.508	0.00
7	-0.57	0.612	1.394	0.35	0.484	0.018	0.49	0.563	0.01
8	0.58	0.687	0.011	0.53	0.539	0.000	0.67	0.614	0.00
9	0.66	0.760	0.010	0.69	0.592	0.010	0.65	0.659	0.00
10	0.74	0.829	0.008	0.61	0.643	0.001	0.73	0.701	0.00
12	1.34	0.962	0.145	0.78	0.737	0.002	0.83	0.775	0.00
14	1.40	1.086	0.100	0.91	0.823	0.007	0.90	0.838	0.00
16	1.57	1.202	0.137	0.98	0.902	0.007	0.96	0.892	0.00
18	3.67	1.311	5.559	1.34	0.975	0.134	1.00	0.939	0.00

20				1.20	1.042	0.024	1.00	0.981	0.00
22	1.75	1.511	0.056	1.13	1.104	0.000	1.05	1.018	0.00
24	1.55	1.602	0.003	1.12	1.162	0.002	1.07	1.051	0.00
25	1.37	1.646	0.075	1.12	1.190	0.006	1.08	1.066	0.00
27				1.17	1.242	0.005	1.10	1.094	0.00
29				1.28	1.291	0.000	1.13	1.119	0.00
31	1.64	1.886	0.060	1.23	1.337	0.011	1.14	1.143	0.00
33	1.57	1.958	0.153	1.35	1.379	0.001	1.16	1.164	0.00
35	1.28	2.026	0.558	1.29	1.420	0.016	1.16	1.183	0.00
37	2.25	2.091	0.024	1.48	1.458	0.001	1.13	1.201	0.00
39	2.37	2.154	0.048	1.51	1.494	0.000	1.19	1.217	0.00
41	2.35	2.213	0.019	1.55	1.528	0.000	1.20	1.233	0.00
43	2.11	2.270	0.026	1.57	1.560	0.000			

Submerged

	WA = 11.4 mg/L			WE = 53.2 mg/L			WI = 92.0 mg/L		
Model Fitting Parameters	k	0.898		k	0.0064		k	0.0661	
	qe predicated	0.000	(μg/mg)	qe	2.8443	(μg/mg)	qe	1.1906	(μg/mg)
	SSE	8.568		SSE	0.5731		SSE	0.5557	
t (days)	q_t(μg/mg)	q_t (model) (μg/mg)	$Error^2$	q_t(μg/mg)	q_t (model) (μg/mg)	$Error^2$	q_t(μg/mg)	q_t (model) (μg/mg)	$Error^2$
0	0.00	0.000	0.00	0.00	0.000	0.000	0.00	0.000	0.000
1	0.14	0.000	0.02	0.12	0.051	0.004	0.22	0.087	0.018
2	0.26	0.000	0.07	0.33	0.100	0.054	0.31	0.162	0.022
3	-0.99	0.000	0.97	0.11	0.148	0.002	0.27	0.227	0.002
4	-0.48	0.000	0.23	0.20	0.193	0.000	0.31	0.285	0.001
5	-1.22	0.000	1.50	0.07	0.238	0.028	0.43	0.336	0.009
6	-0.71	0.000	0.50	0.30	0.281	0.000	0.40	0.382	0.000
7	-0.58	0.000	0.33	0.35	0.322	0.001	0.45	0.423	0.001
8	-0.84	0.000	0.71	0.39	0.362	0.001	0.48	0.460	0.000
9	-1.02	0.000	1.05	0.47	0.401	0.004	0.52	0.494	0.000
10	-0.85	0.000	0.72	0.51	0.439	0.006	0.54	0.524	0.000
12	-0.37	0.000	0.14	0.58	0.511	0.005	0.60	0.578	0.000
14	-0.39	0.000	0.15	0.57	0.579	0.000	0.62	0.624	0.000
16	-0.90	0.000	0.81	0.00	0.643	0.413	0.67	0.664	0.000
18	-0.02	0.000	0.00	0.79	0.703	0.008	0.00	0.698	0.487
20	0.13	0.000	0.02	0.85	0.760	0.008	0.76	0.728	0.001

22	-0.16	0.000	0.02	0.85	0.814	0.001	0.76	0.755	0.000
24	-0.08	0.000	0.01	0.95	0.866	0.007	0.82	0.778	0.002
26	-0.07	0.000	0.00	0.97	0.915	0.003	0.84	0.800	0.002
28	0.06	0.000	0.00	1.05	0.961	0.009	0.86	0.819	0.001
30	-0.47	0.000	0.22	1.01	1.006	0.000	0.88	0.836	0.002
32	-0.12	0.000	0.01	1.15	1.048	0.011	0.90	0.852	0.002
34	-0.12	0.000	0.01	1.09	1.089	0.000	0.90	0.867	0.001
36	0.56	0.000	0.31	1.14	1.127	0.000	0.92	0.880	0.002
38	-0.11	0.000	0.01	1.11	1.164	0.003	0.92	0.892	0.001
41	-0.30	0.000	0.09	1.16	1.217	0.003	0.93	0.909	0.000
43	-0.67	0.000	0.44	1.21	1.250	0.002	0.94	0.919	0.000
45	0.45	0.000	0.21	1.27	1.282	0.000	0.95	0.928	0.000
47	0.87	0.000	0.75	1.35	1.313	0.001	0.95	0.937	0.000
49	0.67	0.000	0.45	1.34	1.342	0.000	0.96	0.945	0.000
51	1.46	0.000	2.14	1.33	1.371	0.001	0.97	0.953	0.000
53	0.53	0.000	0.28	1.40	1.398	0.000	0.97	0.960	0.000
55	0.77	0.000	0.60	1.43	1.424	0.000	0.98	0.967	0.000
57	0.87	0.000	0.75	1.41	1.450	0.001	0.98	0.974	0.000

Salt

	SA = 11.4 mg/L			SE = 51.0 mg/L			SI = 93.0 mg/L		
Model Fitting Parameters	k	0.002		k	0.0273		k	0.0689	
	qe predicated	0.000	(μg/mg)	qe	1.5264	(μg/mg)	qe	1.1781	(μg/mg)
	SSE	12.179		SSE	1.3280		SSE	0.0097	
t (days)	q_t(μg/mg)	q_t (model) (μg/mg)	$Error^2$	q_t(μg/mg)	q_t (model) (μg/mg)	$Error^2$	q_t(μg/mg)	q_t (model) (μg/mg)	$Error^2$
0	0.00	0.000	0.00	0.00	0.000	0.000	0.00	0.000	0.000
1	-1.60	0.000	2.56	-0.27	0.061	0.112	0.06	0.088	0.001
2	-0.59	0.000	0.35	-0.04	0.118	0.024	0.14	0.164	0.001
3	-1.07	0.000	1.15	-0.13	0.170	0.089	0.17	0.231	0.003
4	-1.20	0.000	1.43	0.06	0.218	0.024	0.26	0.289	0.001
5	-0.73	0.000	0.53	0.16	0.263	0.011	0.34	0.340	0.000
6	-0.51	0.000	0.26	0.22	0.306	0.008	0.38	0.386	0.000
7	-0.32	0.000	0.10	0.29	0.345	0.003	0.46	0.427	0.001
8	0.44	0.000	0.19	0.39	0.382	0.000	0.48	0.464	0.000
9	-0.04	0.000	0.00	0.45	0.417	0.001	0.52	0.497	0.000
10	0.32	0.000	0.10	0.51	0.449	0.004	0.52	0.528	0.000
12	-0.21	0.000	0.05	0.56	0.509	0.002	0.60	0.581	0.000
14	-0.21	0.000	0.05	0.51	0.563	0.003	0.61	0.627	0.000
16	-0.29	0.000	0.08	0.68	0.611	0.004	0.67	0.665	0.000
18	0.48	0.000	0.23	0.73	0.655	0.005	0.70	0.699	0.000
20	0.59	0.000	0.35	0.79	0.694	0.009	0.74	0.729	0.000

22	0.55	0.000	0.31	0.81	0.731	0.007	0.77	0.755	0.000
24	0.53	0.000	0.28	0.88	0.764	0.013	0.79	0.778	0.000
26	0.43	0.000	0.18	0.94	0.794	0.021	0.80	0.799	0.000
28	0.32	0.000	0.10	0.88	0.822	0.003	0.82	0.818	0.000
30	0.58	0.000	0.34	1.03	0.849	0.033	0.83	0.835	0.000
32	0.32	0.000	0.10	0.98	0.873	0.012	0.86	0.851	0.000
34	-0.60	0.000	0.37	1.02	0.895	0.015	0.87	0.865	0.000
36	-0.66	0.000	0.43	1.02	0.916	0.011	0.87	0.878	0.000
39	-1.57	0.000	2.48	0.00	0.945	0.894	0.87	0.895	0.001
41	0.40	0.000	0.16	1.11	0.963	0.020	0.90	0.906	0.000

Operational Control

	CA = 11.6 mg/L			CE = 54.4 mg/L			CI = 91.2 mg/L		
Model Fitting Parameters	k	1.000		k	0.0026		k	0.0026	
	qe predicated	0.383	(μg/mg)	qe	3.4451	(μg/mg)	qe	2.8942	(μg/mg)
	SSE	10.796		SSE	0.0420		SSE	0.0665	
t (days)	q_t(μg/mg)	q_t (model) (μg/mg)	$Error^2$	q_t(μg/mg)	q_t (model) (μg/mg)	$Error^2$	q_t(μg/mg)	q_t (model) (μg/mg)	$Error^2$
0	0.00	0.000	0.000	0.00	0.000	0.000	0.00	0.000	0.000
1	-0.49	0.106	0.351				0.02	0.022	0.000
2	-0.33	0.166	0.248	0.06	0.062	0.000	0.03	0.043	0.000
3	-0.29	0.205	0.246	0.08	0.092	0.000	0.06	0.064	0.000
4	0.13	0.232	0.011	0.20	0.121	0.006	0.10	0.085	0.000
5	-0.64	0.252	0.795	0.14	0.150	0.000	0.06	0.106	0.002
6	-0.47	0.267	0.551	0.15	0.179	0.001	0.02	0.126	0.012
7	-0.21	0.279	0.237	0.18	0.207	0.001	0.14	0.146	0.000
8	-0.23	0.289	0.271	0.25	0.234	0.000	0.18	0.166	0.000
9	0.00	0.297	0.088					0.185	0.034
10	-0.31	0.304	0.378	0.28	0.288	0.000	0.22	0.204	0.000
11	-0.27	0.310	0.339	0.29	0.314	0.000	0.23	0.223	0.000
13	-0.52	0.319	0.705	0.37	0.365	0.000	0.28	0.260	0.000
15	0.03	0.327	0.086	0.40	0.415	0.000	0.31	0.296	0.000
17	0.12	0.332	0.043	0.45	0.462	0.000	0.35	0.331	0.000
19	0.18	0.337	0.025	0.48	0.509	0.001	0.37	0.365	0.000

21	1.02	0.341	0.458	0.63	0.554	0.005	0.48	0.398	0.007
23	0.75	0.344	0.161	0.66	0.597	0.003	0.47	0.430	0.002
25	0.58	0.347	0.054	0.62	0.640	0.000	0.47	0.462	0.000
27	0.21	0.350	0.020	0.65	0.681	0.001	0.50	0.493	0.000
29	-0.35	0.352	0.492	0.61	0.721	0.012	0.48	0.523	0.002
31	1.30	0.354	0.892	0.79	0.759	0.001	0.59	0.552	0.002
33	1.34	0.355	0.979	0.85	0.797	0.003	0.59	0.580	0.000
35	1.20	0.357	0.713	0.85	0.834	0.000	0.63	0.608	0.001
37	1.46	0.358	1.204	0.89	0.869	0.001	0.64	0.635	0.000
39	1.07	0.359	0.498	0.95	0.904	0.002	0.68	0.662	0.000
41	1.06	0.361	0.488	0.91	0.938	0.001	0.66	0.687	0.001
43	1.04	0.362	0.464	0.92	0.970	0.003	0.66	0.713	0.003

Appendix E Statistical Notes

Confidence Intervals on Model Predicted Values (also commonly termed Prediction Intervals)

Confidence intervals on model predicted values were determined using the following equation, adapted from Seber & Wild (2003):

$$\hat{y} \pm t_{\frac{\alpha}{2}(n-p)} \sqrt{((H+I)_{ii}\sigma^2)}$$

Where:

$\hat{y}$ is the predicted value from the model, which in this case was the final solid phase concentration, at the given input

$t_{\frac{\alpha}{2}(n-p)}$ is the student t value (test statistic) with a level of confidence of $\frac{\alpha}{2}$ and (n-p) degrees of freedom. The number of experimental points is given by n, and p is the number of parameters in the regression (in this case 2)

H is the "hat" matrix given by

$$H_{ii} = X(X'X)^{-1}X'$$

Where X is the Jacobian matrix evaluated at the points (in this case the final liquid phase MC-LR concentrations of interest). Note where the isotherm data indicated a negative slope (negative 1/n), the slope was assumed to approach 0 (1/n= 10^{-10}) in order to evaluate the Jacobian.

The identity matrix is given as I.

$\sigma^2$is taken as the following:

$$\sigma^2 = \frac{SSE}{n-p}$$

Reference:

Seber, G.A.F. & Wild, C.J. (2003) Nonlinear Regression. John Wiley & Sons, Inc., Hoboken, New Jersey